INVESTIGATION OF A DUAL PUMP/MOTOR HYDRAULIC ACCUMULATOR ENERGY STORAGE AUTOMOBILE

by

SCOTT ALLEN BAUM

A thesis submitted in partial fulfillment of the requirements for the degree of

MASTER OF SCIENCE

(MECHANICAL ENGINEERING)

at the

UNIVERSITY OF WISCONSIN--MADISON

1987

AWO
B347
S367

ACKNOWLEDGEMENT

With this thesis I mark, at least for now, an end to my formal education. Prior to this work my role had been that of a student and my main emphasis was on acquiring knowledge. Subsequent to this work, and for the prior three months, my main task will be to apply this knowledge to the working environment as a practicing engineer. I hope I am able to apply this education fruitfully and for the betterment of mankind. It is my desire to pass on any information which I may have learned to others with a yearning to know why. The ending of my formal education does not signal an end to my learning. I hope the day I stop learning is the day I die. The mind needs to be challenged in order to stay agile.

Just as a ship cannot sail without its crew, this thesis would not have floated without help from others. First I would like to express a deep appreciation to my parents, Allen and Rose, who provided a loving, nurturing environment for me to grow up in so that I could become the person I am today. Gratitude is expressed to professors Frank Fronczak and Norman Beachley for extending a research position to me and for their help during my research work at the University of Wisconsin - Madison. Appreciation is given to General Motors Research Laboratories for their financial support of this research. Credit is also given to Don Benson and Ed Lewandowski who were also research assistants on this

project and are completing their thesis's on other aspects not covered here. A big thanks goes out to Nick and Nancy Zompolas who provided a place to stay, encouragement, and delicious dinners during my weekend journeys to Madison while completing this thesis in spite of a sometimes less than favorable disposition on my part near the end. I also want to thank Lynne Kutzke who proofed and typed the final manuscript, under a somewhat restrictive time frame, which gave me the opportunity to finish other details and complete this thesis on time.

Finally, I would like to close this section with a quote I stumbled across, while nearing the end of my work, which seemed to describe the situation I was in at the time and generally reflects my methods for doing most work of this nature.

Nothing blocks progress like having an ample deadline.

- H. S. Francis

Scott Allen Baum

May 13, 1987

TABLE OF CONTENTS

		Page No.
	Abstract	iii
	List of Figures	iv
	List of Tables	vii
	List of Photographs	ix
	List of Abbreviations	x
	List of Nomenclature	xi
1.0	Introduction	1
1.1	Hybrid Vehicle General Description	1
1.2	Accumulator Energy Storage Hybrid Vehicles	2
1.3	Advantages of Accumulator ESU over Flywheel ESU	5
1.4	Research Scope	6
2.0	Dual Pump/Motor Hydraulic Accumulator Hybrid Vehicle	8
2.1	System Overview	8
2.2	Simulated IC Engine	14
2.3	Engine Pump	17
2.4	Energy Storage Unit	19
2.5	Hydraulic Pump/Motor Unit	22
2.6	Flywheel	27
2.7	Low Pressure Accumulator	28
3.0	Computer Control and Data Acquisition	29
3.1	Introduction	29
3.2	Computer Control	29
3.3	Data Acquisition	31
4.0	Operating Characteristics of the Rexroth Variable Displacement Pump/Motor A2VHD Size 107	33
4.1	Introduction	33
4.2	Spin Losses for Unit as a Pump	34
4.3	Spin Losses for Unit as a Motor	36
4.4	Start-Up and Stall Angles	39
4.5	Pump Efficiency	40
4.6	Chain Drive Efficiency	44
5.0	Accumulator Efficiency Testing	47
5.1	Introduction	47
5.2	Test Set-Up	47
5.3	Instrumentation	51
5.4	Test Procedure	52
5.5	Results	56

TABLE OF CONTENTS (Cont.)

		Page No.
6.0	Regenerative Cycling Testing.....	75
6.1	Introduction.....	75
6.2	Test Set-Up.....	76
6.3	Instrumentation.....	76
6.4	Test Procedure.....	79
6.5	Efficiency Analysis.....	81
6.5.1	Calculation of Flywheel Drag Torque.....	91
6.5.2	Peak Flywheel Speed Method.....	92
6.5.3	Accumulator Energy Transfer Method.....	93
6.6	Results.....	95
7.0	Hybrid Vehicle Control Testing.....	100
7.1	Introduction.....	100
7.2	Control of System.....	101
7.3	Test Configuration.....	104
7.4	Test Procedure.....	107
7.5	Results.....	109
8.0	Conclusions.....	124
	References.....	128
	Appendix A -- Computer Control Programs.....	130
	Appendix B -- Rexroth Test Data.....	137
	Appendix C -- Rexroth Pump/Motor Data.....	148
	Appendix D -- Parker Accumulator Data.....	176
	Appendix E -- Transducer Calibration and Error Bands.....	181

ABSTRACT

A comprehensive test program was conducted to determine the efficiency and controllability of a hybrid passenger vehicle configuration utilizing hydropneumatic accumulators as an energy storage device with dual hydrostatic pump/motor units and a simulated internal combustion engine. In addition to overall system testing, individual component testing was carried out to provide information on component performance and efficiency. The major emphasis of this work is on the experimental methods used and the resulting data obtained from the various tests. Other work gives more detailed information on the design of the system and the control strategies used for the testing. Based on the results of the research, it was concluded that the system is relatively easy to control and has the potential to significantly raise the fuel mileage of passenger vehicles.

LIST OF FIGURES

		Page No.
FIGURE 1.1	Dual Pump/Motor System.....	3
FIGURE 1.2	Single Pump/Motor System.....	3
FIGURE 2.1	Hydraulic Circuit-Hybrid Vehicle Simulation.....	9
FIGURE 2.2	BSFC Map for an IC Engine.....	12
FIGURE 2.3	Hydraulic/Electrical Schematic - Pump.....	18
FIGURE 2.4	Accumulator Energy Storage Control Policy.....	24
FIGURE 2.5	Hydraulic/Electrical Schematic - P/M..	25
FIGURE 3.1	Control and Data Acquisition Schematic.....	30
FIGURE 4.1	Hydraulic Circuit - Spin Loss as a Pump.....	35
FIGURE 4.2	Torque Required to Spin Pump.....	37
FIGURE 4.3	Hydraulic Circuit - Spin Loss as a Motor.....	38
FIGURE 4.4	Start-Up and Stall Angles for Motor as a Function of Pressure.....	41
FIGURE 4.5	Hydraulic Circuit - Efficiency Testing.....	42
FIGURE 4.6	Chain Box Efficiency.....	46
FIGURE 5.1	Hydraulic Circuit - Accumulator Testing.....	48
FIGURE 5.2	Accumulator Oil Pressure.....	57
FIGURE 5.3	Supply Line Oil Pressure.....	58
FIGURE 5.4	Accumulator Gas Pressure.....	59
FIGURE 5.5	Accumulator Piston Position.....	60

LIST OF FIGURES (Cont.)

		Page No.
FIGURE 5.6	Accumulator Gas Temperature.....	61
FIGURE 5.7	Foam Filled Accumulator Oil Pressure..	62
FIGURE 5.8	Supply Line Oil Pressure.....	63
FIGURE 5.9	Foam Filled Accumulator Gas Pressure..	64
FIGURE 5.10	Foam Filled Accumulator Piston Position.....	65
FIGURE 5.11	Foam Filled Accumulator Gas Temperature.....	66
FIGURE 5.12	Accumulator Efficiency versus Holding Time for Fast Charge-Hold-Fast Discharge Cycles With and Without Foam.....	71
FIGURE 5.13	Thermal and Frictional Losses versus Holding Time for Fast Charge-Hold-Fast Discharge Cycles With and Without Foam.....	72
FIGURE 5.14	Accumulator Efficiency versus Holding Time for Fast Charge-Hold-Fast Discharge Cycles With the Accumulator Containing No Foam, Full of Foam and Half-Filled with Foam.....	73
FIGURE 5.15	Thermal and Frictional Losses versus Holding Time for Fast Charge-Hold-Fast Discharge Cycles With the Accumulator Containing No Foam, Full of Foam and Half-Filled with Foam.....	74
FIGURE 6.1	Hydraulic Circuit - Regenerative Cycling.....	77
FIGURE 6.2	Flywheel Losses.....	82
FIGURE 6.3	Flywheel Speed.....	84
FIGURE 6.4	P/M Displacement Angle.....	85
FIGURE 6.5	Accumulator Piston Position.....	86

LIST OF FIGURES (Cont.)

		Page No.
FIGURE 6.6	LVDT Accumulator Pressure.....	87
FIGURE 6.7	Accumulator Pressure.....	88
FIGURE 6.8	P/M Inlet Oil Pressure.....	89
FIGURE 6.9	Flywheel Torque.....	90
FIGURE 6.10	P/M Efficiency 20 Degrees Displacement.....	99
FIGURE 7.1	Computer Control Flow Chart.....	102
FIGURE 7.2	Torque/Speed Curve Simulated Engine...	106
FIGURE 7.3	Command Voltage.....	112
FIGURE 7.4	Flywheel Speed.....	113
FIGURE 7.5	Flywheel Torque.....	114
FIGURE 7.6	Pump/Motor Position.....	115
FIGURE 7.7	Accumulator Pressure.....	116
FIGURE 7.8	Accumulator Position.....	117
FIGURE 7.9	Engine Speed.....	118
FIGURE 7.10	Engine Torque.....	119
FIGURE 7.11	Pump Control Pressure.....	120

LIST OF TABLES

		Page No.
TABLE 1.1	Road Load for a 300 Lb Vehicle.....	7
TABLE 4.1	Torque Required to Spin Pump.....	138
TABLE 4.2	Spin Losses for Motor.....	139
TABLE 4.3	Start-Up and Stall Angles for Motor....	142
TABLE 4.4	Rexroth Pump Data Angle = 1 Degree.....	143
TABLE 4.5	Rexroth Pump Data Angle = 3 Degrees....	144
TABLE 4.6	Rexroth Pump Data Angle = 5 Degrees....	145
TABLE 4.7	Chain Box Data.....	146
TABLE 4.8	Rexroth Efficiency Tables Motor Size 107.....	174
TABLE 4.9	Rexroth Efficiency Tables Pump Size 107.....	175
TABLE 5.1	Accumulator Efficiency Test Identification.....	54
TABLE 5.1	Test Identification Continued.....	55
TABLE 5.2	Results for Tests With 3.45 MPa (500 PSIG) Precharge Pressure, Fast Charge and Fast Discharge.....	68
TABLE 5.3	Effect of Charge and Discharge Time 3.45 MPa (500 PSIG) Precharge Pressure.	69
TABLE 5.4	Results for Tests with 10.35 MPa (1500 PSIG) Precharge Pressure, Fast Charge and Fast Discharge.....	70
TABLE 6.1	Regenerative Cycling Test Identification.....	83
TABLE 6.2	Regenerative Cycling Efficiencies.....	96
TABLE 6.3	P/M Efficiencies 20 Degrees Displacement.....	98

LIST OF TABLES (Cont.)

		Page No.
TABLE 7.1	Test Identification Hybrid Vehicle Control Testing.....	110
TABLE 7.2	Transducer Error Bands.....	184

LIST OF PHOTOGRAPHS

		Page No.
PHOTOGRAPH 2.1	Engine, Gearbox, and Pump Test Stand.....	13
PHOTOGRAPH 2.2	Pump/Motor and Flywheel Test Stand..	13
PHOTOGRAPH 2.3	Simulated Internal Combustion Engine.....	15
PHOTOGRAPH 2.4	Pump Stroke Controller.....	20
PHOTOGRAPH 2.5	P/M Stroke Controller.....	23
PHOTOGRAPH 5.1	Accumulator Efficiency Test.....	50

LIST OF ABBREVIATIONS

A/D	Analog to Digital
BSFC	Brake Specific Fuel Consumption
D/A	Digital to Analog
ESU	Energy Storage Unit
IC	Internal Combustion
I/O	Input/Output
LVDT	Linear Variable Differential Transformer
P/M	Pump/Motor

LIST OF NOMENCLATURE

$A1$ = Piston Area Accumulator Number 1 (26.372 in^2)

$A2$ = Piston Area Accumulator Number 2 (26.421 in^2)

$\frac{d\Omega}{dt}$ = Flywheel Acceleration (rad/sec^2)

E_{acc} = Accumulator Energy (in-lb)

E_{Drag} = Flywheel Drag Losses (in-lb)

$E_{Flywheel}$ = Flywheel Energy (in-lb)

J = Flywheel Inertia (34.783 lb-in/sec^2, 13,492 lb-in^2)

$\Delta L1$ = Change in Accumulator Piston Displacement between Sample Periods (in)

$L1_{(n)}$ = Piston Position Accumulator Number 1 at Sample Interval (n)

$L1_{(n+1)}$ = Piston Position Accumulator Number 2 at Sample Interval (n+1)

N_{accel} = Regenerative Cycling Efficiency During Exchange of Energy from Accumulators to Flywheel

N_{decel} = Regenerative Cycling Efficiency During Exchange of Energy from Flywheel to Accumulators

N_{RT} = Round Trip Regenerative Cycling Efficiency

$\overline{P1}$ = Average Gas Pressure Between Sample Periods Accumulator Number 1 (psig)

$\overline{P2}$ = Average Gas Pressure Between Sample Periods Accumulator Number 2 (psig)

$P1_{(n)}$ = Gas Pressure Accumulator Number 1 at Sample Interval (n) (psig)

$P1_{(n+1)}$ = Gas Pressure Accumulator Number 1 at Sample Interval (n+1) (psig)

$P2_{(n)}$ = Gas Pressure Accumulator Number 2 at Sample Interval (n) (psig)

LIST OF NOMENCLATURE (Cont.)

$P2_{(n+1)}$	= Gas Pressure Accumulator Number 2 at Sample Interval (n+1) (psig)
T	= Flywheel Drag Torque (in-lb)
ω	= Flywheel Speed (rad/sec)

1.0 INTRODUCTION

Several recent studies (1, 2, 6, 7) have been performed to determine the merits of hybrid vehicles. The results of these studies show that a hybrid vehicle has the potential to significantly raise the fuel economy of a passenger vehicle. In particular, a design incorporating a prime mover large enough to handle all of the vehicle's power requirements coupled with a small capacity energy storage unit (ESU) utilizing a hydrostatic transmission has been studied and found to offer good fuel economy (1). Based on the driving cycle simulations of this design, a dual hydraulic pump/motor (P/M) accumulator ESU system was built to further study the proposed design. This system was used to study control policies, verify computer simulation studies, and provide experimental data on system performance.

1.1 Hybrid Vehicle General Description

A type of hybrid vehicle is one which provides for some form of energy storage, in addition to the energy conversion components coupled to the prime mover. This hybrid vehicle can be driven either from the power of the prime mover, from the energy stored in the ESU, or from both simultaneously. One of its advantages over an ordinary

vehicle is increased fuel economy. This increased fuel economy results from the hybrid vehicle's ability to:

(1) decouple the engine load from the driving load allowing the engine to be operated near maximum efficiency at all times

(2) cycle the engine on and off providing power only when needed

(3) recover braking energy regeneratively instead of dissipating this energy as heat.

The system studied uses an operating strategy proposed by Beachley and Frank (3) in which all of the vehicle's power requirements can be met with the prime mover. Coupled with the prime mover is a small capacity ESU which allows for regenerative braking and engine operation at its most efficient point. A system of this type does not require any sacrifice in vehicle performance while still offering significant fuel savings.

1.2 Accumulator Energy Storage Hybrid Vehicles

Currently there are two hydraulic systems which have been studied that employ the above operating strategy. These are the dual P/M system (1) and the single P/M system (2). See Figures 1.1 and 1.2. In the past the dual P/M system was not as attractive as the single P/M system because all of the power had to be transmitted

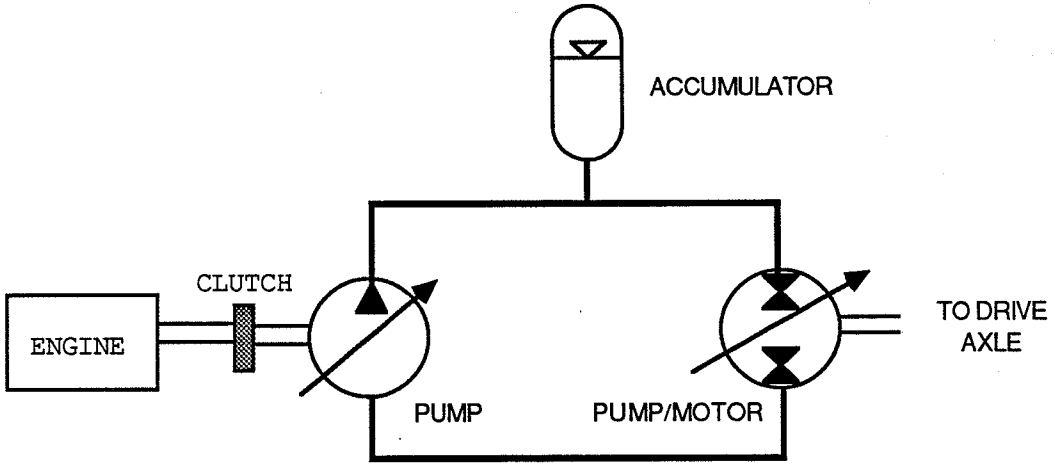


FIGURE 1.1: DUAL PUMP/MOTOR SYSTEM

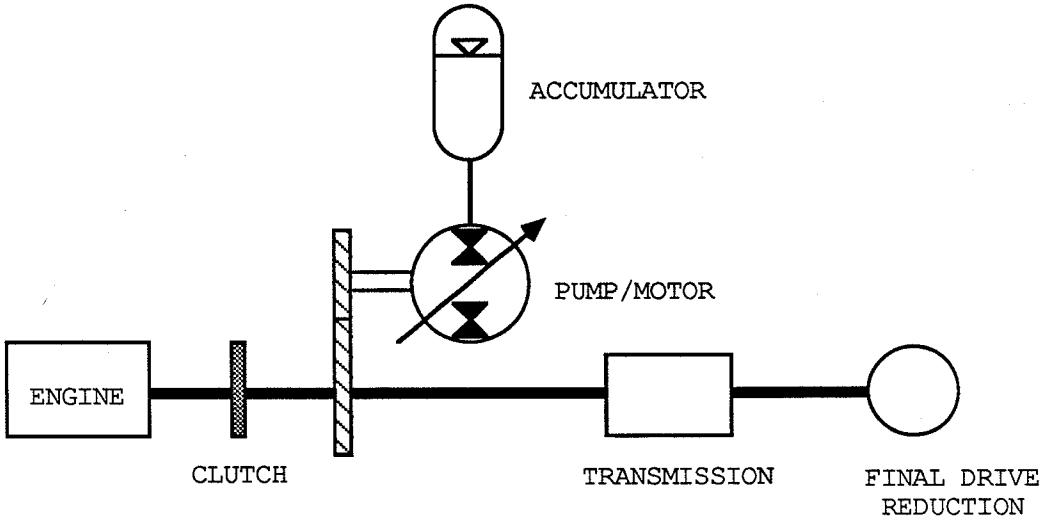


FIGURE 1.2: SINGLE PUMP/MOTOR SYSTEM

hydraulically and system efficiency suffered due to low P/M efficiencies. However, recent improvements in hydraulic P/M units have improved efficiencies (4) and have made a dual P/M system feasible. Studies (5) have shown that hydrostatic transmission efficiency of systems using the newly designed hydraulic pumps can be as high as 92.3% and average 84.9% over the operating range of the hydrostatic transmission.

When comparing the dual P/M system to the single P/M system in Figures 1.1 and 1.2, it is seen that the P/M unit for the single P/M system is used only to transfer energy in and out of the ESU. In the dual P/M system, the P/M units transfer all of the vehicle's driving power. In the single P/M system, the hydraulic unit is driven from the vehicle's transmission. The vehicle's driveline is essential the same as for a conventional automobile. As such, the single P/M system is more of an add-on to the existing driveline of an automobile. In the dual P/M system, the mechanical transmission of the automobile is replaced with a hydrostatic transmission. Both systems have the ability to operate the engine more efficiently and to capture braking energy regeneratively. Each system employs hydropneumatic accumulators as the ESU. Computer modeling simulations have been performed on each system and have shown that each has the potential to raise the fuel

economy of a passenger automobile (1, 2). Further studies need to be performed in order to determine which of the two systems is economically more feasible.

1.3 Advantages of Accumulator ESU Over Flywheel ESU

This study used hydropneumatic accumulators as the ESU. Other studies (6, 7) have focused on the use of flywheels as an energy storage device. It is felt at this time that an accumulator ESU has several advantages over a flywheel ESU. These advantages include reduced overall system weight, elimination of a continuously variable transmission to couple to the flywheel, and capability to store energy indefinitely without parasitic losses. In addition, the concept of a totally hydraulic vehicle (dual P/M system) has several advantages. These advantages include the capability of four wheel drive without additional differentials or gearboxes, elimination of power steering pump, elimination of conventional transmission, and freedom in mounting the engine. Four wheel drive is easily provided by placement of a small P/M unit at each wheel. The engine mounting freedom results from the fact that driveshafts are no longer required since power is transmitted via flexible hoses allowing the engine to be placed without consideration to output shaft orientation.

1.4 Research Scope

The primary focus of this study was to provide experimental data on the performance of a dual P/M accumulator ESU system and to prove that the system was stable and controllable. To provide the required information, a test stand was built. It was felt that a test stand utilizing system components rather than an actual hybrid vehicle would provide the same information, allow for more versatility, and be easier to design and construct. The test stand contained all of the components a vehicle system would require. Figure 2.1 shows the test stand components which included a simulated internal combustion (IC) engine, hydraulic pump unit, gear reduction box, hydraulic P/M unit, hydropneumatic high pressure accumulators, low pressure accumulator, flywheel, and brake system for power dissipation. The flywheel was not used as an ESU for the hybrid simulation. Instead it functioned as an inertia load to simulate the inertia of an automobile.

For the purposes of this study, the system was designed around an assumed vehicle configuration. The vehicle was assumed to weigh 3000 lbs (1300 kg). The simulated IC engine was modeled after the torque/speed curves for a 1983 Pontiac four-cylinder, 152.5 cubic inch (2.5 liter) engine. Road load characteristics were based on several automobile

manufacturer's specifications and are given below in Table 1.1. These vehicle parameters were also the basis used in the computer simulation studies previously cited.

Table 1.1: Road Load for a 3000 lb Vehicle

Speed (MPH)	0	10	20	30	40	50	60	70	80	90	100
Force (Lb)	23.8	28.6	36.9	49.1	65.2	85.1	109.1	137.3	169.5	206.0	246.9

The research work was broken down into four major areas. These areas were:

- Rexroth P/M Efficiency Testing
- Accumulator Efficiency Testing
- Regenerative Cycling Testing
- Hybrid Vehicle Control Testing

The primary focus of the first two test areas was to record performance data to determine component performance and efficiency. The focus of the regenerative cycling testing was to determine total system efficiency in the regenerative cycling mode. The hybrid vehicle control studies were used to verify control system policies and to provide performance data for further computer simulation studies.

2.0 DUAL PUMP/MOTOR HYDRAULIC ACCUMULATOR HYBRID VEHICLE

This section provides the necessary background on the mechanical configuration for the dual P/M hydraulic accumulator ESU vehicle. An entire system overview is provided first, with more detailed information presented later on the individual components.

2.1 System Overview

Figure 2.1 shows the hydraulic schematic for the dual P/M hydraulic accumulator ESU vehicle. Major components are the simulated IC engine, hydraulic pump, high pressure accumulators, hydraulic P/M, and pressurized reservoir. As seen in the figure, the vehicle uses a hydrostatic transmission with an accumulator ESU connected to the high pressure line. The accumulators act as a temporary energy reservoir between the pump and the P/M so each may be controlled independently. This eliminates some of the control problems of a conventional hydrostatic transmission, namely the need to match pump displacement and motor displacement so as to avoid creating large pressure spikes or cavitation in the hydraulic lines. Studies (8) have shown, however, that direct hydrostatic drive may be desirable in certain driving situations where rapid

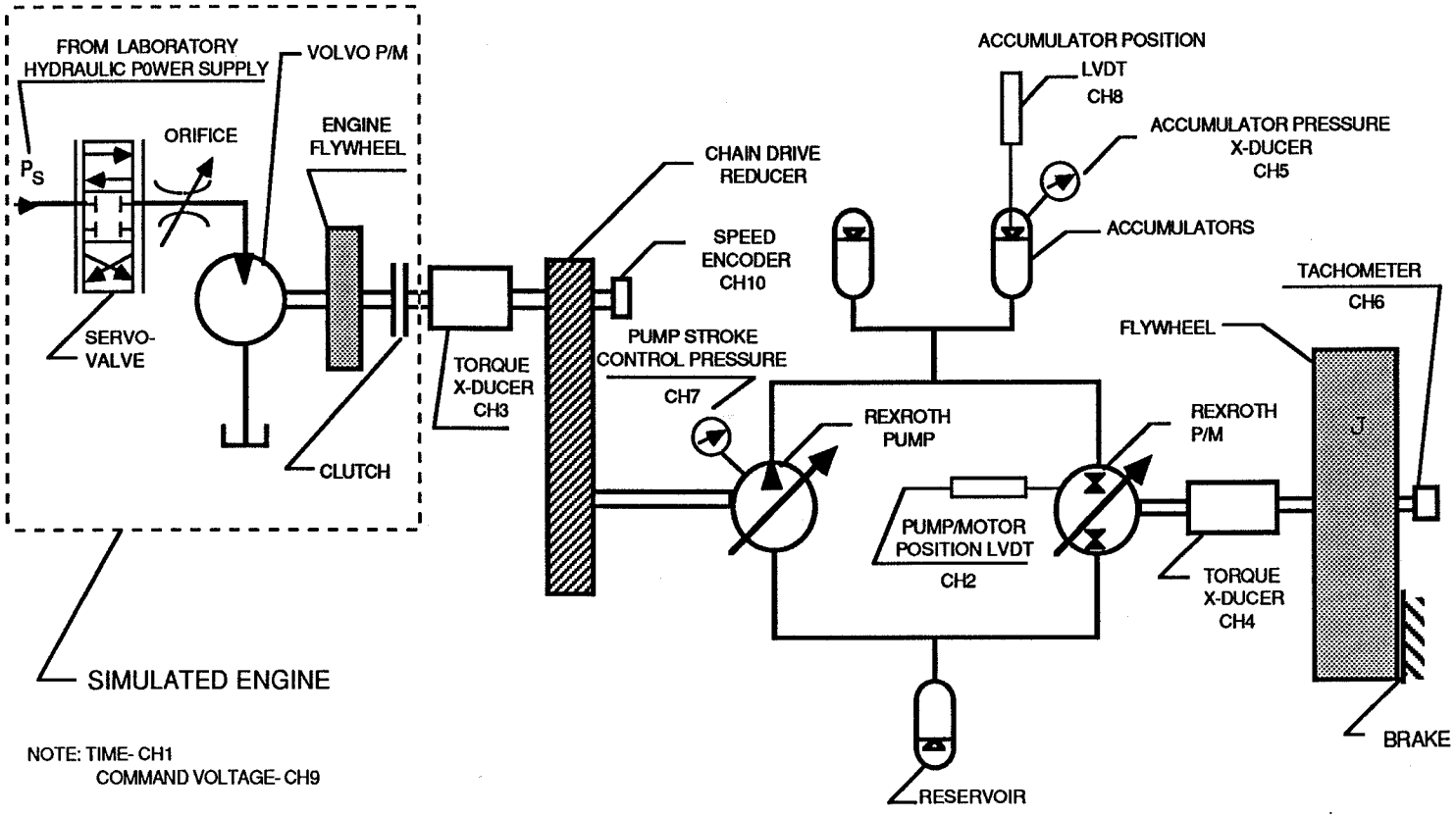


FIGURE 2.1: HYDRAULIC CIRCUIT - HYBRID VEHICLE SIMULATION

acceleration is desired while the accumulator pressure is low. Future research work will entail implementing control strategies developed (9) that allow for direct drive or accumulator driving.

The engine-pump output can be utilized as follows:

(1) provide power to the P/M unit

(2) stored in the accumulators

(3) simultaneously delivered to the P/M and the accumulators.

When the pressure reaches the limit of the high pressure accumulators, the engine is shut off and the displacement of the pump is stroked to zero.

During the entire time the engine and pump are operating, the stroke of the pump is adjusted to maintain engine operation near a point that minimizes fuel consumption with acceptable engine cycling. The minimum value of an IC engine's brake specific fuel consumption (BSFC) is defined as the "ideal point". This ideal point has associated with it a specific torque and speed output determined by the mechanical components of the IC engine. Near the ideal point is a region of different engine power outputs where the BSFC is almost the same as at the ideal point. Therefore, the engine can operate at one of these power values with little sacrifice in economy. The advantage of this is that the power output of the IC engine can be set in

reference to the power demand which can help to reduce engine on/off cycling. However, the engine power output does not have to exactly match the power demand as is required in a conventional automobile allowing for efficient engine operation at all times. Control of the IC engine power output in this manner is known as operating the engine along an "ideal line". The ideal line is a series of power output values that minimize the BSFC. Figure 2.2 shows the ideal line in relation to the BSFC lines for a 109.8 cubic inch (1.8 liter) IC engine. The ideal point is the area at 265 g/kWh (0.44 lb/hp·hr). Operation of the engine on the ideal line allows for a wide range of power outputs with only at most a 25 g/kWh (0.04 lb/hp·hr) increase in the BFSC.

Regenerative braking is provided by the P/M unit which has the capability of going "over center". That is, the hydraulic unit is a variable displacement type which can vary its displacement from negative to positive continuously. This allows for the direction of oil flow to be reversed while still maintaining the same direction of shaft rotation. For hydrostatic units without this ability, valving can be employed to allow for regenerative braking. During regenerative braking the unit uses the kinetic energy of the flywheel (which simulates vehicle inertia) as the energy to power the P/M as a pump which converts the kinetic energy of the vehicle to stored energy in the ESU.

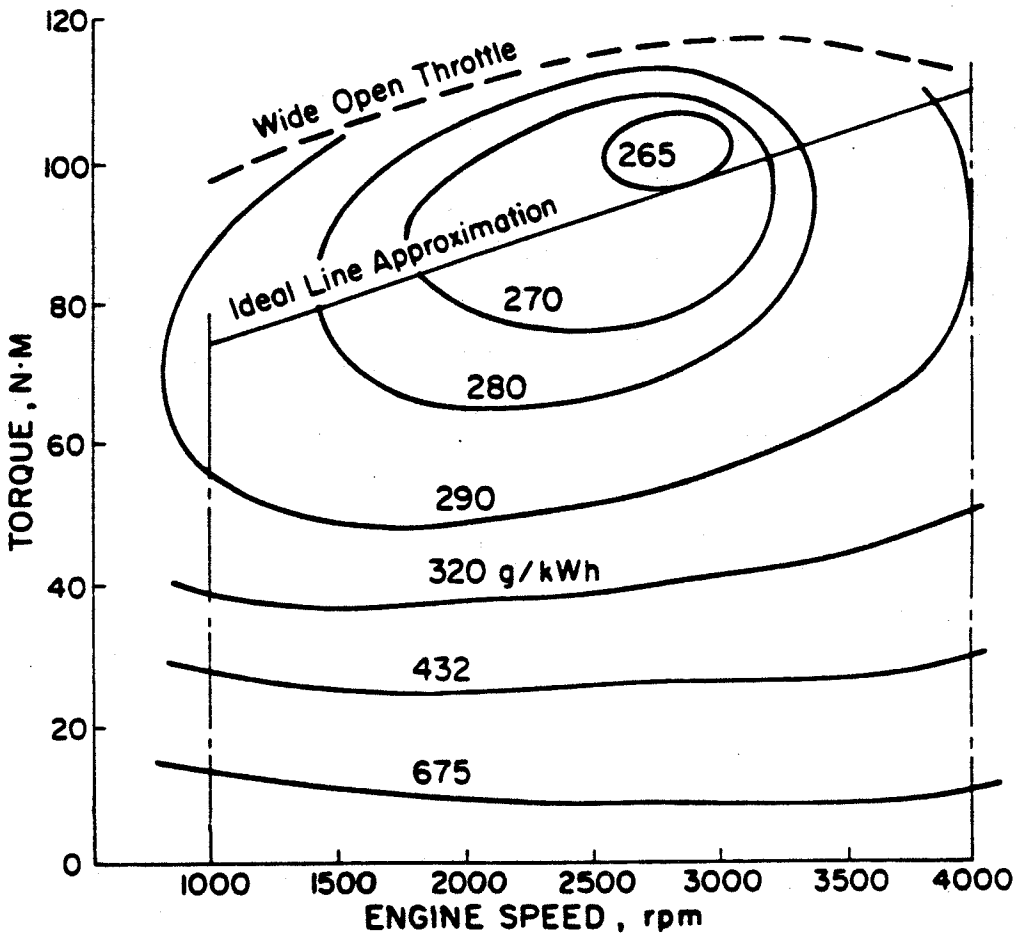
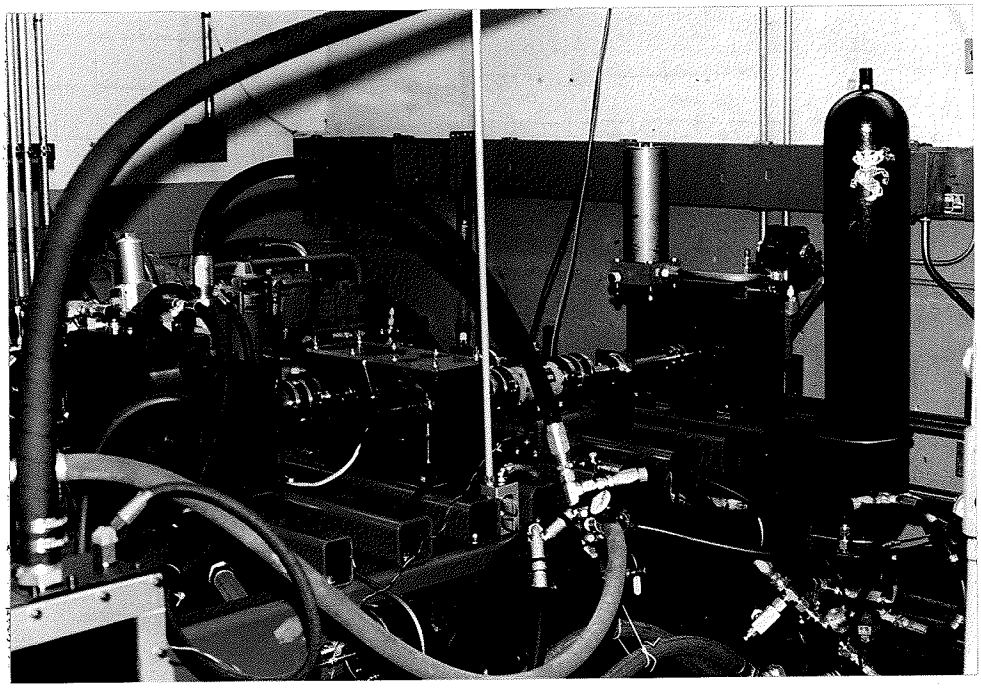
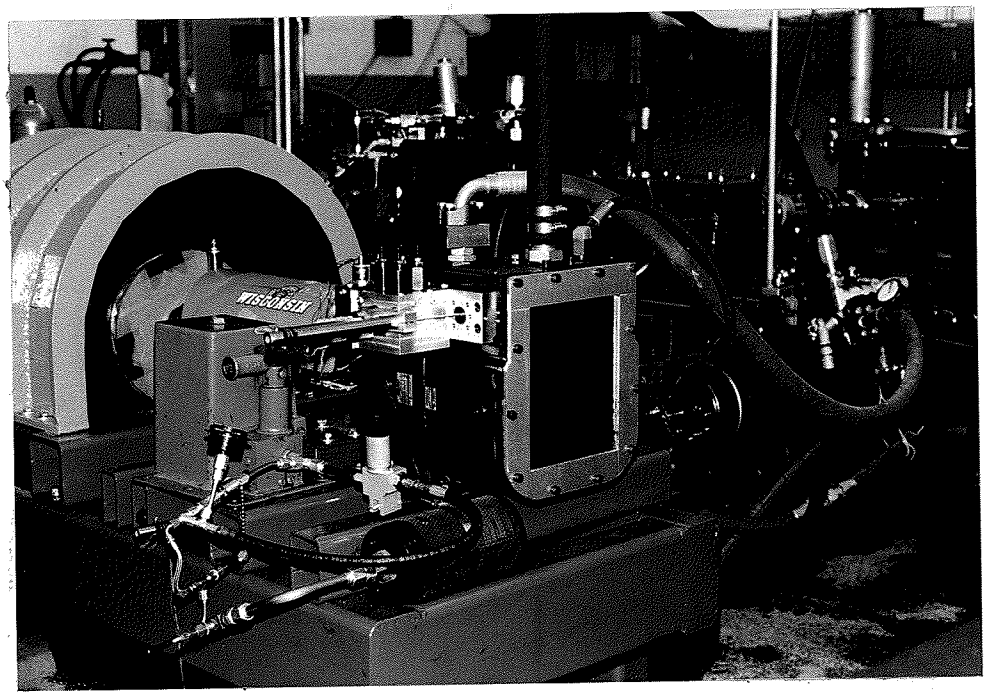


FIGURE 2.2: BSFC MAP FOR AN IC ENGINE

Photograph 2.1 and 2.2 show the actual test stands used for the simulation. Photograph 2.1 is of the test stand which contained the simulated IC engine, gearbox and pump. This stand also supported the high pressure accumulators and the pressurized reservoir. Photograph 2.2 shows the test stand which contained the flywheel (vehicle inertia), pump/motor, and the braking system.



PHOTOGRAPH 2.1: ENGINE, GEARBOX, AND PUMP TEST STAND



PHOTOGRAPH 2.2: PUMP/MOTOR AND FLYWHEEL TEST STAND

2.2 Simulated IC Engine

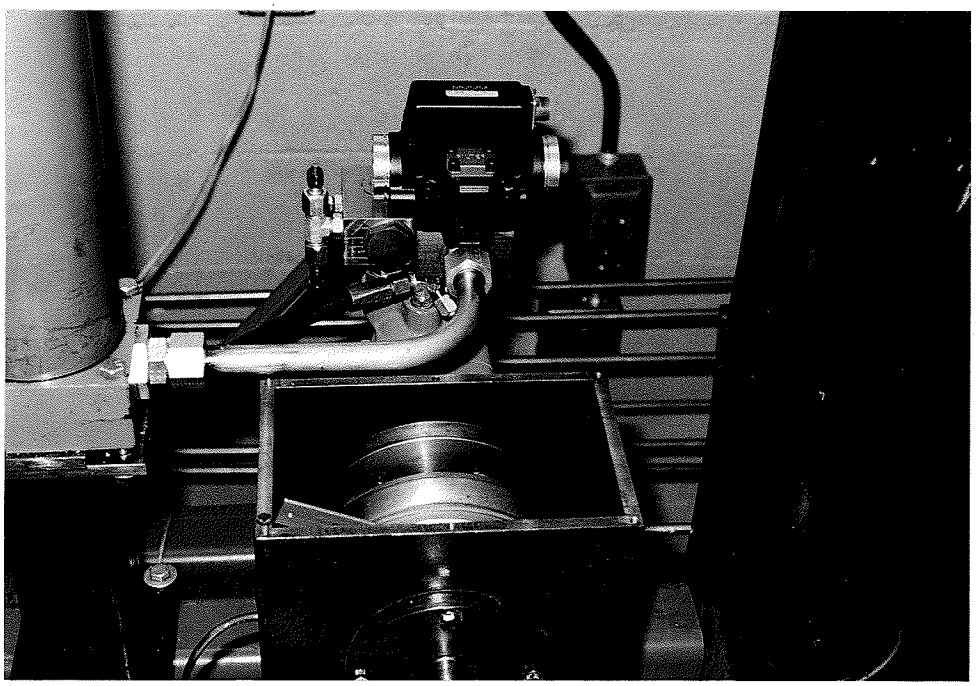
The hydraulic schematic for the simulated IC engine is shown in Figure 2.1 in the boxed area titled: Simulated Engine. A simulated IC engine was used instead of an actual IC engine because it was felt it would eliminate some of the problems associated with an IC engine. The simulated engine eliminated the need for dealing with fuel requirements, exhaust problems, and noise that an actual IC engine would have had. Also a simulated IC engine using a hydraulic motor was more compatible with the rest of the test stand. Since all of the components on the test stand were hydraulic, all of the required power could be conveniently provided by the lab's two 50 hp (37.3 kW) hydraulic power supplies.

For the control strategy utilized, it was not necessary to have an actual IC engine since every motor has its own unique ideal point and ideal line; therefore the control program would have to be adjusted slightly for different engines. What was important, however, was to show that the control scheme was capable of controlling a prime mover with a decreasing torque vs. speed curve at a constant speed and power output.

The basic principle of operation of the hydraulically simulated IC engine is that pressure is directly related to torque in a hydraulic motor, therefore a decrease in

pressure will result in a decrease in torque for a given flow rate. Since the pressure drop across an orifice is proportional to the square root of the flow rate, this results in the torque of a hydraulic motor receiving its flow from an orifice to decrease as the speed of the motor (flow of hydraulic oil) increases thus simulating the torque/speed curve for an IC engine.

The major components of the simulated hydraulic IC engine can be seen in Photograph 2.3. These include a Volvo



PHOTOGRAPH 2.3: SIMULATED INTERNAL COMBUSTION ENGINE

hydraulic motor Model F11-58, Moog servovalve Model 72-161,

Oil Gear variable orifice Model HSTV1200, flywheel, and clutch.

For this particular study the engine was run in an on/off mode maintaining the torque and speed constant during the periods when the engine was running. This would be equivalent to operating the engine at the ideal point. This control was achieved using the computer to control the servovalve to a fully opened or closed position. When power was required a control signal was sent to the servovalve causing it to open fully until the high pressure accumulators reached their maximum pressure limit. At this time another control signal was sent closing the servovalve. Closing the servovalve caused the power of the simulated engine to drop and produced the same effect as shutting off a conventional IC engine.

Future work will entail having the engine operate over the ideal line. As stated earlier, this will allow for the engine's power output to more closely match the vehicle's current power requirements reducing engine on/off cycling while still maintaining efficient engine operation. When this work is carried out, the operation of the servovalve will be similar to the throttle on a conventional IC engine. Further information on the design, construction, and operation of the simulated IC engine is included in E. Lewandowski's thesis: Design of a Test Facility for

Hydropneumatic Accumulator Energy Storage Vehicle Research (10).

2.3 Engine Pump

The pump used for the simulation was a Rexroth A2V107HD. It is a variable displacement unit with pressure control of displacement. The pressure control of the displacement was accomplished using a servovalve, pressure transducer, and servovalve controller. In an actual hybrid vehicle, control of the pump displacement would be accomplished by a digital stroke controller similar to the one which controlled the P/M displacement for this study (see section 2.5). The control of this unit was not modified since the other digital stroke controller was available for control studies and sufficient hardware was not available to modify both units. The hydraulic/electrical schematic for the pressure feedback stroke controller can be seen in Figure 2.3.

Control was accomplished by means of a simple proportional control loop. A voltage command is sent to the servovalve controller which is interpreted as a pressure command. The controller then compares this command to the current pressure obtained from the transducer and if an error is present, a signal is sent to the servovalve which adjusts the flow to maintain the pressure at the desired

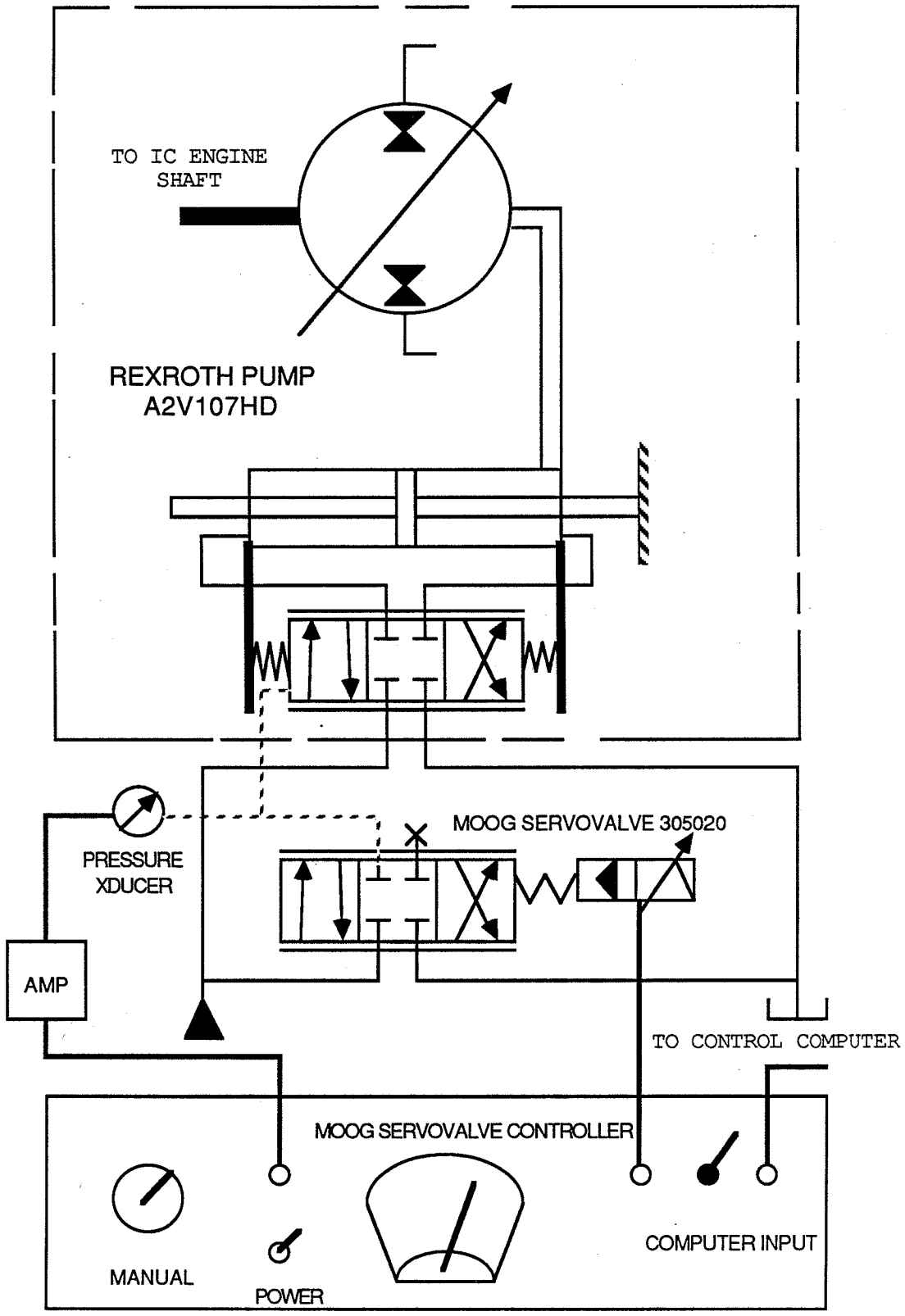


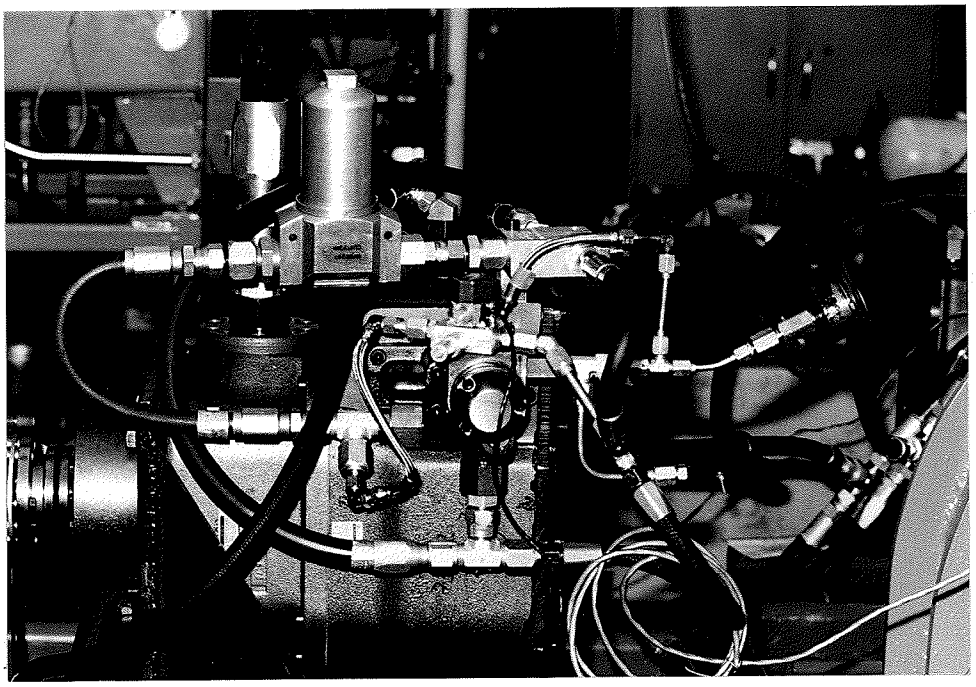
FIGURE 2.3: HYDRAULIC/ELECTRICAL SCHEMATIC - PUMP

point. The servovalve controller was modified to accept either a computer generated control voltage or an operator selected control voltage.

Computer control of this unit is a function of the pressure in the high pressure accumulators. As pressure in the accumulators increases, the stroke of the pump must be decreased so the engine torque and speed will remain constant allowing the engine to operate at the ideal point. The opposite occurs when the pressure in the accumulators decreases. When accumulator pressure reaches the maximum allowable amount (rated maximum pressure) the engine/pump unit is shut off until accumulator pressure drops to near the precharge pressure at which time the engine again is turned on. Photograph 2.4 shows physical hardware used for stroke control of the pump.

2.4 Energy Storage Unit

As mentioned previously, high pressure hydropneumatic accumulators were used as the ESU. The system used two 2.2 gallon (8.2 liter) piston type Parker accumulators Model A6R0462B69E. An accumulator stores energy by compressing a gas. The above accumulators were essentially cylinders with pistons inside which separated the oil from the nitrogen gas. As oil is added to the accumulator the nitrogen gas is compressed, thus storing energy. For



PHOTOGRAPH 2.4: PUMP STROKE CONTROLER

the accumulators used if their total capacity, 4.4 gallons (16.4 liters), could be stored by compressing the nitrogen from 1,000 psig (6.89 MPa) to 3,000 psig (10.34 MPA), 93,069 ft-lbs (.12 MJ) of energy would be stored if the process is assumed to be isothermal. Based on prior studies (11) this amount of energy storage capacity is considered sufficient for our assumed vehicle while limiting the energy storage capacity required.

The accumuators were modified slightly for this study. One of the accumulators was adapted to connect a linear variable differential transformer (LVDT) to the piston. This

allowed for determination of the oil flow rate in or out of the accumulator and could be used to determine the amount of oil (stored energy) in the accumulators. Both accumulators were filled with high density foam on the gas side which previous researchers (12) have found to cause the nitrogen to behave more isothermally. This allows for more energy storage during charging since less thermodynamic losses occur if the gas behaves isothermally and not adiabatically. Increased energy storage results from the fact that the gas temperature will remain nearly constant during compression or expansion eliminating the thermodynamic losses associated with changes in the gas temperature.

The charge policy of the accumulators is such that part of the total energy storage capacity is reserved for regenerative braking. Therefore the maximum accumulator pressure allowed is a function of the vehicle's speed. As vehicle speed increases, the accumulators are charged to a lower pressure so when the brakes are applied there is room in the accumulator to store the regenerative braking energy. Figure 2.4 shows the accumulator's stored energy as a function of vehicle speed for this type of energy allocation policy (11).

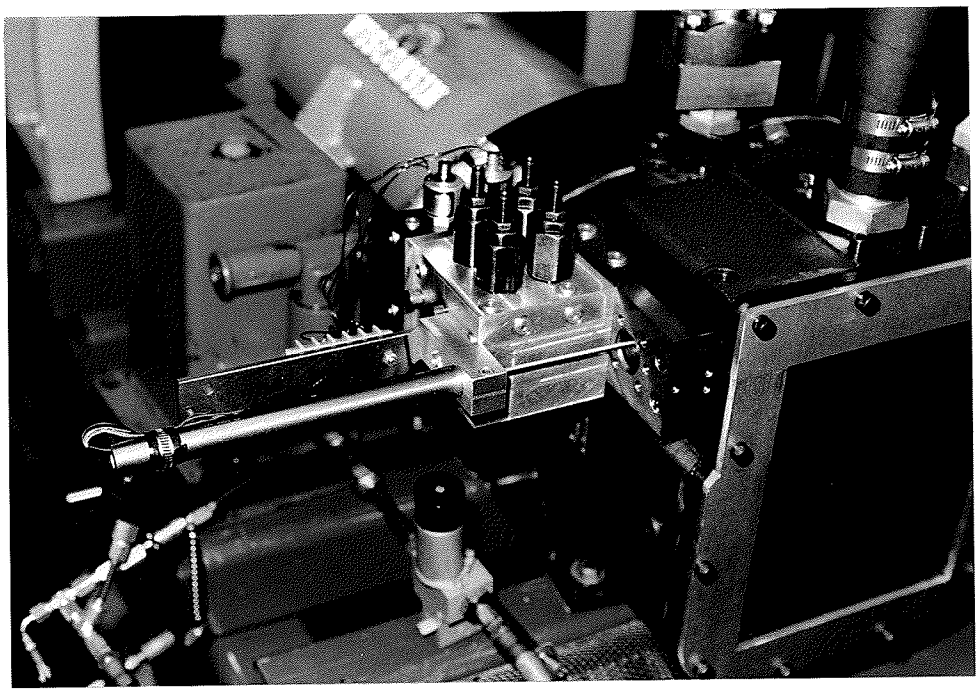
During the vehicle simulation studies, the accumulators were precharged to a pressure of 1,000 psig (6.89 MPa). This is the starting pressure of the nitrogen before any oil

is added to the accumulators. Prior studies (1) have shown that a precharge pressure that is approximately 1/3 the maximum rated pressure of an accumulator will maximize its energy storage capacity.

2.5 Hydraulic Pump/Motor Unit

The P/M used for the hybrid vehicle simulation is a Rexroth A2V107HD which has the ability to go "over center". The displacement control of this unit was modified to incorporate direct digital control. This controller utilized high speed solenoid valves which in turn operate poppet valves that control the flow of oil to the displacement cylinder in the P/M unit. Displacement feedback is provided via a LVDT connected to the trunnion of the piston cylinder block. Figure 2.5 shows the hydraulic/electrical schematic for this digital control system. The hardware used for this controller is shown in Photograph 2.5.

The major reason for modifying the existing pressure feedback control is that a pressure displacement servovalve system would be too expensive to install in an automobile. Servovalves and servovalve controllers are very expensive while solenoid valves and poppet valves are fairly inexpensive. The system used has the advantage of being directly controlled by the computer and inexpensive valve



PHOTOGRAPH 2.5: P/M STROKE CONTROLLER

drivers. It is also felt that the LVDT can be replaced with a less costly feedback system without affecting the controllability of the system. Once a complete control algorithm is established, a micro-processor would take the place of the computer.

In addition to the cost advantages this controller has to offer, digital displacement control does not have the contamination problems associated with servovalves. A servovalve, in order to operate reliably, needs extremely clean hydraulic oil which requires the use of 3 micron

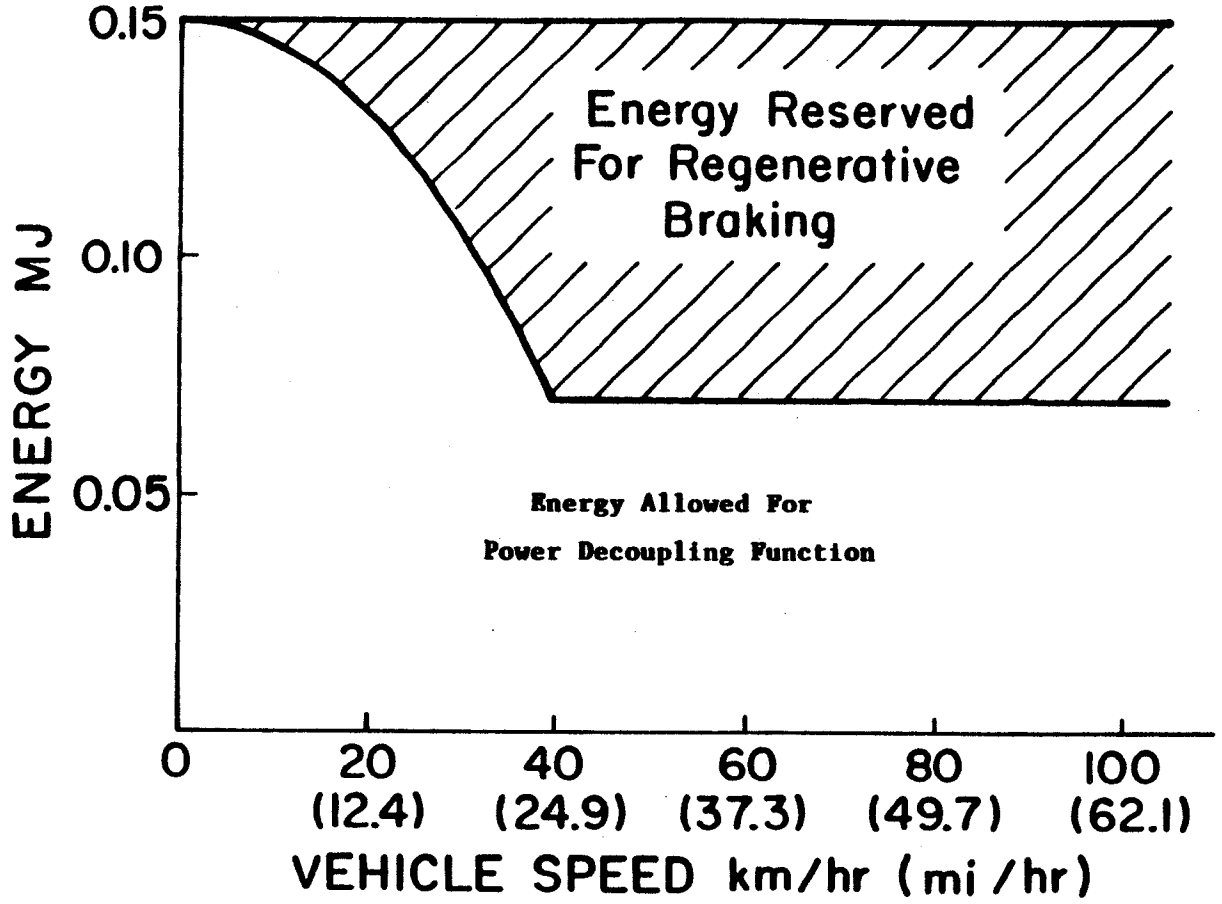


FIGURE 2.4: ACCUMULATOR ENERGY STORAGE CONTROL POLICY

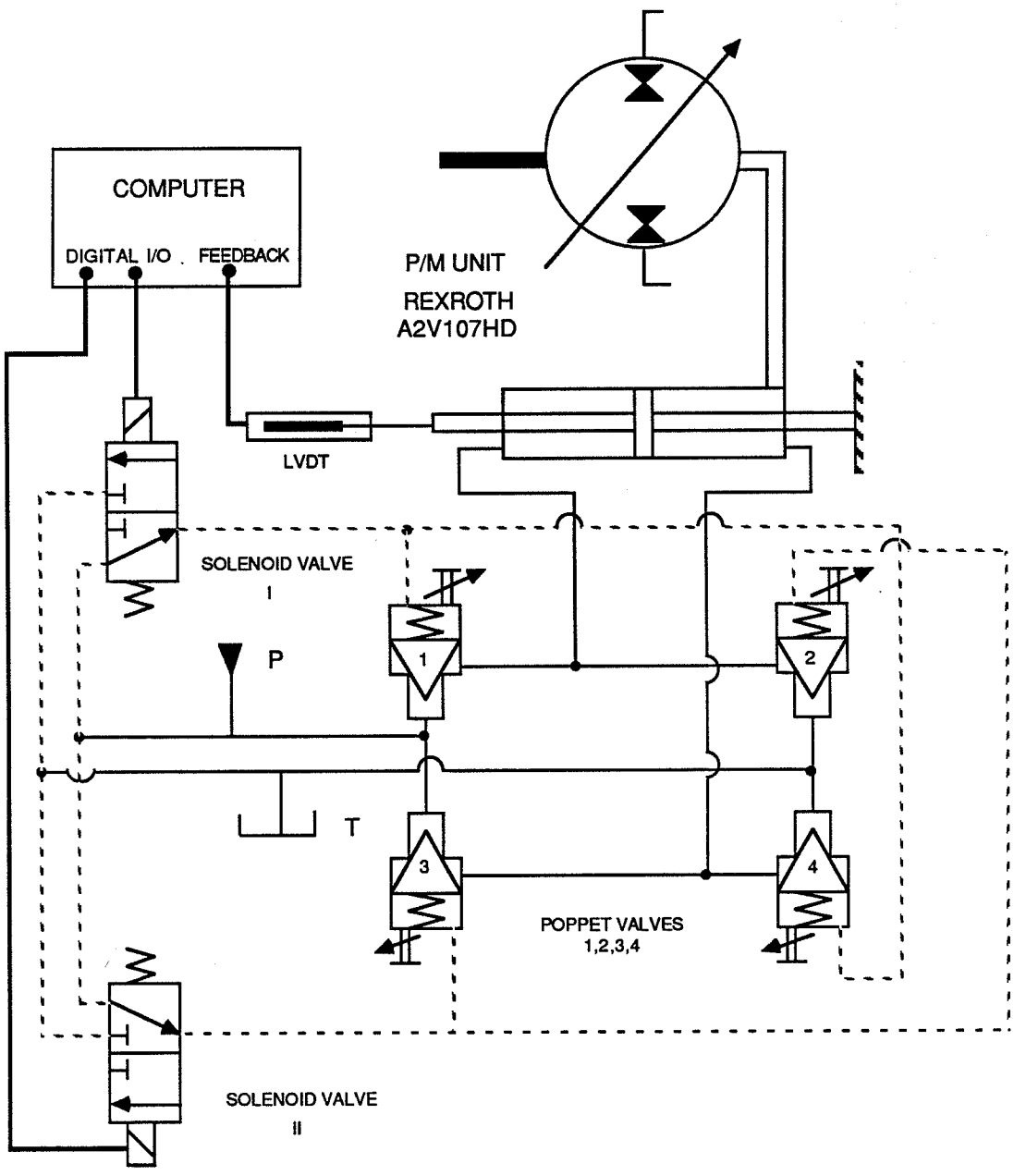


FIGURE 2.5: HYDRAULIC/ELECTRICAL SCHEMATIC - P/M

particle filters. This is due to the fact that small particles may jam on the close tolerances of the servovalve causing it to malfunction. A digital control system is more reliable than a servovalve system since the components are more rugged and simpler to build. Finally, a digital controller can achieve the same level stroke control as the pressure feedback system. No decrease in positional accuracy is required with this controller.

The required displacement of this unit is a function of accumulator pressure. The control is such that the unit maintains a constant command torque output irrespective of accumulator pressure. This is accomplished by limiting the torque output of the P/M to a value that could be achieved with maximum displacement and minimum accumulator charge. If the accumulator charge is at a value higher than the minimum charge, the P/M is destroked to a smaller displacement by the control computer so as to maintain the same maximum torque output. Therefore if the desired torque command is held constant, the stroke of the P/M is automatically increased as accumulator pressure drops and automatically decreased as accumulator pressure increases maintaining a constant output torque.

This policy was needed in order to maintain the driveability of the vehicle. If the displacement of the unit was not changed with increasing accumulator pressure

the driver would, for a constant P/M displacement, have more torque with higher accumulator pressures than with lower accumulator pressures. This variable torque could result in an unsafe vehicle since the driver would not know how the vehicle would respond to his commands. A more complete discussion on the hardware and control of the P/M is included in E. Lewandowski's thesis: "Design of a Test Facility for Hydropneumatic Accumulator Energy Storage Vehicle Research"(10).

2.6 Flywheel

Vehicle inertia was simulated by a 363 lb (164.6 kg) flywheel. The flywheel used had an inertia of 34.783 lb-in/sec^2 (13,429.3 lb-in^2, 3.93 kg-m^2). For the simulation parameters assumed, this would result in a rotational speed for the flywheel of 2,280 rpm equivalent to a 3,000 lb (1300 kg) vehicle traveling 29 mph (46.7 km/hr). The flywheel shaft had rotors and disk brakes attached to it which dissipated energy allowing for various road loads to be simulated. These simulated road loads were applied to the P/M in addition to the inertia load during hybrid vehicle simulation testing.

2.7 Low Pressure Accumulator

The low pressure accumulator functioned as a pressurized reservoir during the hybrid vehicle simulation testing. Its primary functions are to store the hydraulic fluid when the accumulators are discharged and to prevent cavitation in the P/M when functioning as a pump. Pressures were in the range of 50-100 psig (345-690 kPa) which provided the required boost pressure for the Rexroth A2V107HD. Depending on the amount of oil in the high pressure accumulators, reservoir oil volumes ranged between 1 and 5 gallons (3.8 and 18.9 liters).

3.0 COMPUTER CONTROL AND DATA ACQUISITION

3.1 Introduction

This section provides a brief overview of the computer control and data acquisition techniques used while conducting tests with the dual P/M hydraulic, accumulator ESU test stand. Additional information for specific methods can be found in the separate sections outlining the various testing performed. A more comprehensive treatment of the subject is included in D. Benson's thesis: "Experimental Evaluation of the Controllability of a Dual Pump/Motor Hydraulic Accumulator Energy Storage Automobile" (13).

3.2 Computer Control

Figure 3.1 shows a schematic of the control and data acquisition system. The various components on the test stand were controlled using an IBM computer, Model PC, and a Data Translation board, Model DT2801. The Data Translation board had capabilities for 8 analog to digital (A/D) inputs (double ended), 2 digital to analog (D/A) outputs, and 16 digital input and output ports (I/O). The board is based on a 12 bit A/D and D/A conversion.

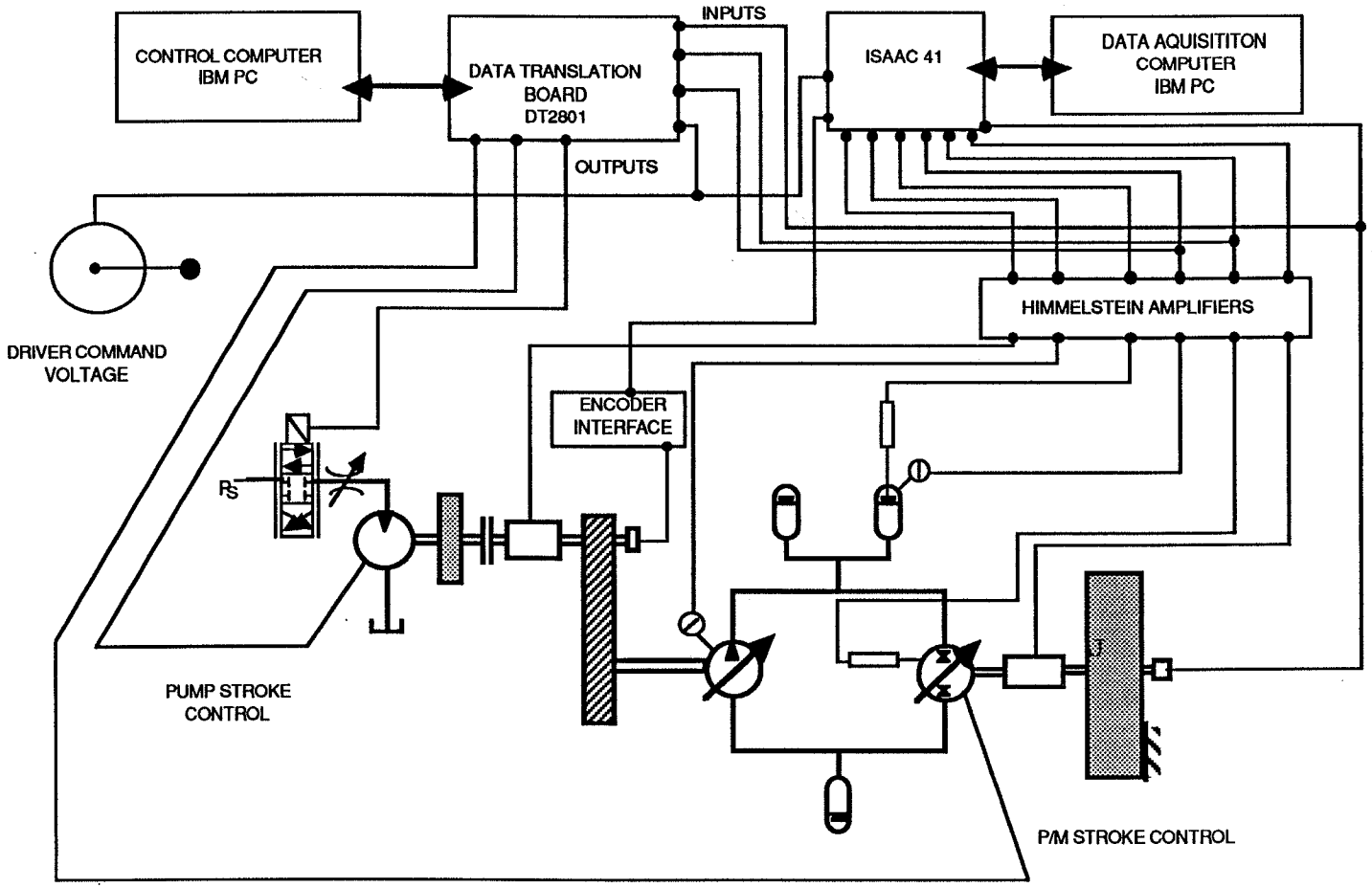


FIGURE 3.1: CONTROL AND DATA ACQUISITION SCHEMATIC

Two of the digital I/O ports were used to control the digital displacement controller on the P/M. One of the D/A ports provided a signal to the servovalve to control the pump. The other controlled the servovalve for the simulated IC engine. Three of the A/D ports were used to monitor the system and provide feedback for the control algorithm. The three variables needed to control the simulated hybrid vehicle were accumulator pressure, flywheel speed (vehicle speed), and P/M displacement.

The Data Translation board is designed to be controlled by commands written in IBM Personal Computer's BASIC language. One control program was written to control the P/M during the regenerative cycling testing (Chapter VI). A separate control program was written for the hybrid vehicle control testing (Chapter VII). An overview of each of these control programs can be found in the separate sections on these topics. The complete control program for each test can be found in Appendix A.

3.3 Data Acquisition

Data acquisition was initially handled by an Isaac 2000 data acquisition system and an IBM computer, Model PC. The Isaac 2000 was found to be inadequate for the necessary sample rates, due to a slow interface with the computer, requiring the system to be upgraded to an Isaac 41 data

acquisition system. The Isaac 41 had the ability to record 16 analog inputs, and 16 bits of binary input. It has a maximum sampling rate of 10,000 Hz for a single channel of input. Simultaneous sampling of binary input and several analog inputs limits the maximum sampling rate to approximately 20 Hz.

Signal conditioning was provided by Himmelstein System 6 amplifiers. The amplifiers have an output range of ± 5 volts. The System 6 has built in filtering for each amplifier circuit that allows a choice of a .1, 1, 100, or 500 Hz filtering if desired. The system is designed to accept amplifier modules which are specially built for either strain gage transducers, LVDT transducers, or thermocouples. Sensitivity is rated at 0.1 mv/v and signal-to-noise-ratio is 0.05% rms.

Various transducers were used for data acquisition purposes. These were Schaevitz pressure and displacement transducers, Himmelstein torque transducers and a Hewlett Packard optical encoder. Details concerning transducer linearity can be found in the specific test sections.

4.0 OPERATING CHARACTERISTICS OF THE REXROTH VARIABLE DISPLACEMENT PUMP/MOTOR A2VHD SIZE 107

4.1 Introduction

This section presents the results of preliminary testing to determine the operating characteristics of the Rexroth model A2V size 107 hydrostatic P/M. This information was obtained to provide data for computer modeling of the system. Included in this section is a description of the test set-ups, the calibration procedures, and the test procedures used. Tests were conducted to determine spin losses for the unit as both a pump and motor, start-up and stall angles for the unit as a motor, and efficiency of the unit as a pump (with data taken primarily at conditions of low power). Additional testing was done to determine the efficiency of the chain drive used in the test stand.

Although the data presented are felt to be reasonably accurate, some of the efficiencies calculated were larger than 100 percent. While this is obviously incorrect, the source of the error was felt to lie in flow meter accuracy and noises superimposed on the transducer signals causing inaccurate values. This was the first series of tests

conducted and this experience led to improved data acquisition techniques. Later testing allowed for improved accuracy in the generation of data made possible by the use of better flowmeters, an improved data acquisition system (Isaac 41), and improved data acquisition algorithms.

4.2 Spin Losses for Unit as a Pump

The purpose of this test was to determine the torque required to operate the Rexroth unit as a pump with no load. The circuit for this test is shown in Figure 4.1. The Rexroth P/M is driven via a chain drive by a hydraulic motor (which is powered by a 50-hp (37.3 kW) Vickers power supply). A Himmelstein torque transducer is coupled between the Rexroth and the chain drive box. The suction line, 16 feet (4.8 m) long, 3/4 in (1.9 cm) hydraulic hose, draws from a reservoir open to atmosphere. The return line is 3/4 in (1.9 cm) hose, 5 feet (1.5 m) in length. A pressure gauge (0-100 psig) measures the pressure out of the pump (which ideally should be zero psig). This pressure was as high as 3 psig (20.7 kPa) at large displacements and high speeds. For most tests the pressure was between 1 and 2 psig (6.7-13.8 kPa).

The torques were measured at 0, 100, 200, 400, 800, and 1100 rpm (the maximum speed attainable with the Vickers

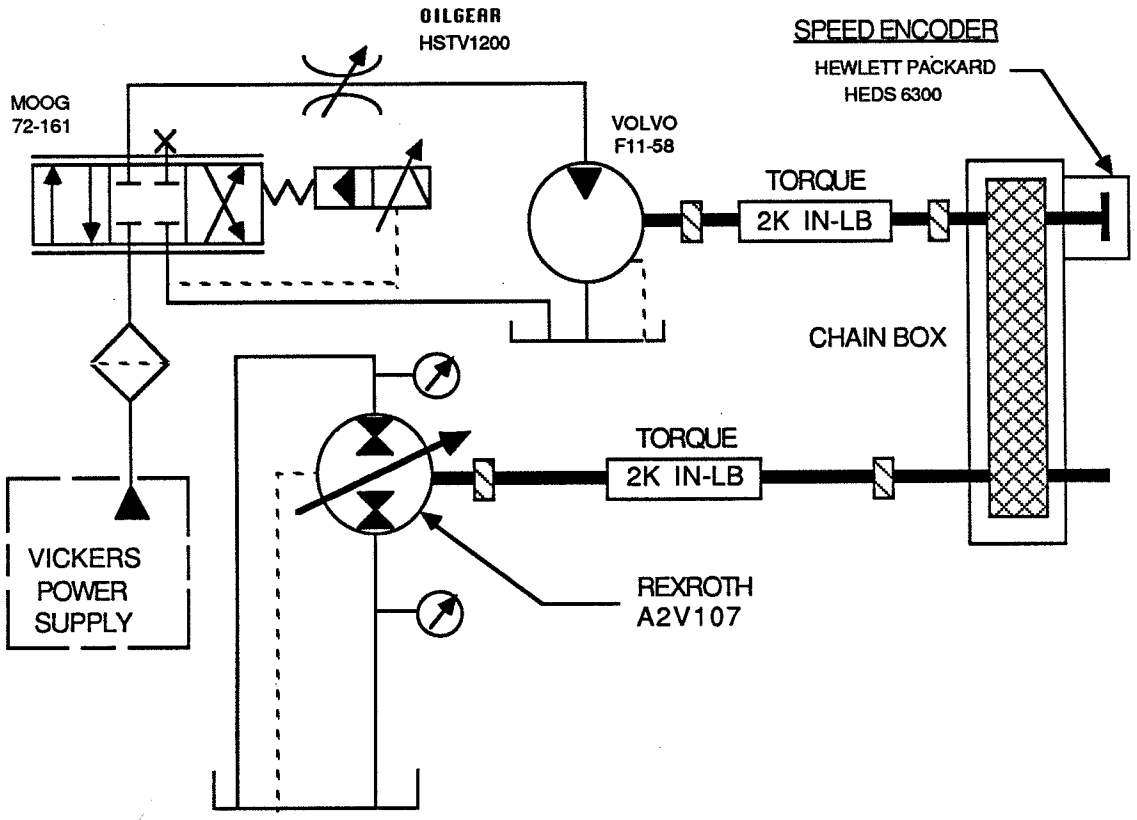


FIGURE 4.1: HYDRAULIC CIRCUIT - SPIN LOSS AS A PUMP

power supply), and for 0, 1, 3, 5, 10, 15, 20, and 25 degrees displacement. The readings at 0 rpm indicate the torque needed to overcome stiction and start the pump turning. Since this test produced little heating of the oil, the oil temperature was constant at 95°F (35°C). The data are shown in Table 4.1 in Appendix B and are plotted in Figure 4.2. From this figure it is apparent that stiction is four to six times greater than running friction at low speeds. No load torque increases with speed, as would be expected. At high speeds and large displacements the measured operating torque is slightly higher than the true no load torque due to the flow losses in the hydraulic hoses.

4.3 Spin Losses for Unit as a Motor

This test determined the pressure required to spin the Rexroth unit with no load. The circuit for this test is shown in Figure 4.3. The Rexroth P/M is driven by the Vickers power supply, which has both a variable displacement and a variable relief pressure. Pressure gauges and transducers were inserted at the inlet and outlet to the Rexroth unit. The Rexroth shaft was disconnected from all external loads. The speed was read using a tachometer. Data were taken at 0, 50, 100, 200, 400, 800, 1500, and 3200 rpm, unless limited by the flow output of the Vickers power

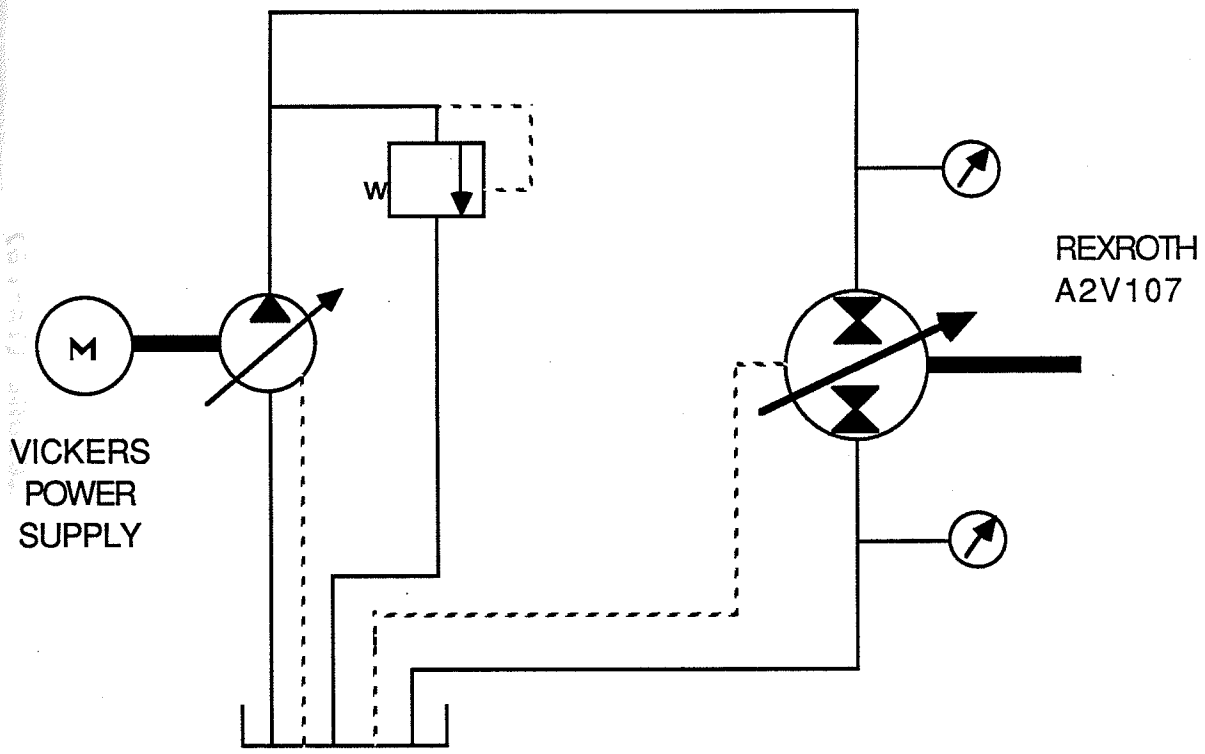


FIGURE 4.3: HYDRAULIC CIRCUIT - SPIN LOSS AS A MOTOR

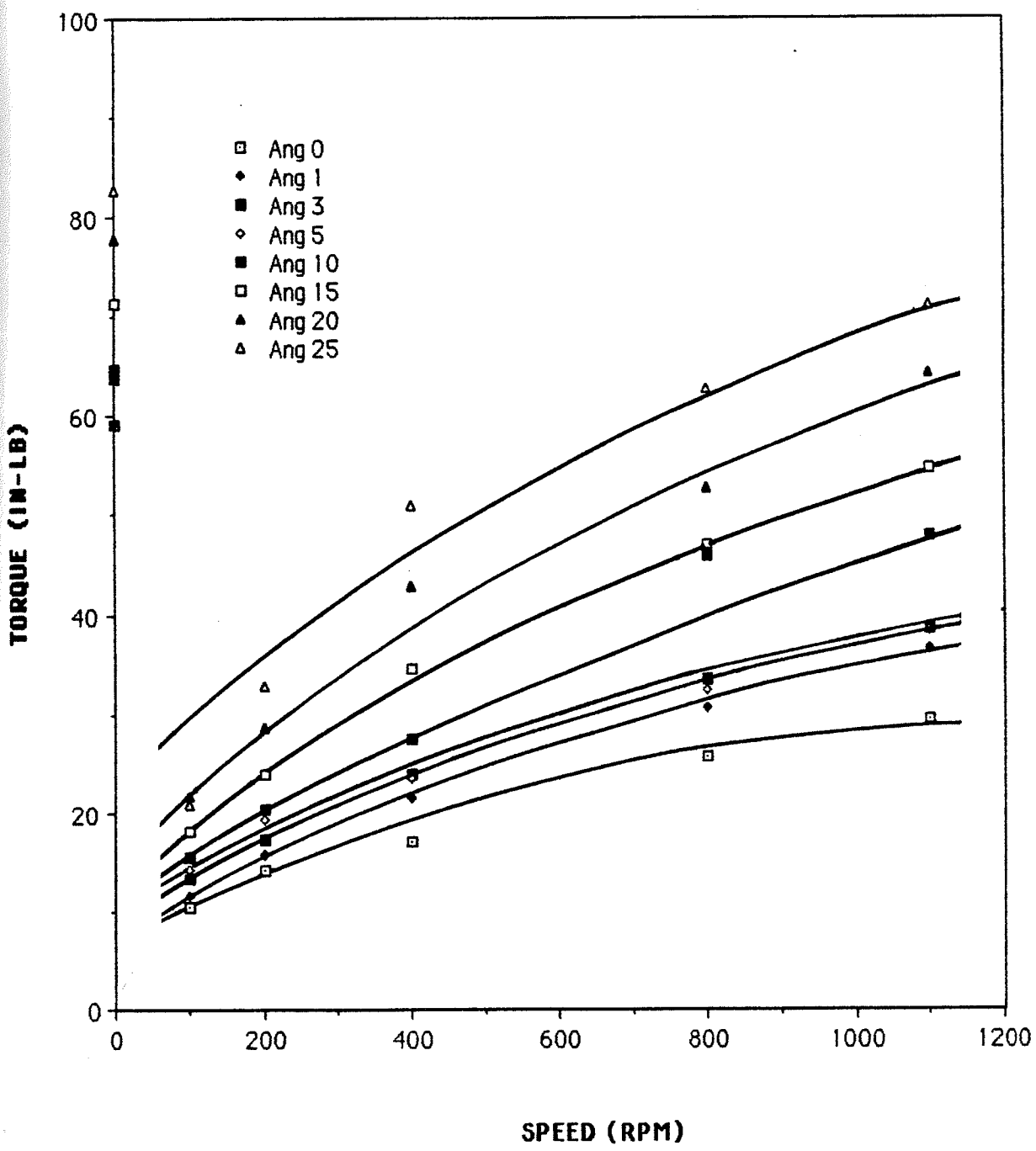


FIGURE 4.2: TORQUE REQUIRED TO SPIN PUMP

supply. The displacement was varied from 1 to 25 degrees and -1 to -10 degrees. Negative angles refer to the fact that the displacement is "over center" which causes rotation in the opposite direction. The data are listed in Table 4.2 of Appendix B. The pressure at 0 rpm is the pressure needed to start the motor spinning, that is, to overcome stiction. Note that there is much scatter in these data points. The probable reason for this scatter is that the required start-up torque varies with the position at which the Rexroth unit previously stopped. Recall that this is a piston-type unit, and a piston produces no torque at top dead center.

The lowest speed listed in the data for each angle is the minimum speed at which the unit can be run. Any reduction in flow results in the motor stalling. As the displacement was reduced, the unit would stall at higher speeds (and pressures). Note that at low displacements much greater pressure is required to start the motor turning than is required to keep it turning. At 1 degree these pressures are approximately 3000 and 300 psig (20.7 MPa and 2.1 MPa) respectively.

4.4 Start-up and Stall Angles

This test determined the angles at which the Rexroth unit would start and stop turning as a function of pressure. The circuit diagram for this test is the same as for spin

losses as a motor (Figure 4.3). The procedure used here was to set the motor supply pressure while the Rexroth unit was not running and then slowly increase the displacement until it began to spin. The displacement was then decreased until the unit stalled. The first angle was considered the start-up angle; the latter the stall angle. These data are found in Table 4.3 of Appendix B, and are shown plotted in Figure 4.4. Because the Rexroth should be symmetrical about the zero displacement point, no distinction between negative and positive angles was made when plotting the results. Both negative and positive angles were plotted as positive angles. It appears that this unit can start up at very low angles, and can spin as a motor even at 0.25 degrees. Some of the scatter in the data can be attributed to the tolerances in the linkage of the displacement controller. However all measurements should be within 0.005 inches, or approximately 0.15 degrees. Also, the angular position at which the Rexroth unit stopped rotating could vary the start-up angle due to the position of the piston in the bore.

4.5 Pump Efficiency

The hydraulic circuit to test pump efficiency is shown in Figure 4.5. The Rexroth unit is driven by the Volvo hydraulic motor through the chain drive. A torquemeter

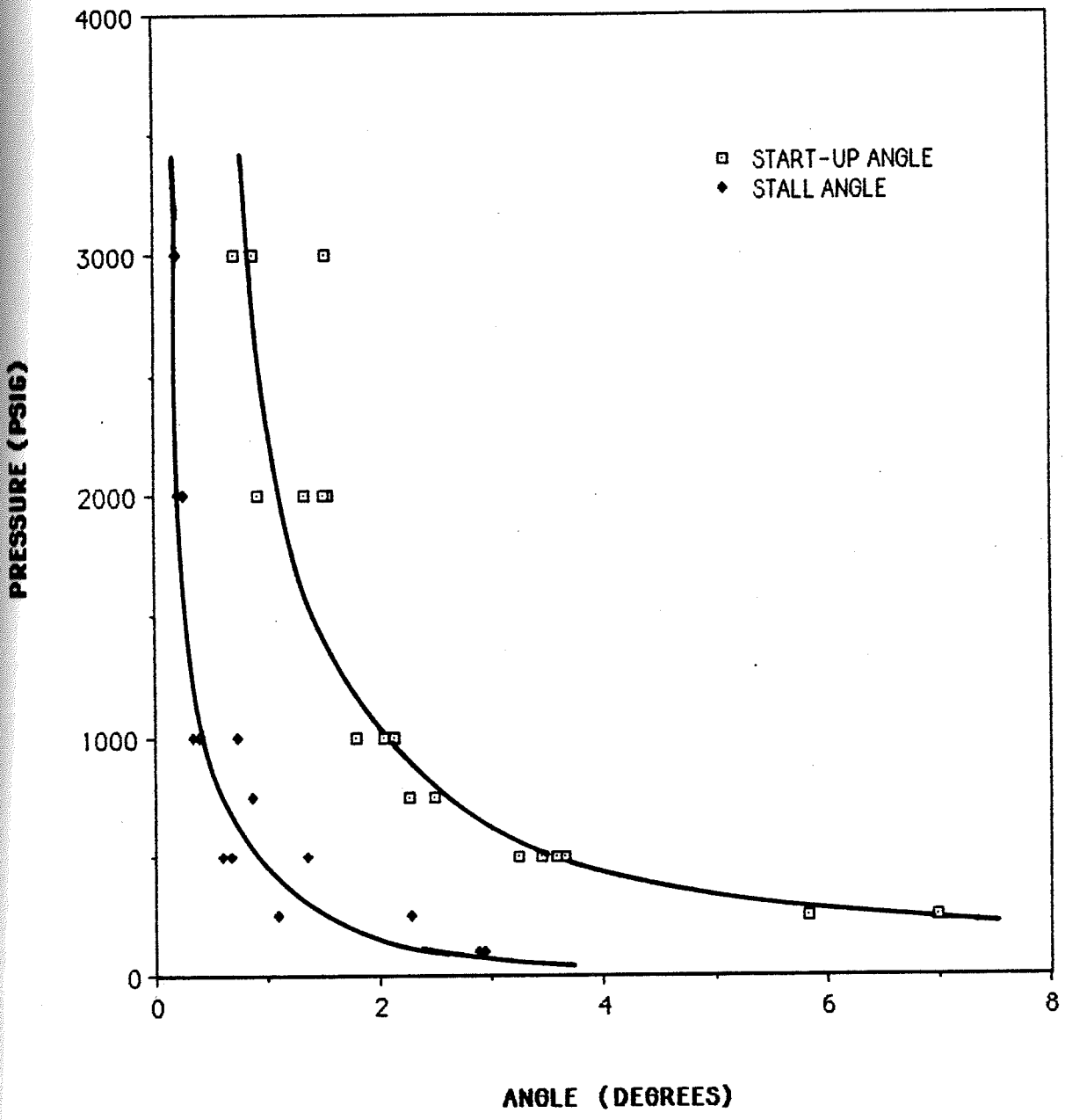


FIGURE 4.4: START-UP AND STALL ANGLES FOR MOTOR AS A FUNCTION OF PRESSURE

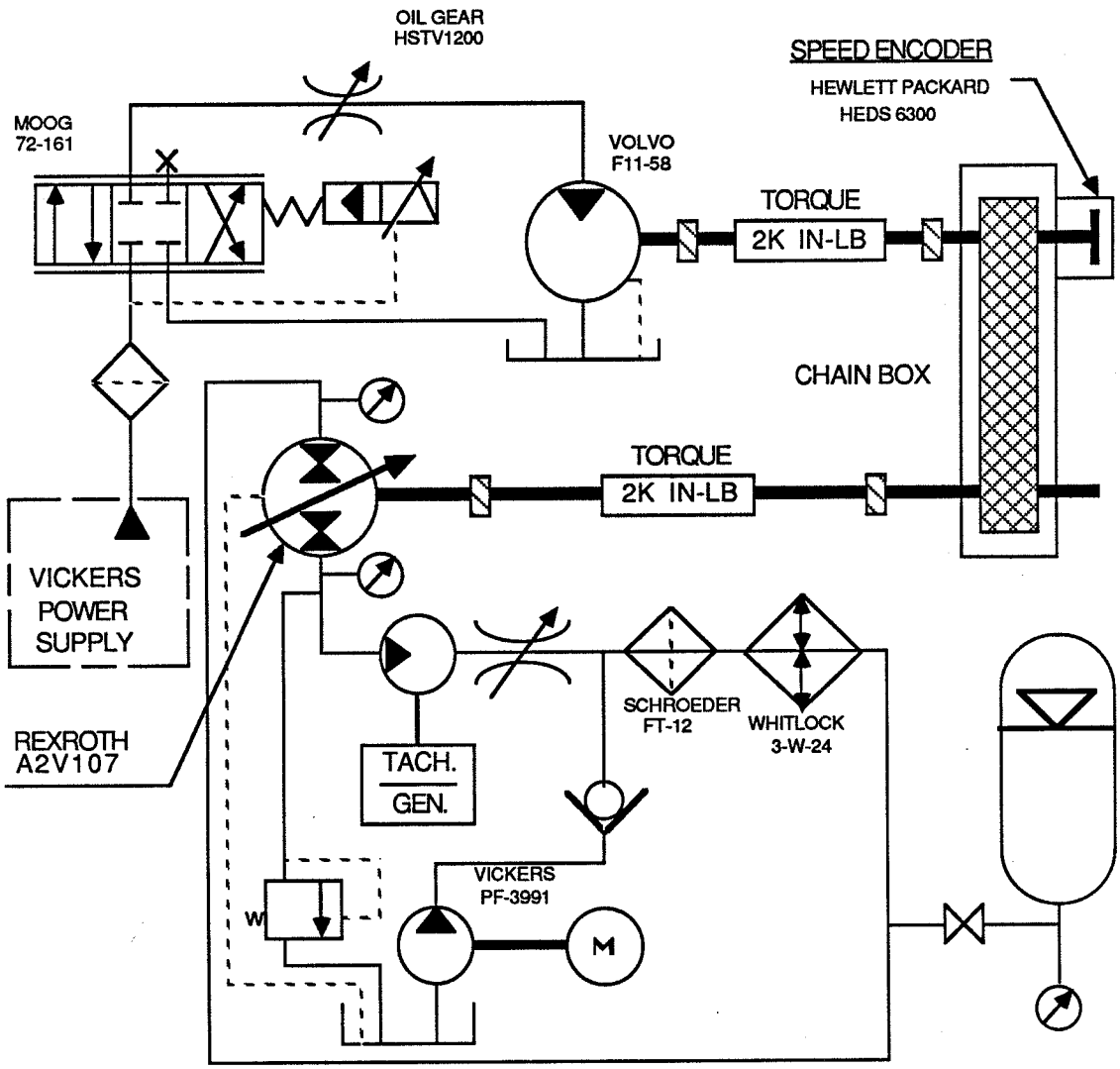


FIGURE 4.5: HYDRAULIC CIRCUIT - EFFICIENCY TESTING

records the input torque. Two pressure transducers record inlet and outlet pump pressure. A flow meter (a hydraulic motor) measures the output (high pressure) pump flow. This is followed by a variable orifice for setting the outlet pump pressure. The speed was varied using controls on the Vickers power supply and the servovalve.

The test data obtained are shown in Tables 4.4-4.6 in Appendix B. Comparing these data with those supplied by the manufacturer of the unit (Appendix C), it is seen that the measured mechanical and volumetric efficiencies are consistently higher. Also, a few volumetric efficiencies appear to be over 100%. There are several possible explanations for this. The data from Rexroth are based on an oil viscosity of 36 cSt. Since the tests were run at temperatures between 115 and 130°F (46.1 and 54.4°C) our viscosity was from 12 to 24 cSt. A lower viscosity tends to increase mechanical efficiency and decrease volumetric efficiency. To get true pump efficiencies there should be no boost pressure (inlet pressure = 0 psig). Our system had a boost pressure of 85 to 110 psig (586 to 758 kPa) which is approximately the pressure in the pressurized reservoir. The flow meter, a hydraulic motor, generally would be fairly accurate. Volumetric efficiency for no load is often near 99 percent. It seemed, though, that we were getting a greater case drain flow than normal: 0.25 to

0.32 gpm (0.95 to 1.21 l/min) at 3,000 to 5,000 psig (20.7 to 34.5 MPa). Also, since we were concerned with low displacement efficiency, our flow rates were generally small. For slow speeds the motor speed was not always constant. The tachometer reading is also questionable at these speeds. In addition volumetric efficiency drops off at slower speeds. Finally, the data may have been skewed. The five analog signals were sampled over a period of about 1.6 seconds. Then they were displayed on the screen. There was perhaps a 5 second delay before the speed (binary) was sampled. To reduce or eliminate many of these sources of error in subsequent testing the following was incorporated: the "motor" flowmeter was replaced with a turbine-type flowmeter with much greater accuracy. The optical encoder interface was redesigned to provide accuracy of 0.1 rpm. The computer program was rewritten to reduce skewing error by sampling the speed immediately after sampling the analog signals.

4.6 Chain Drive Efficiency

The chain drive unit on the test stand was incorporated in the system in order to allow for more versatility. Its design was such that variable backlash could be introduced in order to study these effects on the system and control strategies. In addition, the chain box

was designed in such a way that conversion from a dual P/M system to a single P/M system was fairly rapid and possible with existing components. A chain drive is not needed for an actual hybrid system in an automobile, however, since the unit was an integral part of the test stand, its efficiency was also determined.

The chain drive consists of a 75-link 2-inch-wide Morse silent chain, a 21-tooth drive sprocket, and a 38-tooth driven sprocket. The shafts are supported by four ball bearings. The housing is sealed by 4 oil seals, and spray lubrication is provided on all bearings and on the chain.

For the purposes of determining chain drive efficiency, the input and output torque were measured and recorded during the pump efficiency testing. The ratio of output torque to input torque determined the chain drive efficiency. The results are listed in Table 4.7 of Appendix B and plotted in Figure 4.6. From these results it is evident that the efficiency is mainly a function of torque.

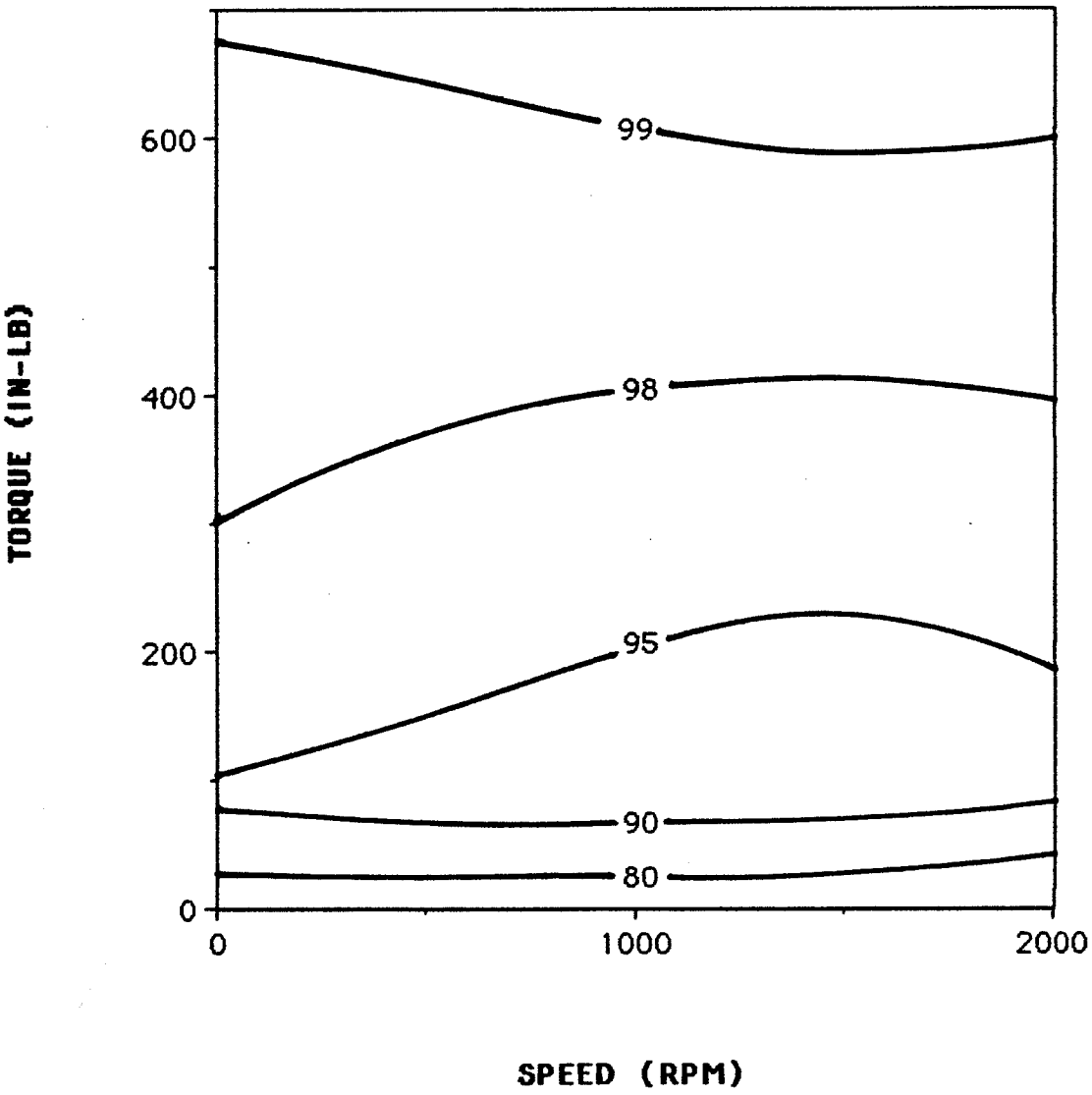


FIGURE 4.6: CHAIN BOX EFFICIENCY

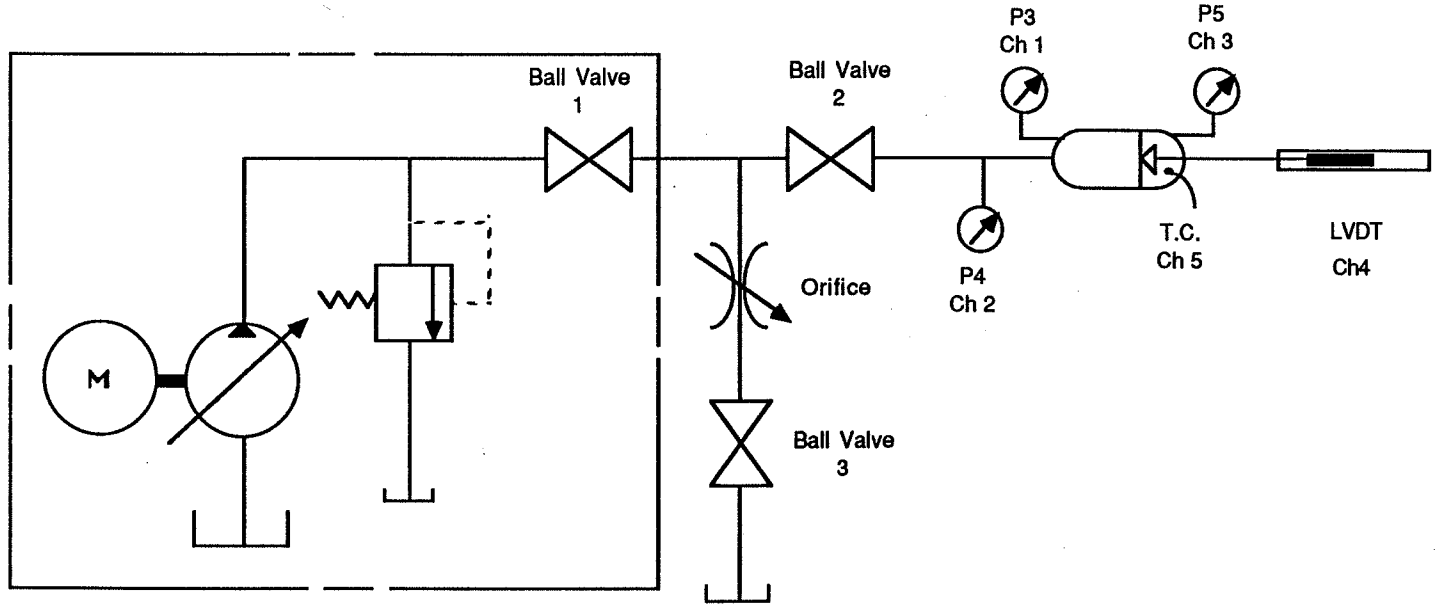
5.0 ACCUMULATOR EFFICIENCY TESTING

5.1 Introduction

This section presents results of accumulator test data used to determine accumulator efficiency. One of the two Parker 2.2 gallon (8.2 liters) piston-type accumulators rated at 3000 psig (20.7 MPa) was used in the tests. During the charging and discharging of the accumulator, five parameters were recorded: accumulator gas pressure, accumulator oil pressure, oil pressure at the inlet to the accumulator, accumulator gas temperature, and the piston position. Data were taken for different rates of charging and discharging, various holding times, and with the gas side of the accumulator containing no foam, half-full of foam, and full of foam. Tests were conducted with foam since prior studies (12) have shown foam increases an accumulator's efficiency.

5.2 Test Set-Up

The circuit used for these tests is shown in Figure 5.1. Hydraulic power was provided by a 50-hp (37.3-kW) unit manufactured by the Oilgear Company. It uses two Hydura type "PVW" variable delivery pumps (swashplate

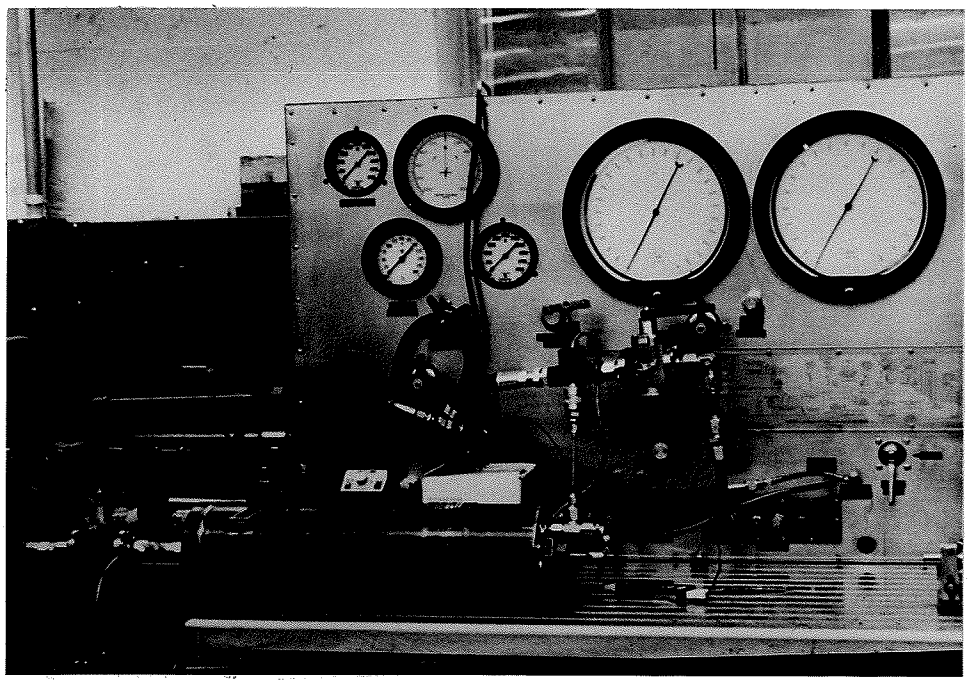


Oilgear Power Supply

FIGURE 5.1: HYDRAULIC CIRCUIT - ACCUMULATOR TESTING

type). This power supply has a relief valve which was set to 3100 psig (21.4 MPa) and an Apollo ball valve (ball valve 1) which controlled the output flow. The output of the power supply was connected to the accumulator by several feet of hose and tubing and another ball valve (ball valve 2). This ball valve was manufactured by Hydromatics, Inc. and has 3/8 inch SAE ports. As mentioned above, the accumulator tested was a 2.2 gallon (8.2 liter) piston-type manufactured by Parker, model no. A6RO462B69E. Appendix D contains the manufacturer's data on this particular accumulator. To discharge the accumulator, a line with a variable orifice and a ball valve (ball valve 3) was included in the circuit. The orifice is manufactured by Marsh Instrument Company, and the ball valve is the same style as the second valve listed above. The discharge line ran into the Oilgear power supply reservoir and had about 20 psig (137.9 kPa) backpressure while the power supply was running. Ball valves were used because they were quick opening and leaked very little. The actual test components can be seen in Photograph 5.1.

The accumulator contained foam during several of the tests. The accumulator was filled with 1.68 lbs (762 grams) of foam consisting of 20 disks, each 1-in (2.54-cm) thick. The first two disks near the piston were reduced in diameter to fill the piston cavity. The remaining 18 disks



PHOTOGRAPH 5.1: ACCUMULATOR EFFICIENCY TEST

were used to fill the bore of the accumulator. These disks did not meet flush with the end cap and had to be compressed approximately 1/4 in (6.4 mm) when the end cap was installed.

After running the full-foam tests, the foam was removed and was found to weigh 1.69 lbs (765 grams). For the half-foam tests, disks 1 through 11 were removed leaving a total of 0.77 lbs (351 grams) of foam in the accumulator. The thermocouple was located in the same position as for the full foam tests. For these tests, however, the thermocouple

was located at the foam/gas surface rather than between two foam disks.

5.3 Instrumentation

Instrumentation included three pressure transducers, two thermocouples, one thermometer, and one LVDT. The pressure transducers were manufactured by Schaevitz, type P2503-0001, and were rated at 0 to 6000 psig (0 to 41.4 MPa). Their outputs were amplified by Himmelstein transducer amplifiers Model 6-201, which had an output of 0-5 volts. These transducers were calibrated using a dead-weight pressure tester. The calibration was checked every day and drifted by no more than 5 psig (34.5 kPa). The two thermocouples were copper-constantan. The one in the accumulator was made of 30-gauge wire. It was connected to an Omega thermocouple amplifier, Model Omni Amp 1. The nitrogen gas thermocouple was located at a position 8.75-in (22.2-cm) from the end cap and 1.5-in (3.81-cm) from the center of the accumulator's bore on the nitrogen side of the piston. The oil thermocouple was located on the inlet to the accumulator. It was made with 24-gauge wire soldered directly onto the 1/2-in (1.27-cm) diameter steel inlet tube about 16-in (40.6-cm) from the end of the accumulator. The reservoir oil temperature was measured using a thermometer.

The piston position was measured using a Schaevitz LVDT model 10000HR with a range of ± 10 inches (25.4 cm) and 0.24% linearity. A 1/4-in (6.4-mm) diameter rod connected the accumulator piston to the LVDT core. The LVDT output signal was conditioned using a Himmelstein LVDT amplifier model 6-203A, which has an output of -5 to +5 volts. The LVDT was calibrated using a vernier caliper. The calibration was checked daily.

Five of the signals were continuously sampled during each test using the Isaac 41, a 12-bit A-D data acquisition system manufactured by Cyborg Corporation. This system was controlled by an IBM computer, Model PC.

5.4 Test Procedure

The general test procedure is discussed first. Certain tests had slight variations which will be explained later.

The power supply pump displacement was set to provide the desired flow rate, which determined the accumulator charging time (fast or slow). The power supply relief valve was set to 3100 psig (21.4 MPa). At the start of the test, valves 1 and 3 were closed and valve 2 was open. Valve 1 was then opened, allowing oil to flow into the accumulator. When the accumulator pressure reached about 3100 psig (21.4 MPa), the charge was held for 0, 15, 50, 100,

or 200 seconds. With zero holding time, valve 3 was opened and valve 1 closed simultaneously. For the other holding times, valve 2 was closed upon reaching 3100 psig (21.4 MPa). Then valve 1 was closed and valve 3 was opened. Thus, there was a 3100 psig (21.4 MPa) pressure differential across valve 2. Some leakage across the valve may have occurred, which would be indicated by a drifting in the LVDT position during the holding time. After the appropriate holding period, valve 2 was opened. The discharge time was determined by the setting of the orifice. After the accumulator was completely discharged, the Oilgear power supply was turned off. There was a minimum of five minutes between test runs to allow the accumulator temperature to stabilize somewhat.

An extensive amount of testing was performed on the accumulator and data was gathered for a total of 45 charging/discharging cycles. The main parameters varied were the precharge pressure, charge rate (fast or slow), holding time, discharge rate (fast or slow), volume of foam (full, half, or none), and maximum piston displacement allowed. A matrix of testing was established to cover changes in all of the variables, while at the same time not requiring testing all of the combinations possible. Table 5.1 lists all of the tests performed.

TABLE 5.1: ACCUMULATOR EFFICIENCY TEST IDENTIFICATION

TEST NUMBER	OUTPUT FILENAME	DATE 1986	FOAM (GRAMS)	INLET TUBE WALL ·F	RESERVOIR TEMP. ·F
1	5FF0	5-22	0	101	100
2	5FF15	5-22	0	90	98
3	5FF50	5-22	0	97	98
4	5FF100	5-22	0	98	100
5	5FF200	5-22	0	96	99
6	5FS0	5-23	0	96	101
7	5FS50	5-23	0	96	101
8	5FS100	5-23	0	96	103
9	5SS0	5-23	0	103	104
10	5SS50	5-23	0	102	104
11	5SS100	5-23	0	100	104
12	5SF0	5-23	0	104	103
13	5SF50	5-23	0	103	103
14	5SF100	5-23	0	101	102
15	5FS15	5-23	0	98	104
16	15FF0	5-27	0	100	108
17	15FF15	5-27	0	100	106
18	15FF50	5-27	0	100	107
19	15FF100	5-27	0	100	109
20	15FF200	5-27	0	99	109
21	15FS0	5-27	0	99	107
22	15FS15	5-27	0	99	106
23	15FS50	5-27	0	95	106
24	15FS100	5-27	0	95	106
25	15SS0	5-27	0	105	110
26	15SS50	5-27	0	102	110
27	15SS100	5-27	0	104	113
28	15SF0	5-27	0	112	115
29	15SF50	5-27	0	111	113
30	15SF100	5-27	0	107	112
31	F5FF0	5-28	762	98	100
32	F5FF100	5-28	762	96	101
33	F5FS100	5-28	762	98	101
34	F5FC	5-28	762	98	101
35	F15FF100	5-28	762	95	99
36	F15FC	5-28	762	94	100
37	F15FS100	5-28	762	96	101
38	F15FFL	5-28	762	99	106
39	F5FFL	5-28	762	101	105
40	H15FF0	5-29	351	101	106
41	H15FF100	5-29	351	102	109
42	F0FF12A	6-4	765	90	99
43	F0FF12B	6-4	765	91	97
44	FAFF12A	6-4	765	91	97
45	FAFF12B	6-4	765	91	97

TABLE 5.1: TEST IDENTIFICATION CONTINUED

TEST NUMBER	SAMPLING RATE (HZ)	CHARGE RATE	DISCHARGE RATE	HOLD TIME (SEC)	PRECHARGE PRESSURE (PSIG)
1	30	FAST	FAST	0	500
2	12	FAST	FAST	15	500
3	9	FAST	FAST	50	500
4	5	FAST	FAST	100	500
5	2	FAST	FAST	200	500
6	6	FAST	SLOW	0	500
7	5	FAST	SLOW	50	500
8	4	FAST	SLOW	100	500
9	4	SLOW	SLOW	0	500
10	3	SLOW	SLOW	50	500
11	3	SLOW	SLOW	100	500
12	5	SLOW	FAST	0	500
13	5	SLOW	FAST	50	500
14	3	SLOW	FAST	100	500
15	5	FAST	SLOW	15	500
16	15	FAST	FAST	0	1500
17	12	FAST	FAST	15	1500
18	9	FAST	FAST	50	1500
19	5	FAST	FAST	100	1500
20	2	FAST	FAST	200	1500
21	6	FAST	SLOW	0	1500
22	5	FAST	SLOW	15	1500
23	5	FAST	SLOW	50	1500
24	4	FAST	SLOW	100	1500
25	4	SLOW	SLOW	0	1500
26	3	SLOW	SLOW	50	1500
27	3	SLOW	SLOW	100	1500
28	5	SLOW	FAST	0	1500
29	5	SLOW	FAST	50	1500
30	3	SLOW	FAST	100	1500
31	4	FAST	FAST	0	500
32	4	FAST	FAST	100	500
33	3	FAST	SLOW	100	500
34	90	FAST	----	---	500
35	4	FAST	FAST	100	1500
36	90	FAST	----	---	1500
37	3	FAST	SLOW	100	1500
38	4	FAST	FAST	100	1500
39	4	FAST	FAST	100	500
40	10	FAST	FAST	0	1500
41	5	FAST	FAST	100	1500
42	3	FAST	FAST	120	0
43	3	FAST	FAST	120	0
44	3	FAST	FAST	120	20
45	3	FAST	FAST	120	20

5.5 Results

Typical results are shown in Figures 5.2 through 5.6 for a test with no foam and in Figures 5.7 through 5.11 for a test with the accumulator full of foam. Each of the tests had an accumulator precharge pressure of 500 psig (3.45 MPa) and consisted of a fast charge followed by a 100 second holding period and then a fast discharge of the accumulator. Referring again to Figure 5.1, the variable corresponding to the channel number can be determined.

As stated earlier, the inclusion of the foam causes the nitrogen gas to behave more isothermally during charging and discharging. This can be seen by comparing Figures 5.6 and 5.12. Without foam the temperature in the accumulator varies from just under 400°F (204°C) to approximately -90°F (-67.8°C). This causes the gas pressure in the accumulator to drop from 3,150 psig (21.7 MPa) to 2,000 psig (13.8 MPa) as seen in Figure 5.4. Inclusion of foam limits the maximum temperature to 142°F (61.1°C) and the minimum to 85°F (29.4°C). The result is the pressure during the holding period drops by only about 200 psig (1.38 MPa)(see Figure 5.9) instead of the previous 1,150 psig (7.9 MPa).

Not only does the inclusion of the foam help to minimize thermal losses in the accumulator, it also allows for more energy to be stored. This can be seen by

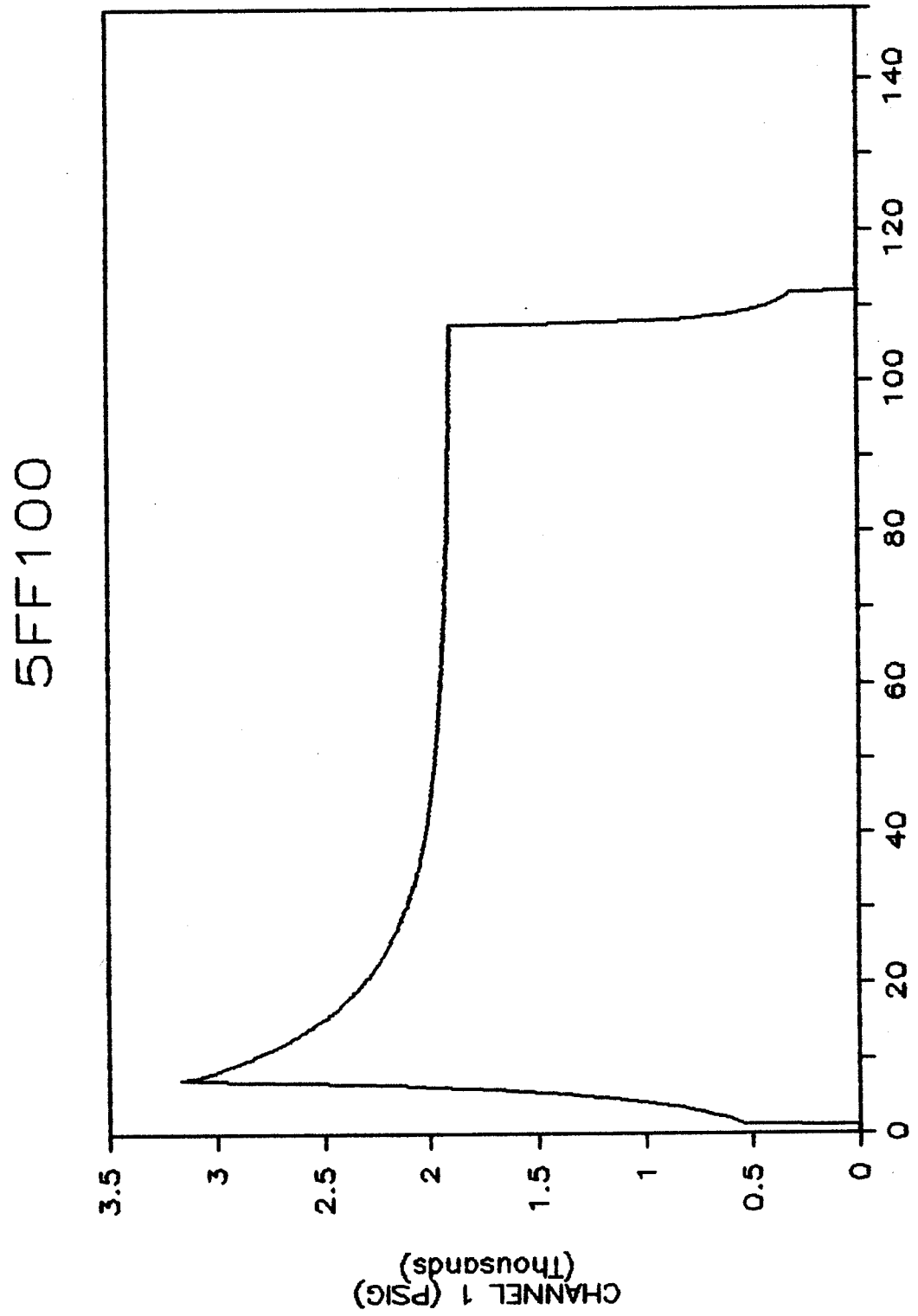


FIGURE 5.2: ACCUMULATOR OIL PRESSURE

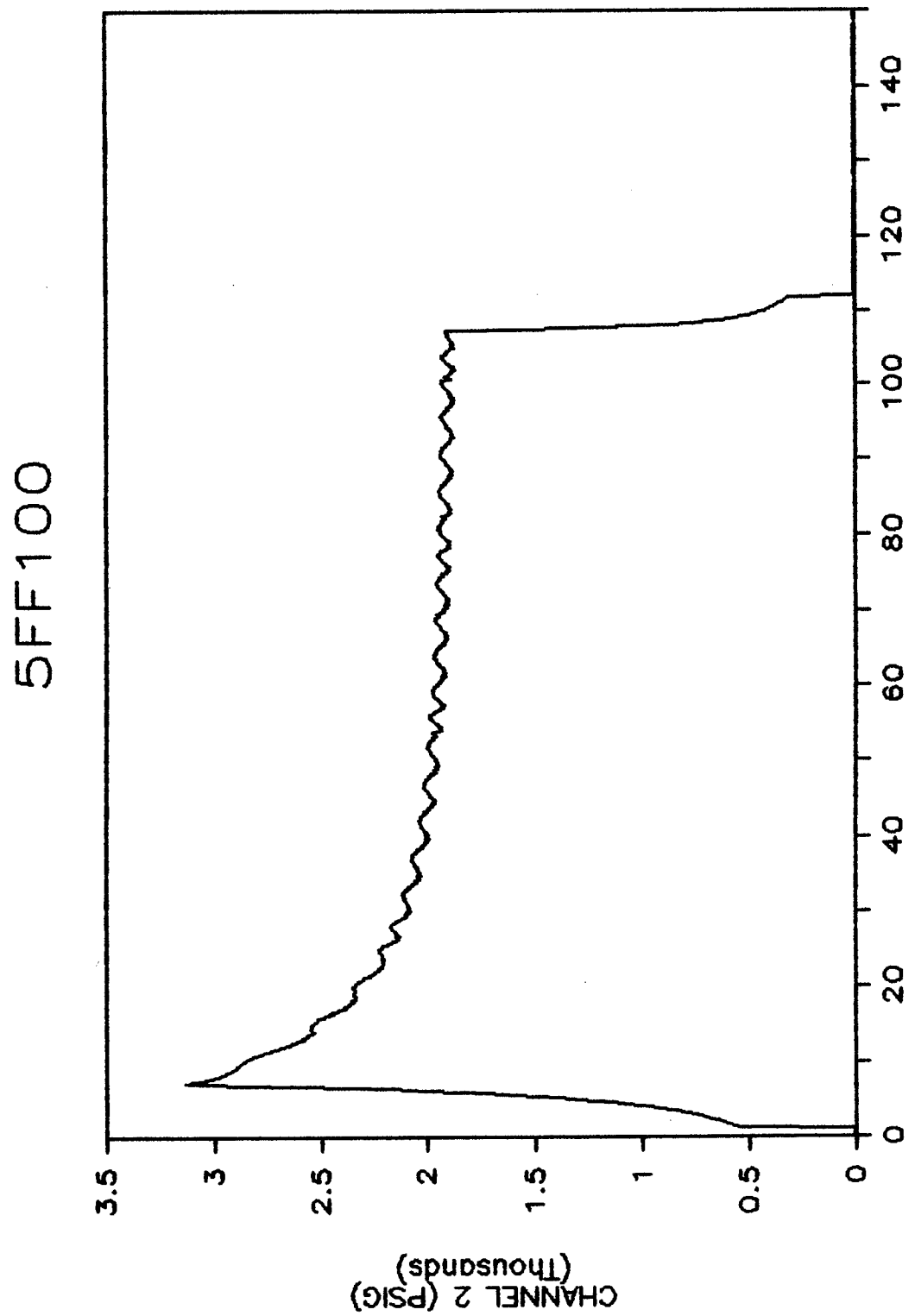


FIGURE 5.3: SUPPLY LINE OIL PRESSURE

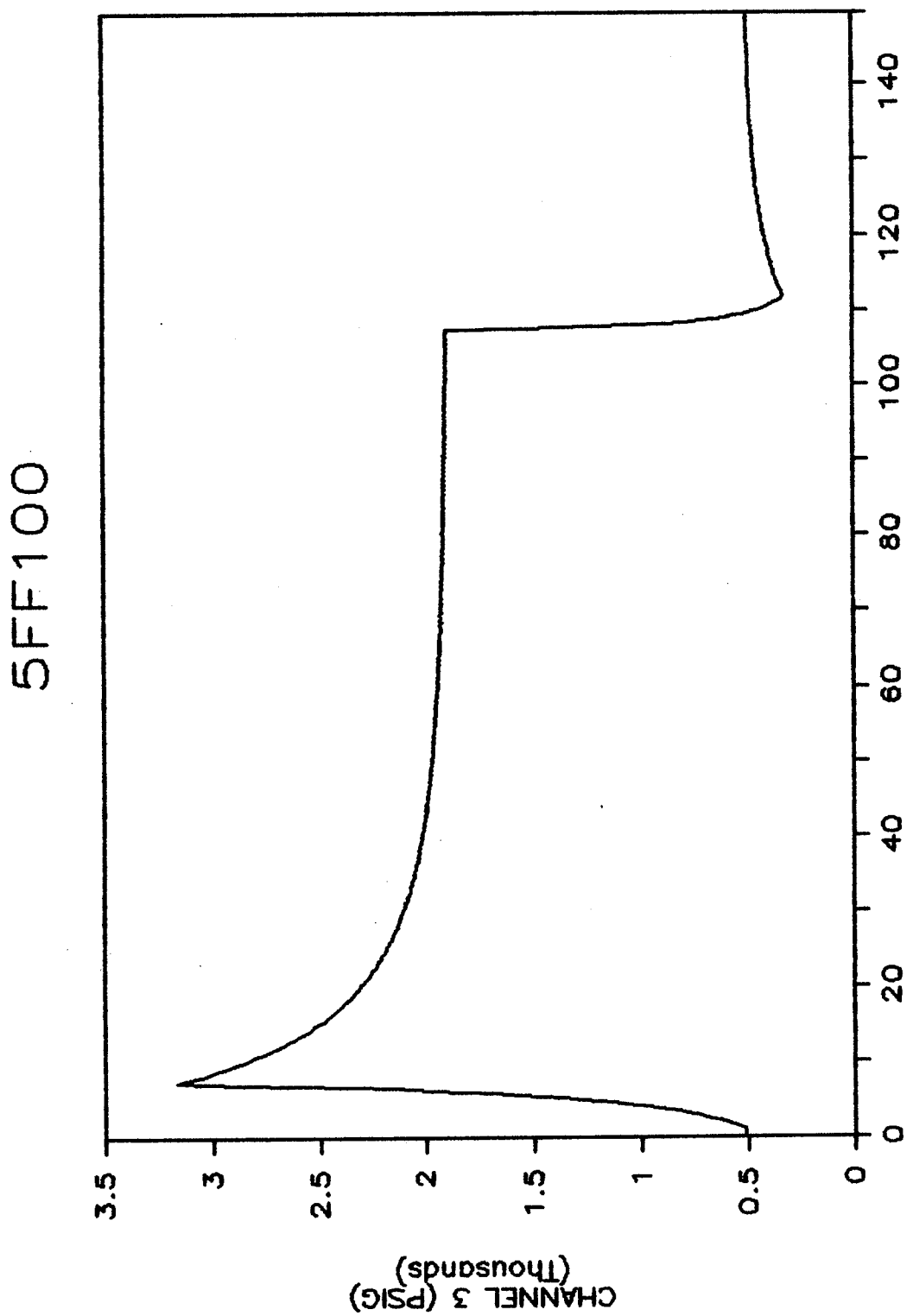


FIGURE 5.4: ACCUMULATOR GAS PRESSURE

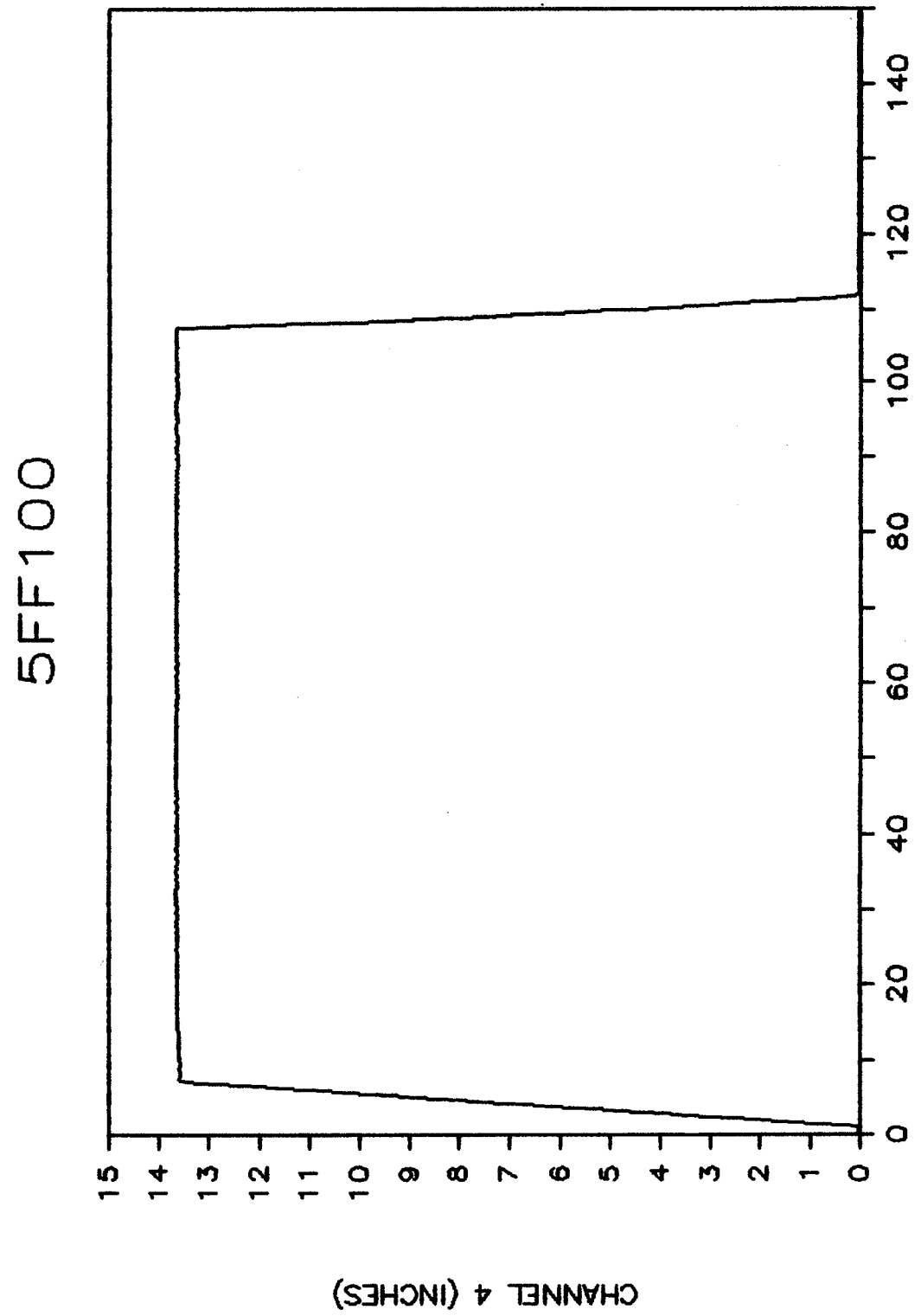


FIGURE 5.5: ACCUMULATOR PISTON POSITION

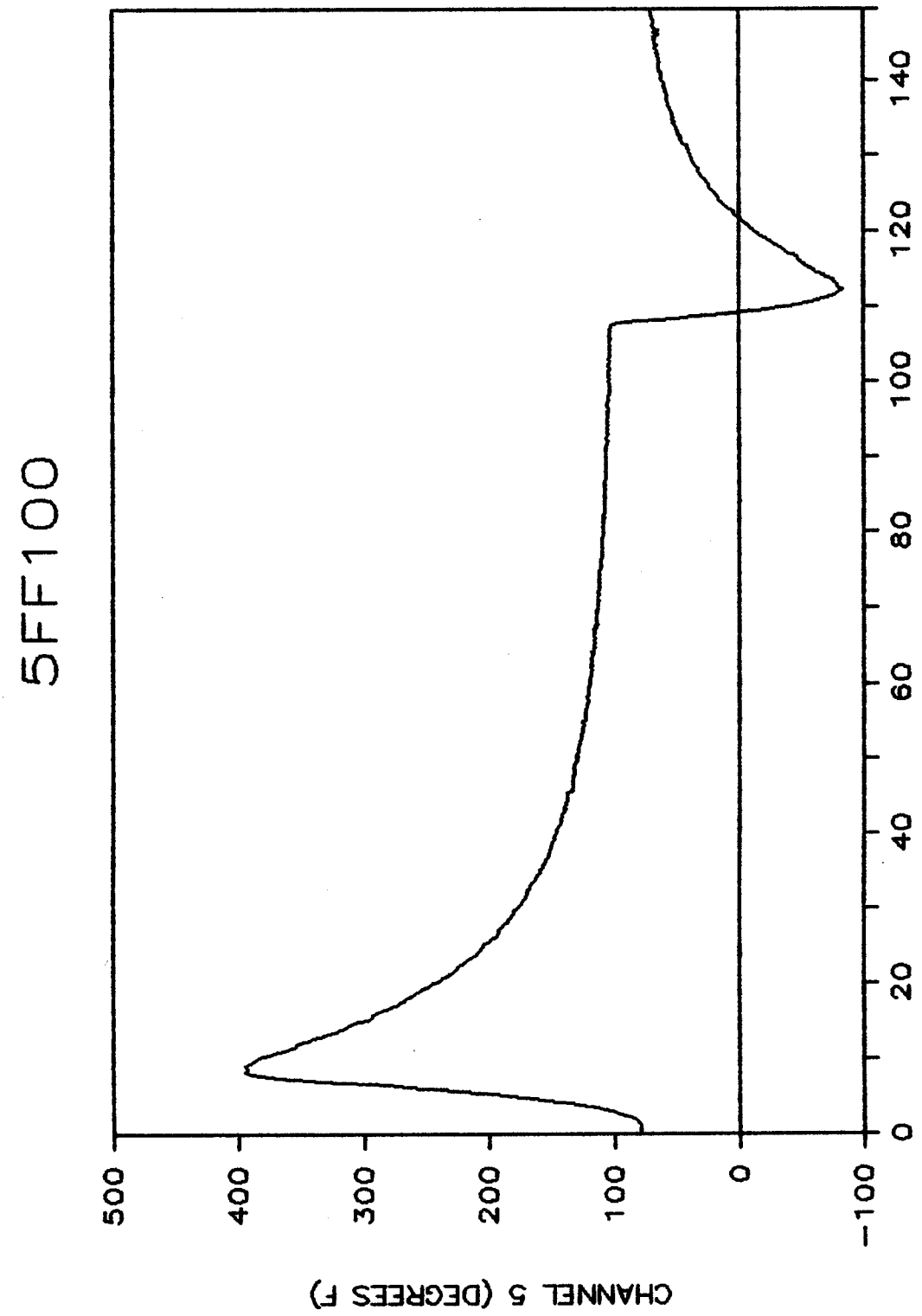


FIGURE 5.6: ACCUMULATOR GAS TEMPERATURE

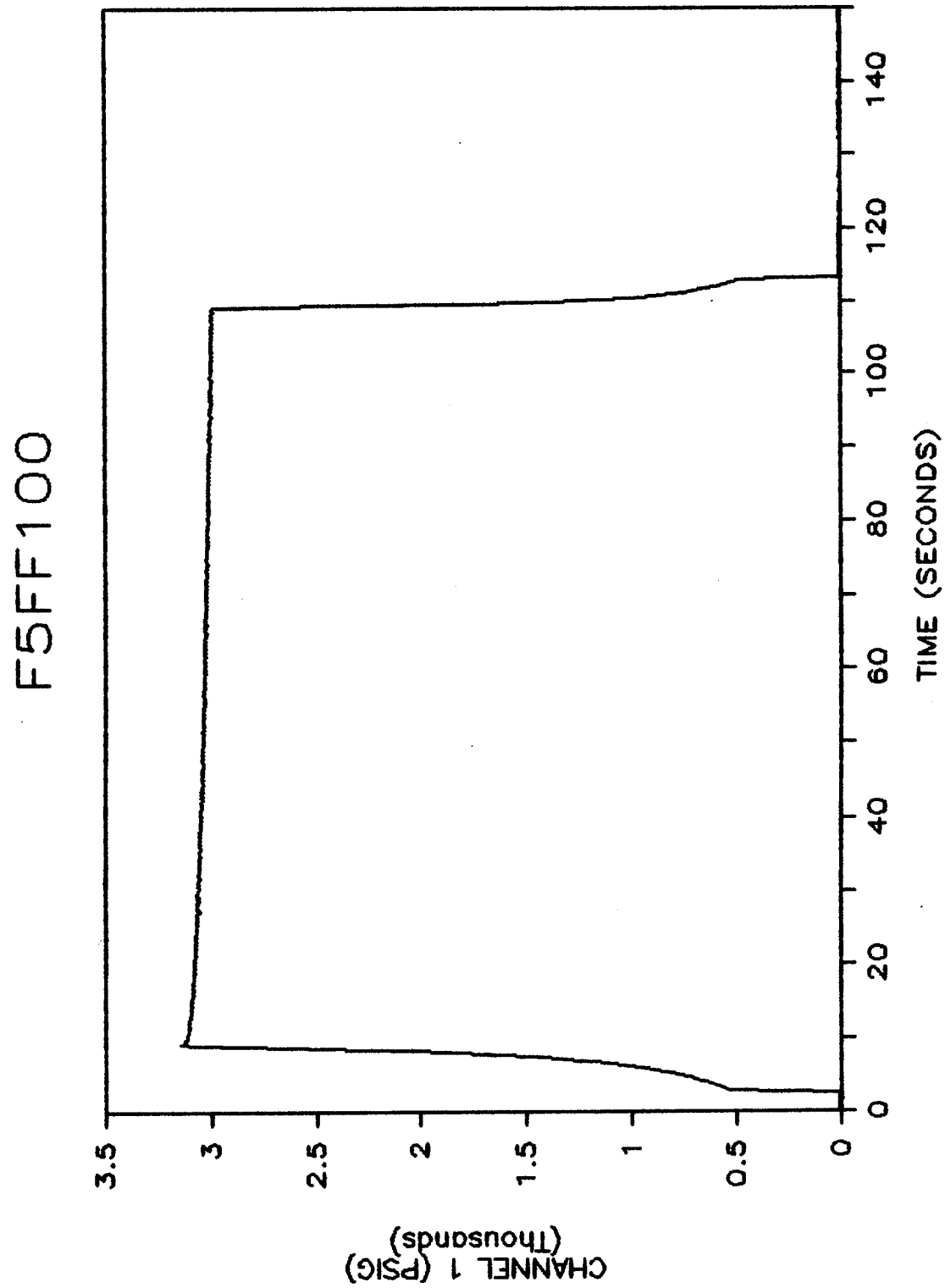


FIGURE 5.7: FOAM FILLED ACCUMULATOR OIL PRESSURE

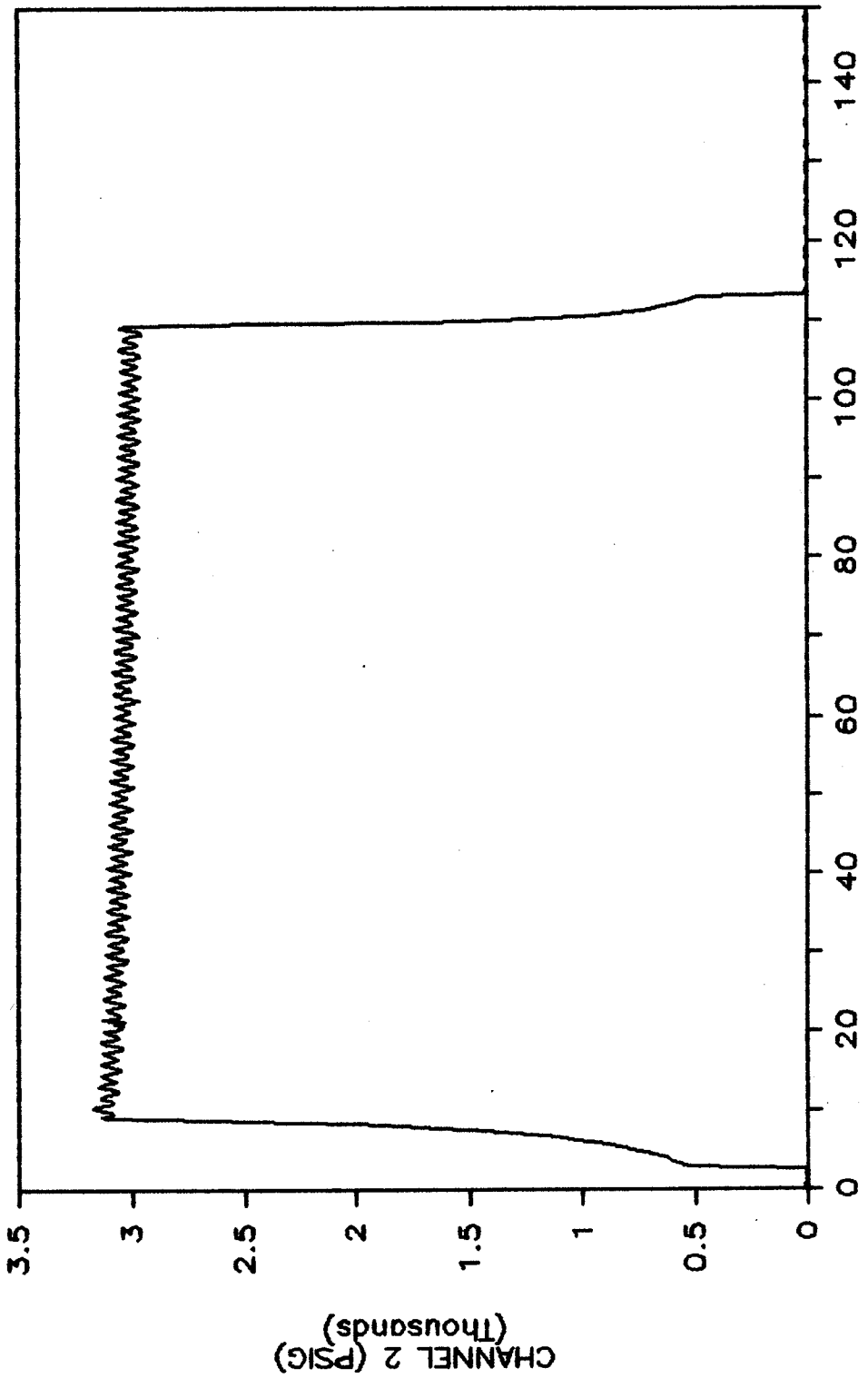


FIGURE 5.8: SUPPLY LINE OIL PRESSURE

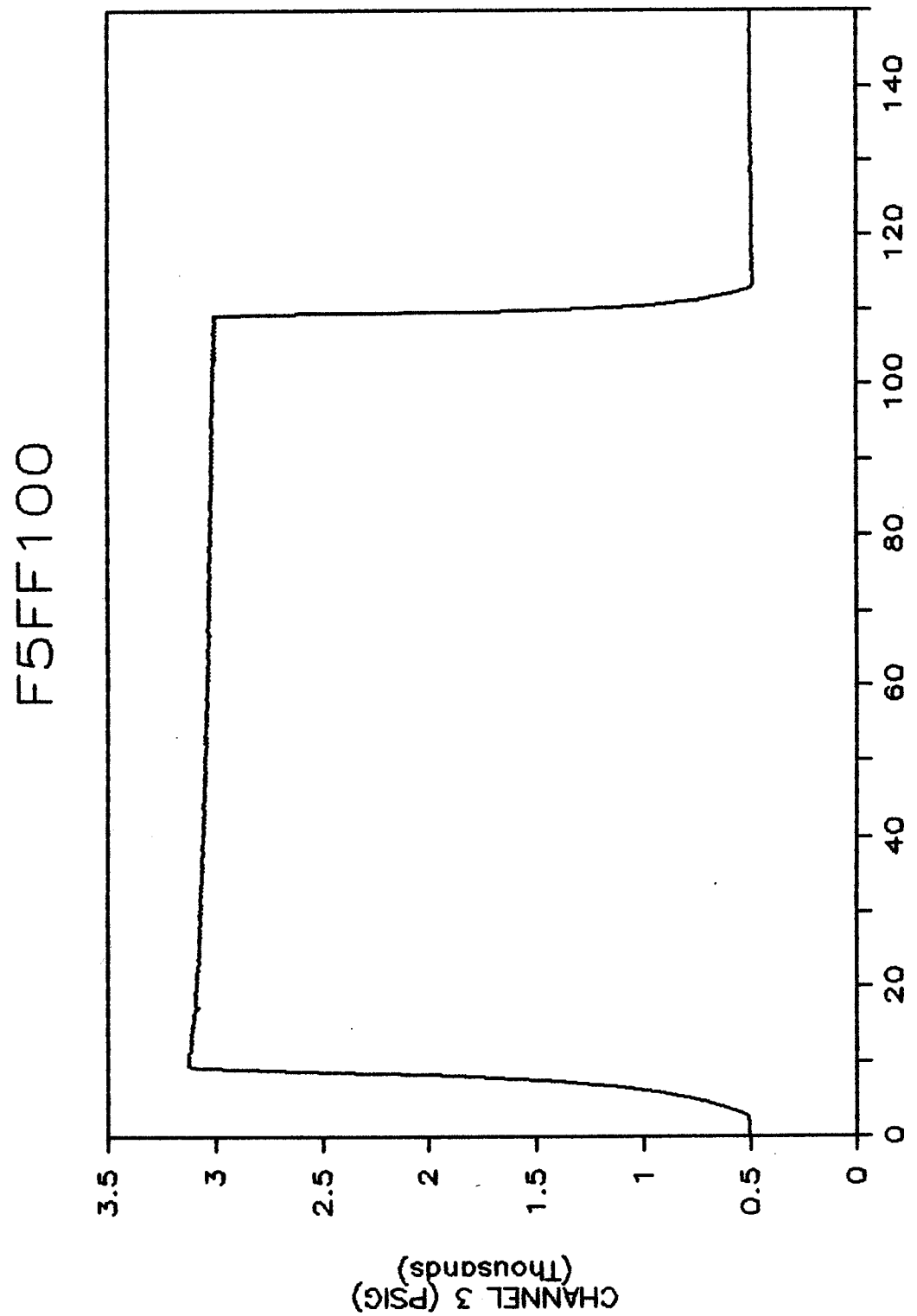


FIGURE 5.9: FOAM FILLED ACCUMULATOR GAS PRESSURE

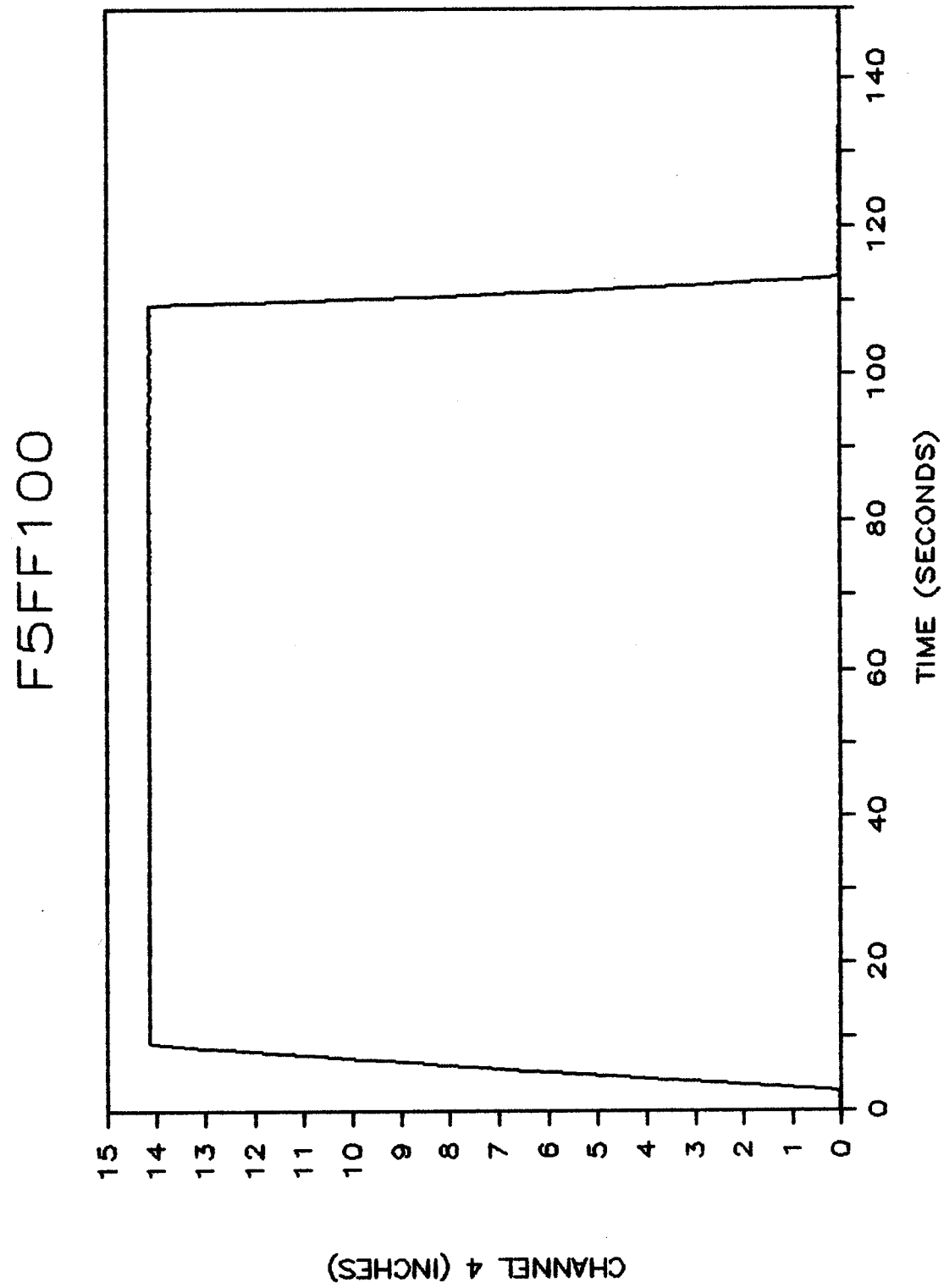


FIGURE 5.10: FOAM FILLED ACCUMULATOR PISTON POSITION

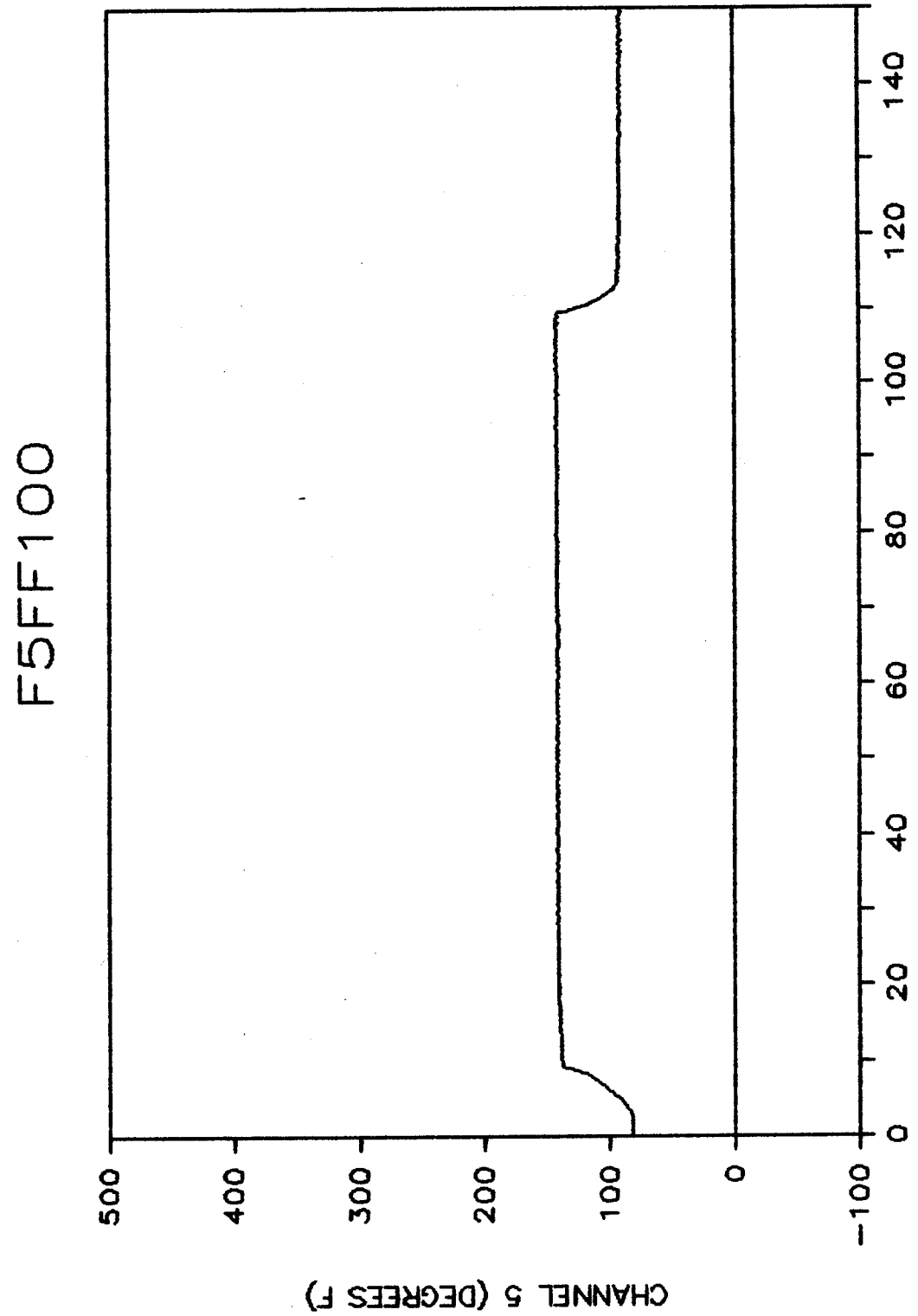


FIGURE 5.11: FOAM FILLED ACCUMULATOR GAS TEMPERATURE

comparing Figures 5.5 and 5.10. Introduction of the foam increases the maximum displacement from 13.6 inches (34.5 cm) to 14.1 inches (35.8 cm). This results in the accumulator with foam included to store about 4 percent more energy than its counterpart without foam.

The specific efficiency calculations for the data obtained was performed by A. Pourmovahed and are presented in: "Experimental Evaluation of Hydraulic Accumulator Efficiency With and Without Elastomeric Foam"(15). The results of this analysis are included in Tables 5.2 - 5.4. The data are also presented in a graphical form in Figures 5.12 - 5.15. Figure 5.13 shows that the inclusion of foam in the nitrogen side of an accumulator significantly increases its efficiency. The foam does, however, increase the frictional losses of the accumulator slightly as seen in Figure 5.14.

TABLE 5.2

RESULTS FOR TESTS WITH 3.45 MPa (500 psig) PRECHARGE PRESSURE, FAST CHARGE AND FAST DISCHARGE
Piston Stroke = 35 cm (13.7 in)

TEST No.	Foam Mass (grams)	Maximum Gas Pressure (MPa, abs)	Holding Time (s)	Energy Input (kJ)	Thermal Loss (%)[5]	Frictional Loss (%)	Accumulator Efficiency (%)
1	0	22.08	0	49.7	7.7	2.4	90.0
2	0	22.06	14.5	51.2	30.7	2.4	66.9
3	0	22.01	48.9	54.4	36.6	2.8	60.6
4	0	21.92	100.0	53.0	38.9	1.7	59.5
5	0	21.98	200.5	52.1	39.9	1.7	58.5
31	762[6]	18.94	0	48.1	0.1	4.3	95.6
39	762	18.94	100.5	47.1	1.1	3.7	95.2

5 Percent of energy input to the accumulator

6 The foam occupied 100% of the gas-side volume.

TABLE 5.3

EFFECT OF CHARGE AND DISCHARGE TIME
3.45 MPa (500 psig) PRECHARGE PRESSURE

TEST No.	Charge/Discharge (Holding Time, s)	Max. Gas Pressure (MPa, abs)	Energy Input (kJ)	Thermal Loss (%)	Frictional Loss (%)	Accumulator Efficiency (%)
6	fast/slow (0)	21.96	49.8	14.1	3.3	82.6
8	fast/slow (100.0)	21.93	54.2	30.5	2.8	66.7
15	fast/slow (15.2)	21.99	50.8	26.8	2.3	70.9
33	fast/slow (foam) (100.3)	21.81	52.0	0.5	4.1	95.3
9	slow/slow (0)	21.04	52.8	18.4	4.3	77.4
10	slow/slow (51.7)	21.04	55.4	24.3	4.3	71.4
12	slow/fast (0)	20.76	52.7	22.7	5.4	71.9
13	slow/fast (50.0)	21.15	54.9	34.7	4.5	60.8
14	slow/fast (100.0)	20.96	56.1	34.0	5.0	61.1

TABLE 5.4

RESULTS FOR TESTS WITH 10.35 MPa (1500 psig) PRECHARGE PRESSURE, FAST CHARGE AND FAST DISCHARGE
Piston Stroke = 19 cm (7.5 in) for Tests 40,41
Piston Stroke = 17 cm (6.6 in) for all other tests

TEST No.	Foam Mass (grams)	Maximum Gas Pressure (MPa, abs)	Holding Time (s)	Energy Input (kJ)	Thermal Loss (%)	Frictional Loss (%)	Accumulator Efficiency (%)
16	0	21.88	0	43.3	1.5	2.6	95.9
17	0	21.74	14.9	44.3	11.8	3.1	85.1
18	0	21.88	50.4	46.8	17.5	1.1	81.5
19	0	21.86	99.6	45.5	19.9	3.4	76.6
38	762	18.96	98.8	41.4	1.0	3.5	95.6
40	351[7]	22.12	0	48.9	2.4	3.1	94.5
41	351	22.15	99.6	48.8	12.2	2.9	84.9

7 The foam occupied 46% of the gas-side volume at precharge state.

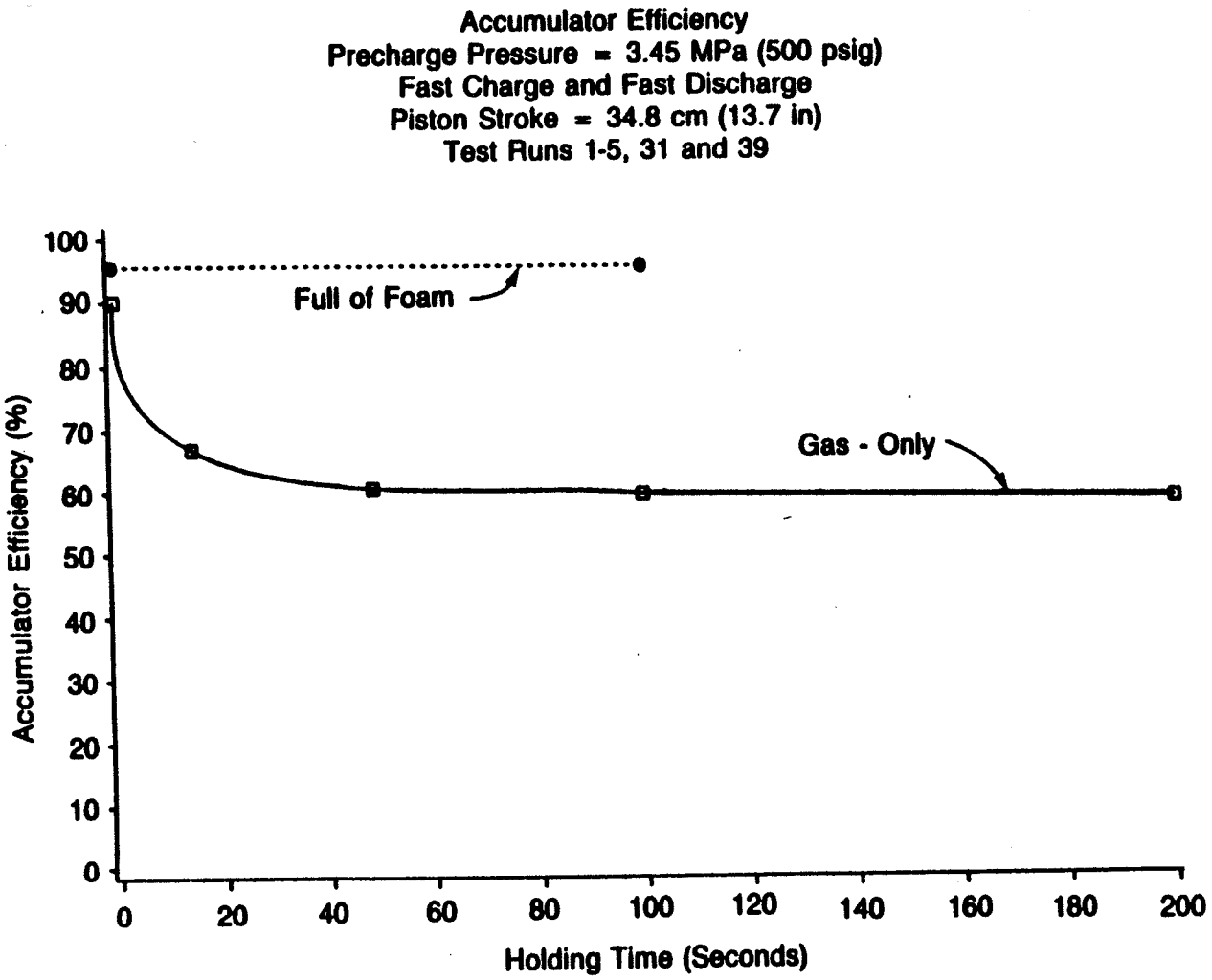


Fig: 5.12 Accumulator efficiency versus holding time for fast charge-hold-fast discharge cycles with and without foam (precharge pressure = 3.45 MPa (500 psig))

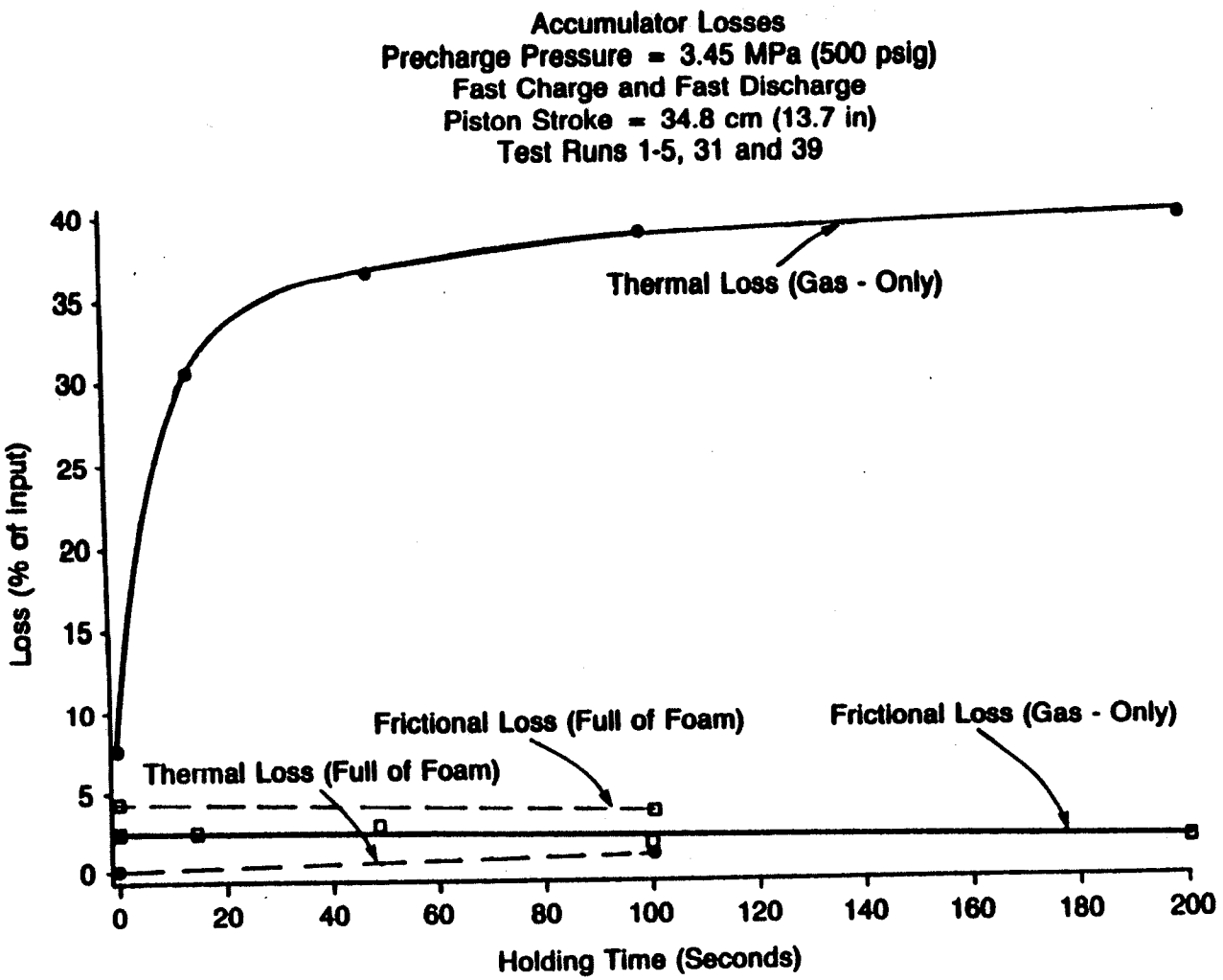


Fig: 5.13 Thermal and frictional losses versus holding time for fast charge-hold-fast discharge cycles with and without foam (precharge pressure = 3.45 MPa (500 psig))

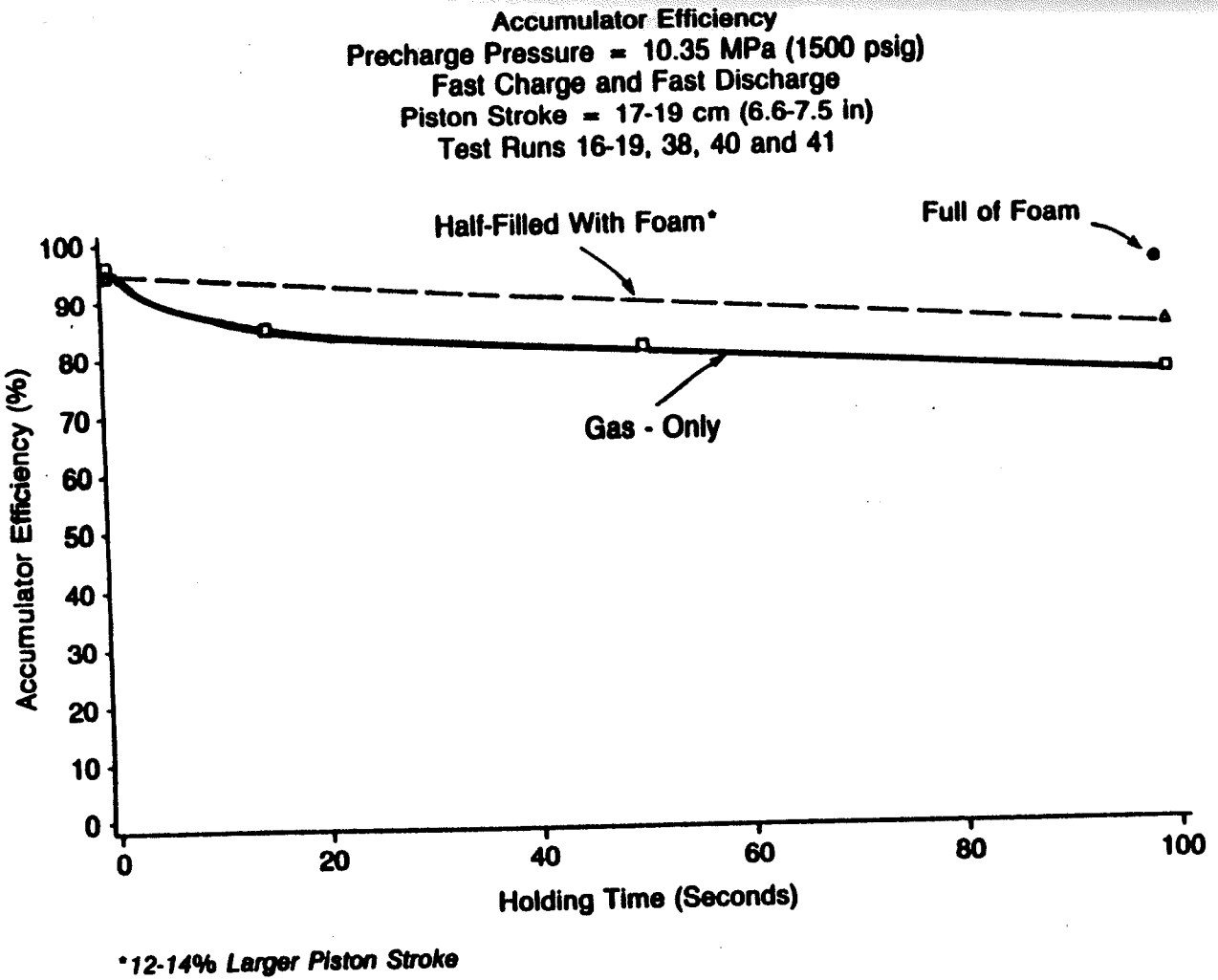


Fig: 5.14 Accumulator efficiency versus holding time for fast charge-hold-fast discharge cycles with the accumulator containing no foam, full of foam and half-filled with foam (precharge pressure = 10.35 MPa (1500 psig))

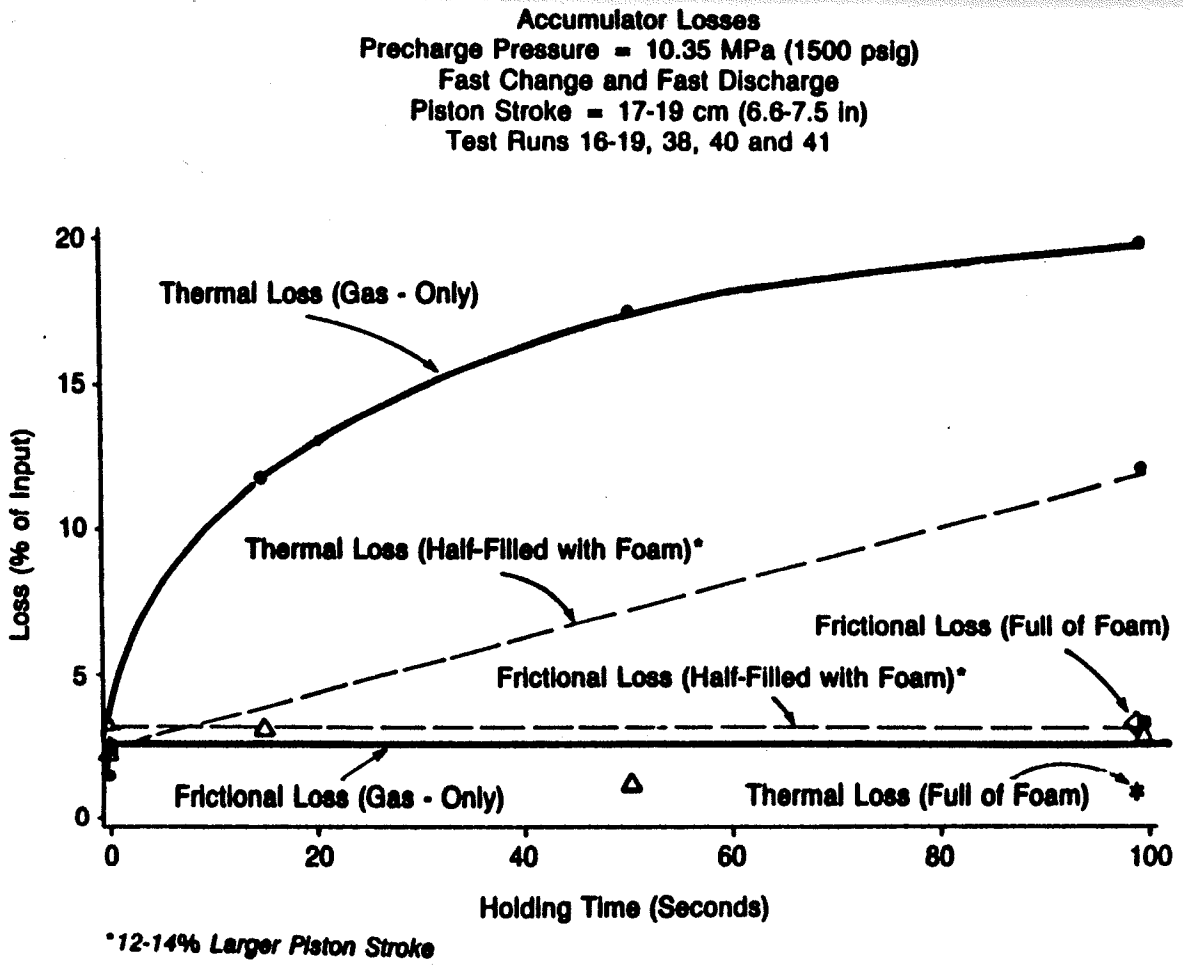


Fig: 5.15 **Thermal and frictional losses versus holding time for fast charge-hold-fast discharge cycles with the accumulator containing no foam, full of foam and half-filled with foam (precharge pressure = 10.35 MPa (1500 psig))**

6.0 REGENERATIVE CYCLING TESTING

6.1 Introduction

This section presents regenerative cycling test data gathered during the experimental hybrid vehicle simulation. Basically the test consisted of charging the accumulators, then using this energy to accelerate the flywheel. When the accumulators were nearly discharged, the Rexroth P/M was displaced "over center" causing the unit to then operate as a pump. This reversed the flow of oil, again storing the energy in the accumulators. The process was continued until all of the energy was dissipated through losses. Both of the test stand's Parker 2.2-gallon (8.2-liters) piston-type accumulators rated at 3000 psig (20.7 MPa) were used in the tests. During the cycling of the energy between the accumulators and the flywheel, a data acquisition computer recorded seven parameters: the P/M position, the piston position in an accumulator, the inlet oil pressure of the pump, both accumulator gas pressures, the torque between the P/M and flywheel, and the flywheel speed. Data was taken for different P/M displacements and for different oil temperatures. Determination of the percent energy lost

during each cycle allowed for efficiency estimates when the hybrid vehicle was operated in the regenerative braking mode.

6.2 Test Set-Up

The circuit used for these tests is shown in Figure 6.1. Power to provide the initial accumulator charge was provided by a 50-hp (37.2-kW) power supply manufactured by Oilgear Corporation. The power supply relief valve was set to approximately 3100 psig (21.4 MPa) to set the maximum pressure in the accumulators when they were being charged. Ball valve 1 and an orifice separated the power supply from the rest of the circuit. As mentioned, two 2.2 gallon (8.2 liters) piston-type Parker accumulators Model A6RO462B69E were used as the ESU. The rest of the circuit consisted of two ball valves and a 10 gallon (37.9 liters) accumulator used as a pressurized reservoir.

The accumulators were both filled with foam during all of the tests. One accumulator contained 1.68 lb (762 grams) of foam and the other contained 1.62 lb (734 grams) of foam.

6.3 Instrumentation

Instrumentation included three pressure transducers, two LVDT's, one torquemeter, and one digital encoder. The pressure transducers were manufactured by Schaevitz, type

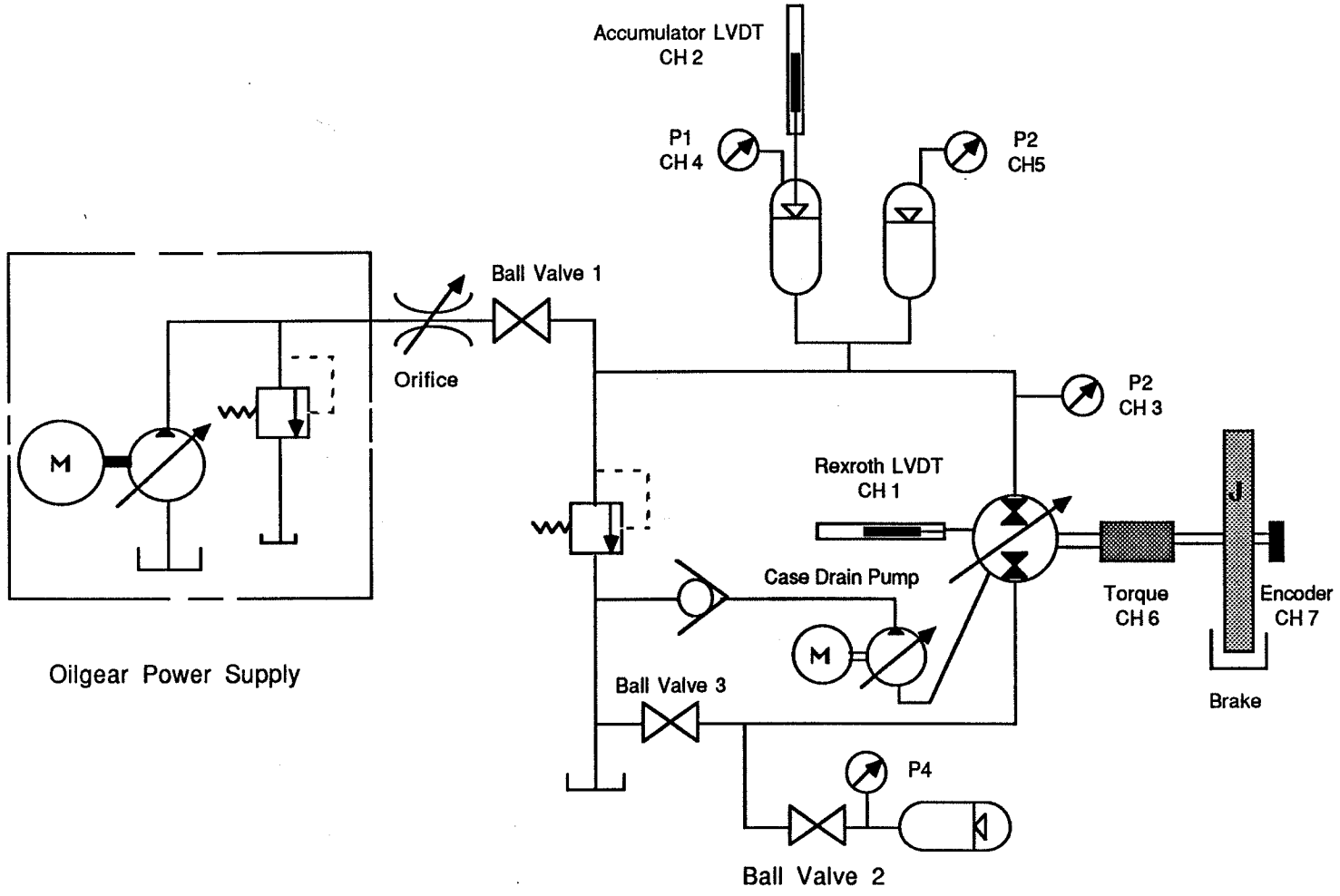


FIGURE 6.1: HYDRAULIC CIRCUIT - REGENERATIVE CYCLING

P2503-0001, and were rated at 0 to 6000 psig (0 to 41.4 MPa). Their outputs were amplified by Himmelstein transducer amplifiers Model 6-201, which have an output of ± 5 volts. These transducers were calibrated using a dead-weight pressure tester.

The accumulator piston position was measured with a Schaevitz LVDT Model 10000HR with a range of ± 10 inches (25.4 cm) and 0.24% linearity. A 1/4 inch (0.64 cm) diameter rod connected the accumulator piston to the LVDT core. The P/M displacement was measured using a Schaevitz LVDT Model 2000HR with a range of ± 2 inches (5.1 cm) and 0.15% linearity. A 1/8 inch (0.32 cm) diameter rod connected the P/M piston block to the LVDT core. The LVDT output signals were conditioned using Himmelstein LVDT amplifiers Model 6-203A, which has an output of ± 5 volts. The LVDT's were calibrated using a vernier caliper.

Flywheel torque was measured using a Himmelstein MCRT torquemeter Model 9-02T with a range of 4000 in-lb (452 N-m) and 0.1% linearity. The torquemeter output signals were conditioned by Himmelstein transducer amplifiers Model 6-201, which have an output of ± 5 volts.

Flywheel (vehicle) speed was measured using a Hewlett Packard optical encoder Model HEDS-6000. An encoder interface converted the signal from the encoder into a binary number which was read by the data acquisition system.

The seven signals were continuously sampled at a rate of 4 Hz (4 times a second) during each test using the Isaac 41, a 12-bit A/D and binary data acquisition system manufactured by Cyborg Corporation, and an IBM computer Model PC. A second IBM PC computer with a Data Translation Corporation data acquisition and control card was used to control the displacement of the P/M.

6.4 Test Procedure

For each test the following procedure was followed. Ball valves 1, 2, and 3 were opened and oil was circulated through the system until it was at the desired test temperature. Ball valve 3 was then closed and oil allowed to flow into the low pressure reservoir. The reservoir was charged with oil until the pressure was 30 psig (138.9 kPa), the amount of boost pressure required by the pump. At this point the flywheel was braked to a stop and the two high pressure accumulators were charged to 3100 psig (21.4 MPa). When the relief valve of the Oilgear power supply started to relieve, the data acquisition was started. Ball valve 1 was closed and the brake released. This allowed the flywheel to accelerate while the accumulators were discharging. When the accumulators were nearly discharged, the displacement of the P/M was changed by going "over center". The accumulator piston position LVDT functioned

as the trigger signal to the control computer to determine the proper time to change the P/M displacement. Once the displacement of the P/M became negative the unit started functioning as a pump and began charging the accumulators. When the flywheel stopped spinning, the accumulators started the P/M turning in the opposite direction, since the stroke of the P/M was not changed at this point. The system then continued cycling the energy between the flywheel and the high pressure accumulators until it was dissipated through losses in the system.

Two components shown on Figure 6.1 have purposes which may not be readily apparent. These are the orifice and ball valve 2. The orifice's only function was to allow for a safe discharge of the oil in case of problems during the test. Since the orifice is not part of the regenerative circuit, its inclusion does not affect the efficiency of the system. Ball valve 2 is part of the low pressure reservoir and is sometimes closed when the system is configured differently.

In addition to the regenerative cycling tests, a flywheel spin down test was conducted in order to determine flywheel losses. These losses could then be taken into account when analyzing the regenerative cycling data. For this test the P/M was not used. Instead, the flywheel was driven by a small hydraulic motor. This change was

done to allow the motor to be quickly disengaged from the flywheel so its drag was not part of the spin down test. The mounting of the motor allowed it to be slid back and forth. The motor was coupled to the flywheel and torquemeter by means of a faceplate mounted to a flexible coupling which engaged two pins mounted on the torquemeter coupling plate. Speed of the flywheel versus time was monitored using the data acquisition equipment previously mentioned. The test consisted of accelerating the flywheel to 2250 rpm by means of the small hydraulic motor, then disengaging the motor and starting the data acquisition equipment. The speed of the flywheel was then sampled at a rate of once per second until the flywheel stopped. Figure 6.2 shows the results of this test.

6.5 Efficiency Analysis

Table 6.1 summarizes the regenerative cycling tests performed and Figures 6.3-6.9 show the obtained data plotted for Test 6. Figure 6.3 is a plot of the flywheel speed showing its acceleration and deceleration as the energy was cycled from the accumulator to the flywheel and back. From the height of consecutive peak flywheel speeds one can obtain a rough visual estimate of cycling efficiency. Figure 6.4 shows the P/M displacement alternating between ± 5 degrees. Figure 6.5 shows the

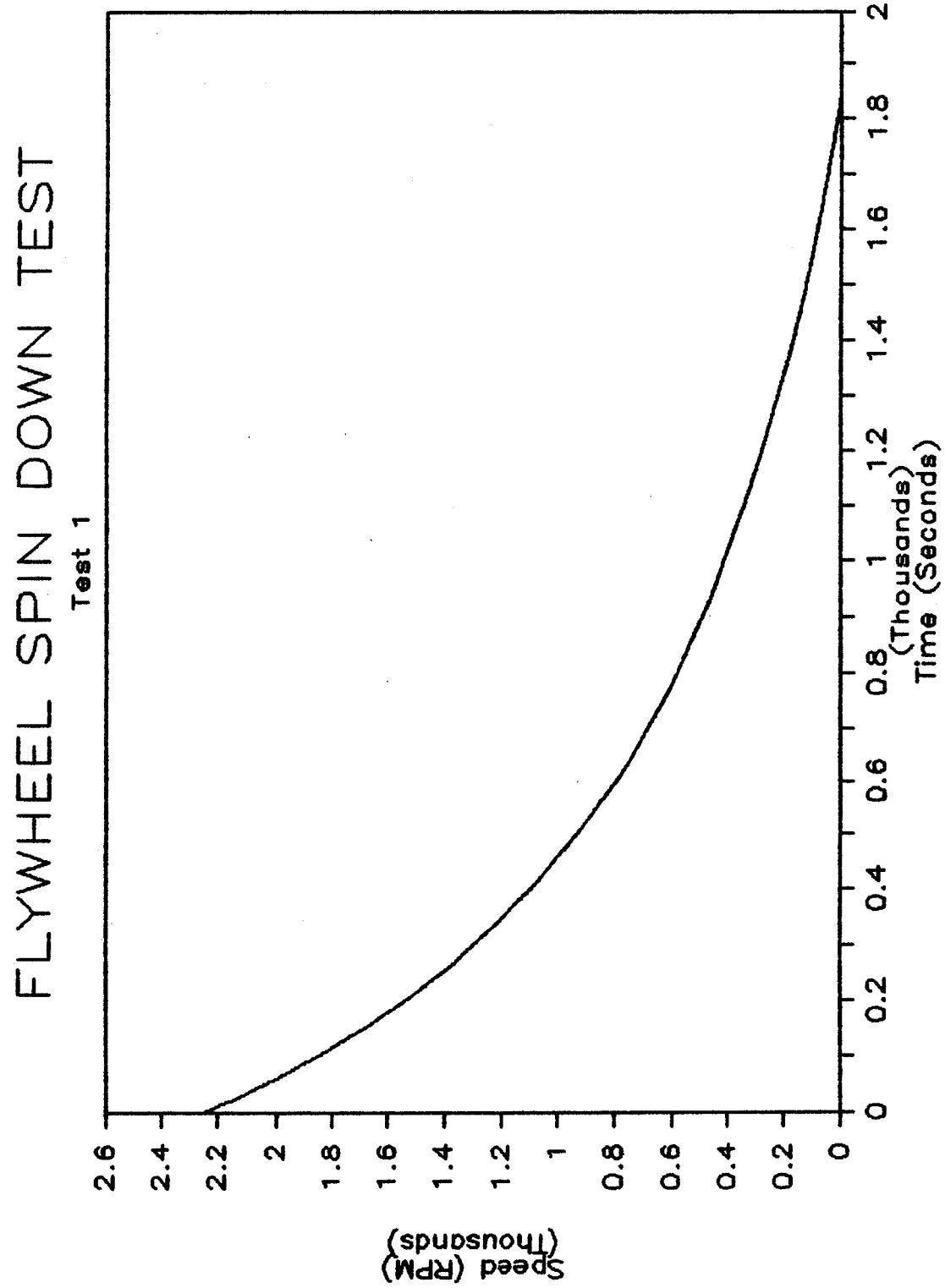


FIGURE 6.2: FLYWHEEL LOSSES

TABLE 6.1: REGENERATIVE CYCLING TEST IDENTIFICATION

TEST NUMBER	OUTPUT FILENAME	DATE 1986	STARTING OIL TEMP (·F)	ENDING OIL TEMP (·F)
1	O20C	7-23	85	80
2	O10C	7-23	82	78
3	O3C	7-23	80	77
4	O3H	7-23	125	98
5	O2H	7-23	130	111
6	O5H	7-23	127	106
7	O10H	7-23	130	109
8	O15H	7-23	129	111
9	O20H	7-23	130	110

TEST NUMBER	PRECHARGE PRESSURE (PSIG)	PUMP/MOTOR ANGLE (DEGREES)	STARTING RESERVOIR PRESSURE (PSIG)	ENDING RESERVOIR PRESSURE (PSIG)	CASE DRAIN FLOW (GALLONS)
1	1000	20	30	55	0.0476
2	1000	10	30	53	0.0793
3	1000	3	30	53	0.1004
4	1000	3	30	53	0.1110
5	1000	2	30	41	0.0819
6	1000	5	30	50	0.1559
7	1000	10	30	52	0.1374
8	1000	15	30	52	0.1030
9	1000	20	30	53	0.0740

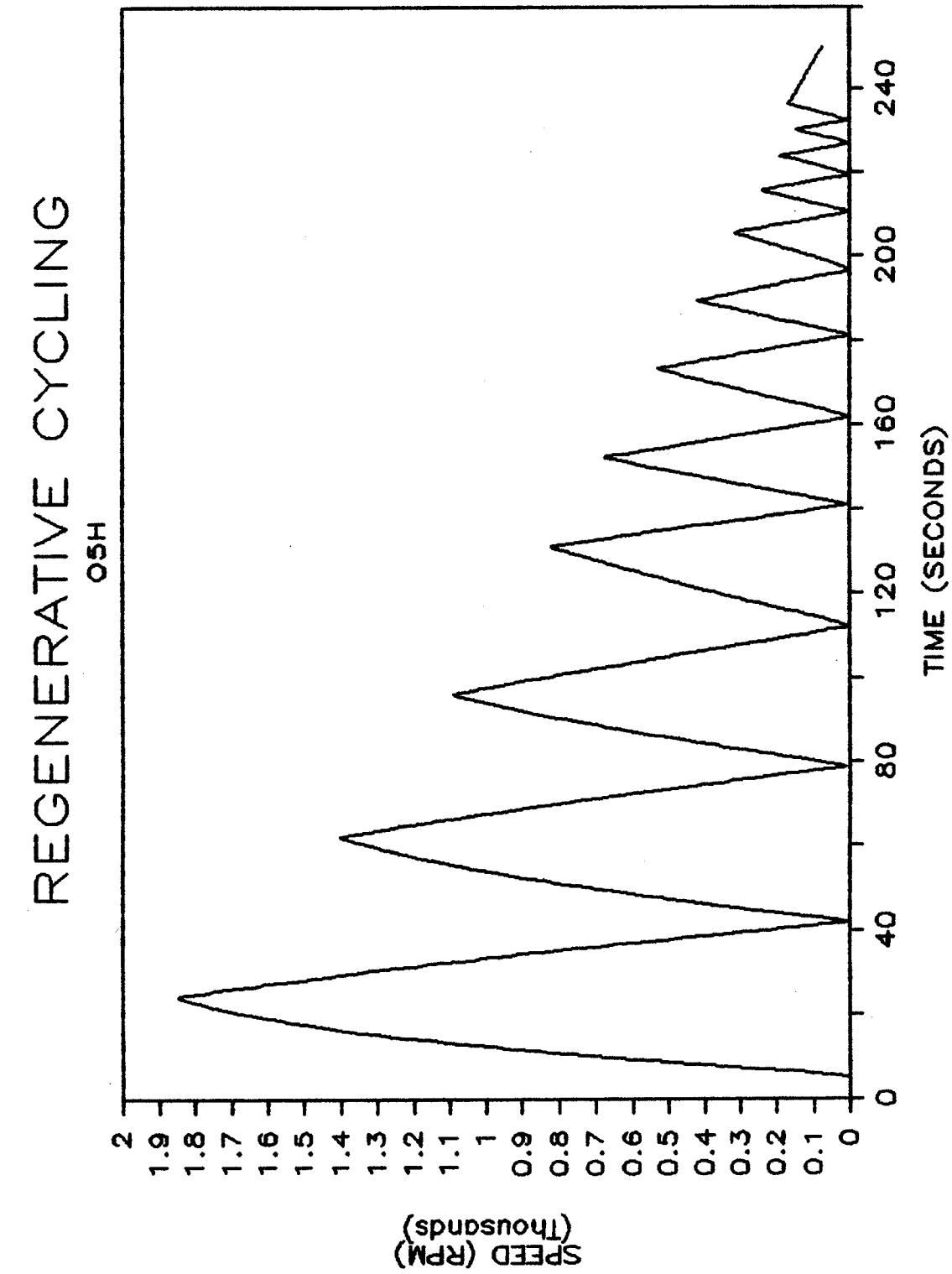


FIGURE 6.3: FLYWHEEL SPEED

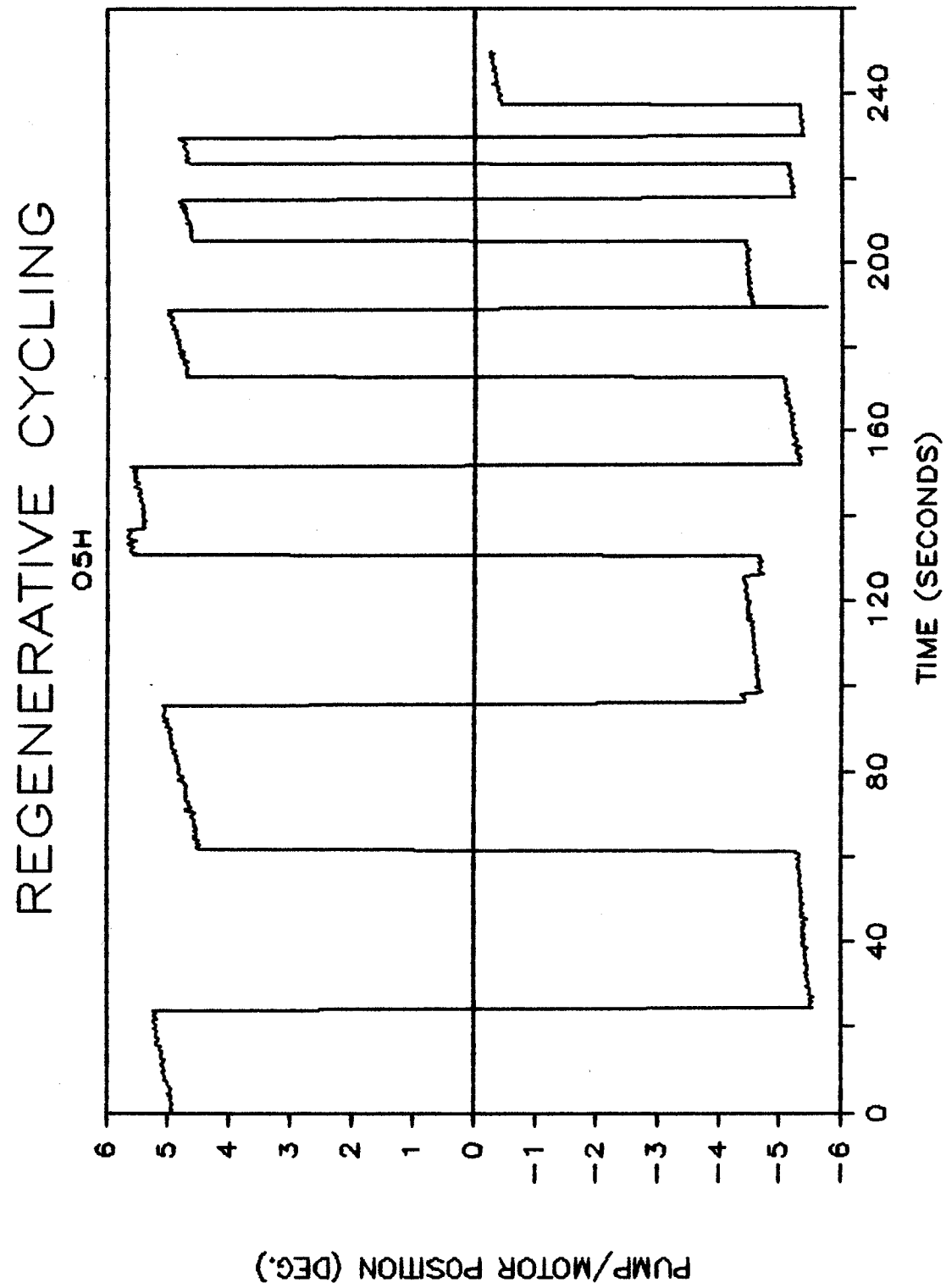


FIGURE 6.4: P/M DISPLACEMENT ANGLE

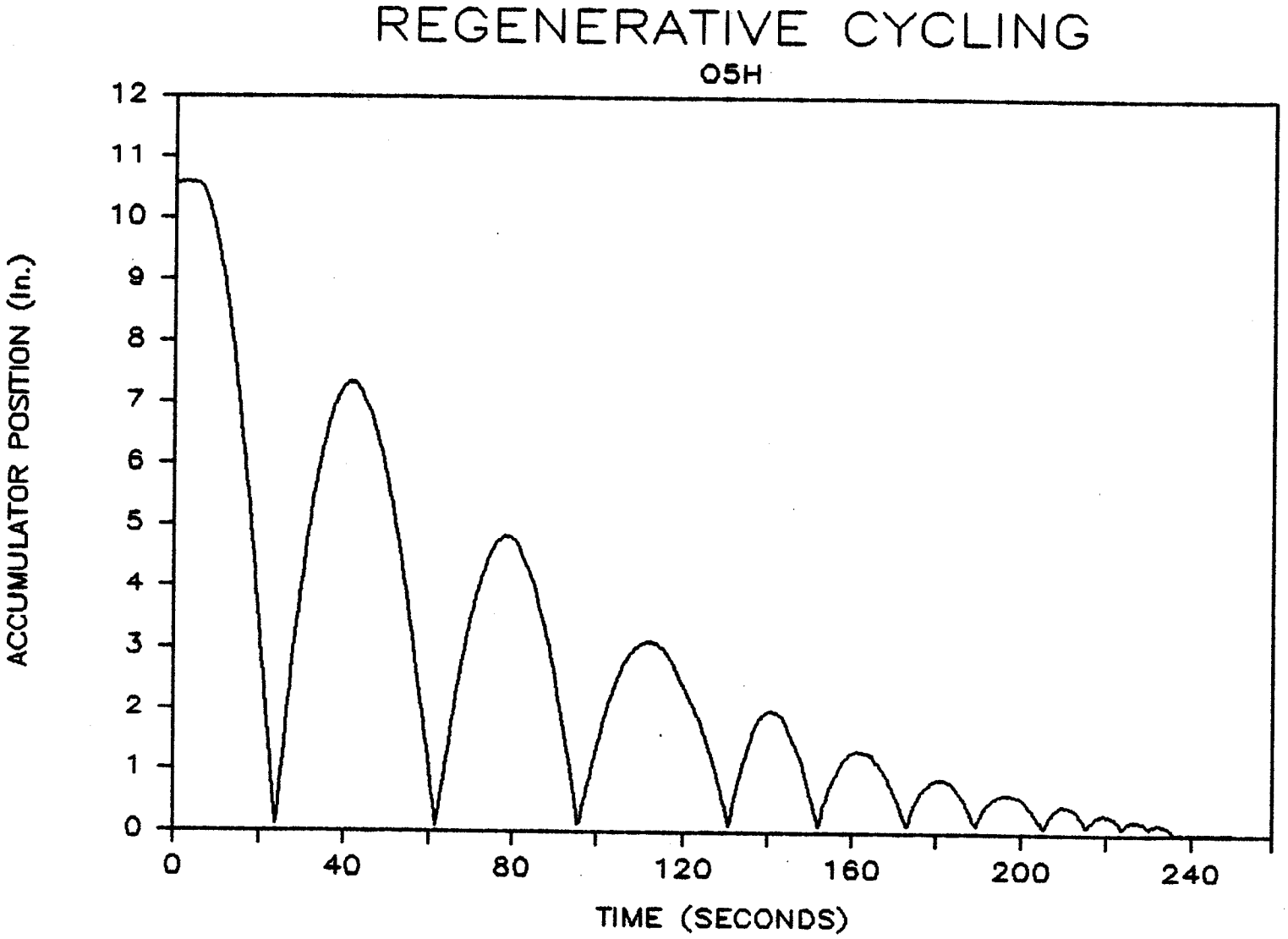


FIGURE 6.5: ACCUMULATOR PISTON POSITION

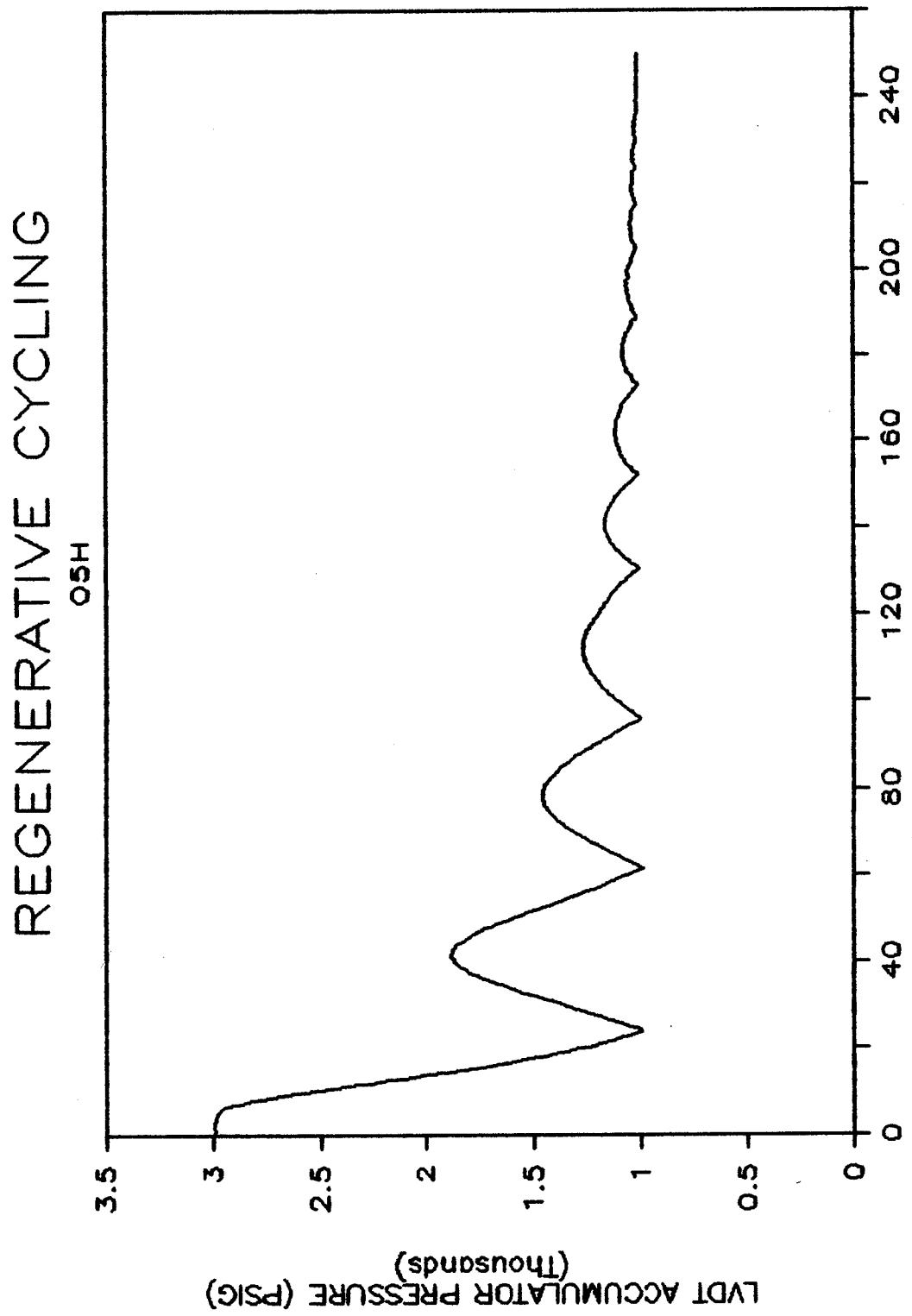


FIGURE 6.6: LVDT ACCUMULATOR PRESSURE

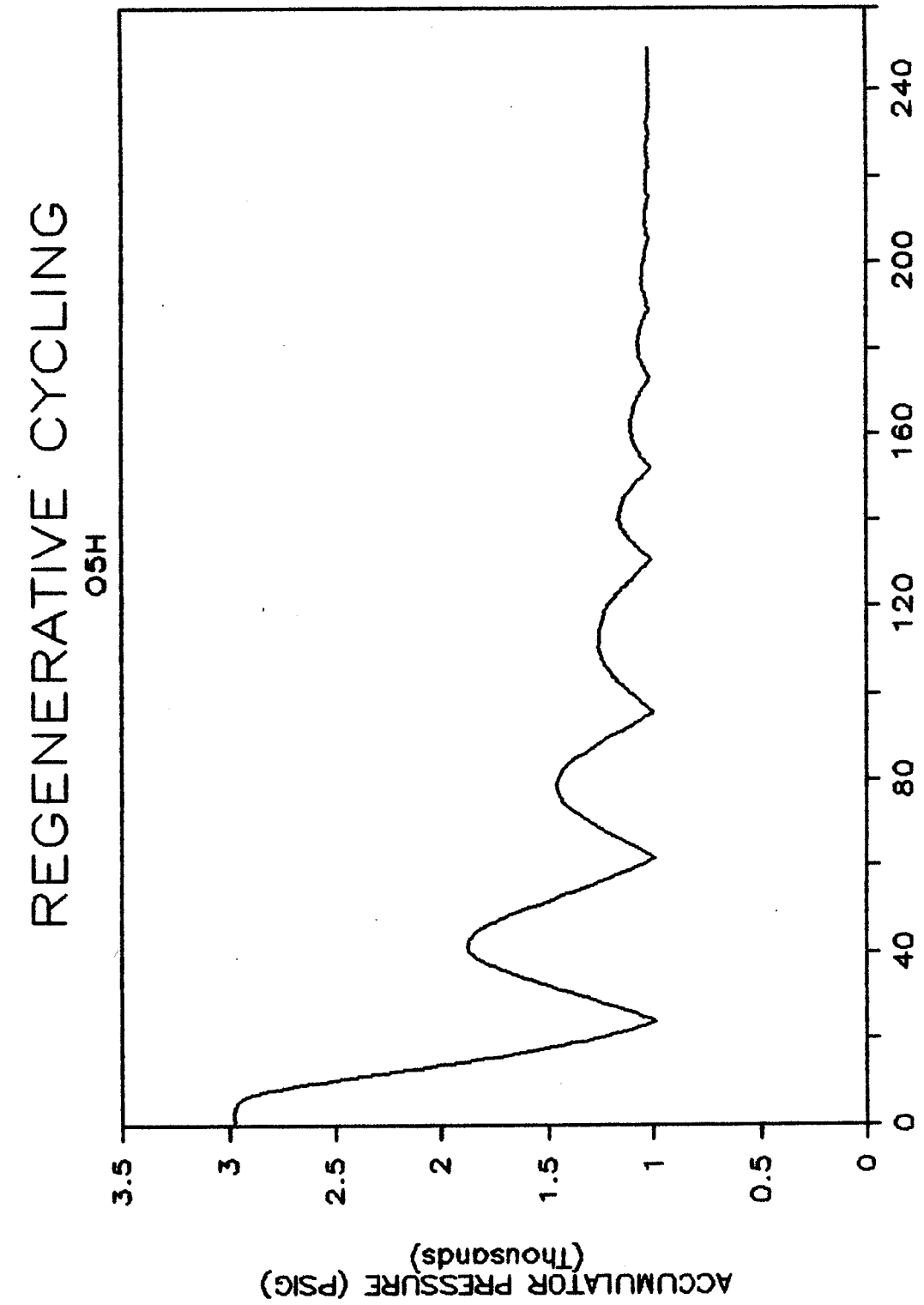


FIGURE 6.7: ACCUMULATOR PRESSURE

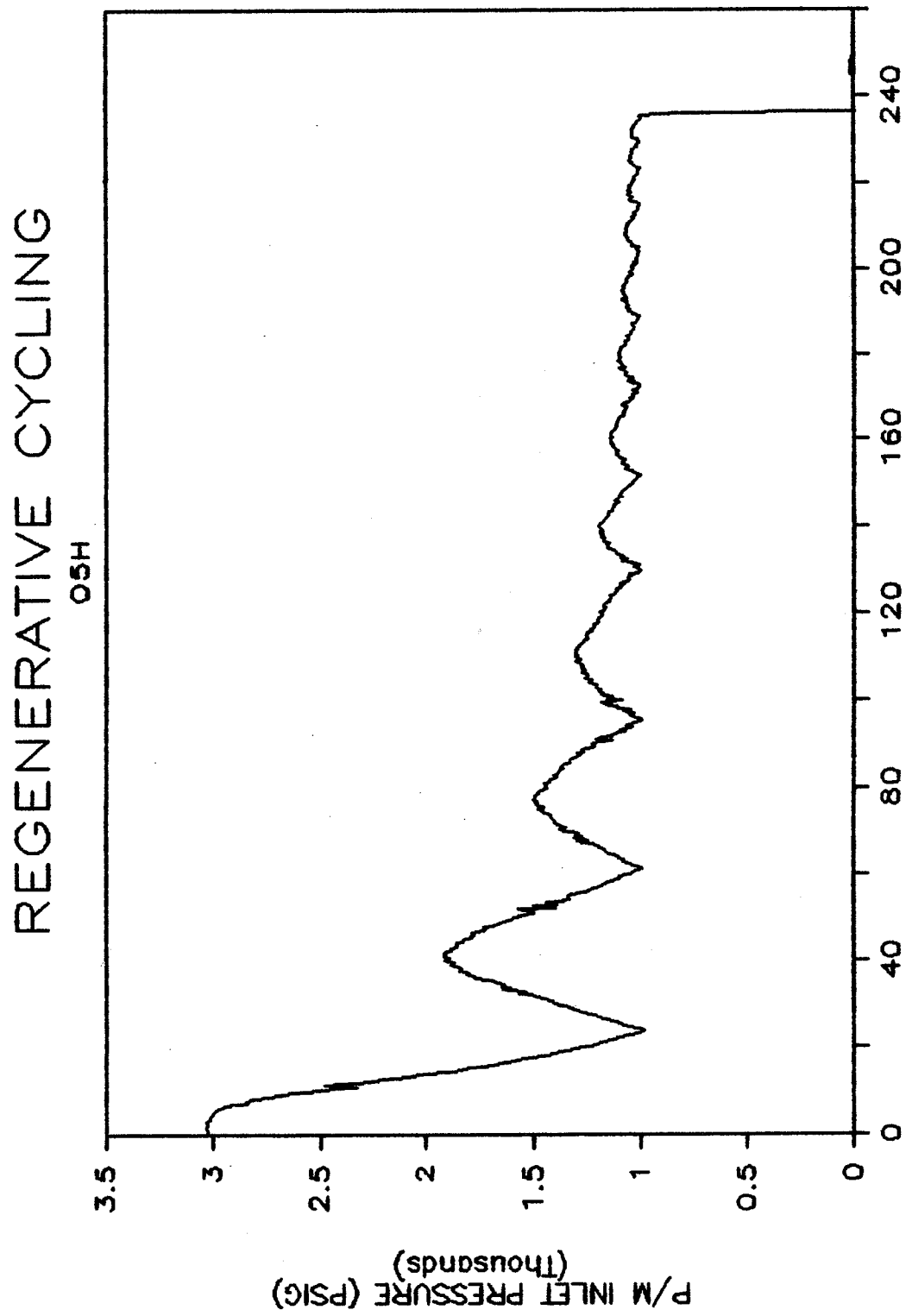


FIGURE 6.8: P/M INLET OIL PRESSURE

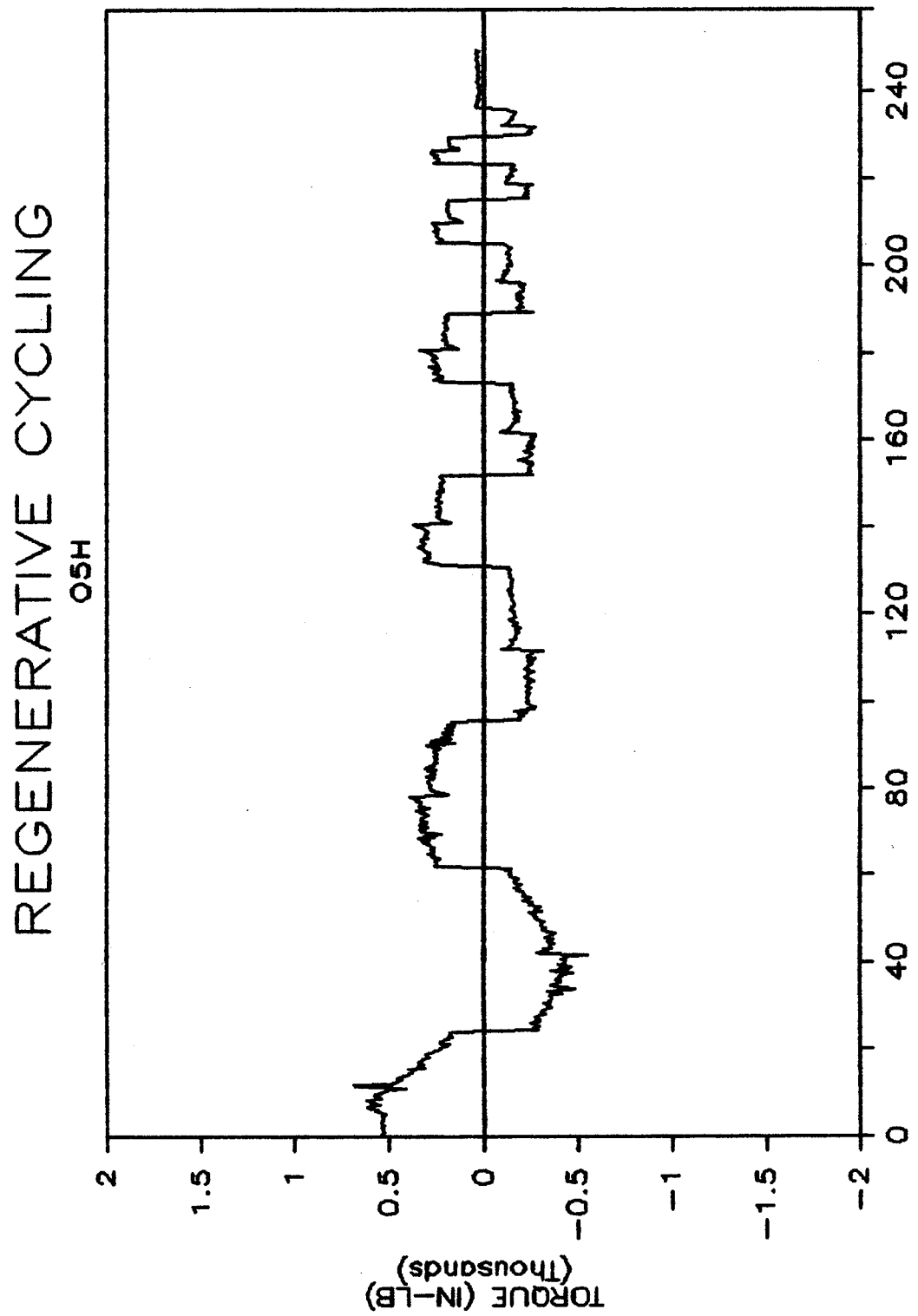


FIGURE 6.9: FLYWHEEL TORQUE

accumulator piston position as a function of time. Figures 6.6 and 6.7 detail each accumulator's gas pressure during the test. The oil pressure at the P/M is shown in Figure 6.8. The slight ripple on this graph is due to pump piston pulsations and from pressure spikes due to small changes made in the P/M displacement by the controller to maintain the displacement angle at 5 degrees. Figure 6.9 shows the torque required to accelerate and decelerate the flywheel.

Two methods were used to calculate the round trip regenerative cycling efficiencies. The first method was based on looking at consecutive peak flywheel speeds then calculating the percent energy recovered for each cycle. The second method was based on calculating the energy transferred from the accumulators or flywheel and then comparing this to the energy obtained by the flywheel or accumulators. The second analysis method allowed for efficiency calculations during flywheel acceleration and during flywheel deceleration in addition to the round trip efficiency calculations. In both methods the calculated efficiencies were corrected for flywheel losses.

6.5.1 Calculation of Flywheel Drag Torque

Since flywheel torque is related to speed by the following relationship:

$$T = J\frac{d\Omega}{dt} \qquad (1)$$

the results of the flywheel spin down test could be used to determine the flywheel drag torque as a function of flywheel speed. The data obtained from the flywheel spin down test (Figure 6.2) were numerically differentiated. This result was multiplied by the flywheel inertia and then curvefit to obtain an expression for the flywheel drag torque as a function of speed. The result is given as equation 2.

$$T = (1.1644 \times 10^{-4})\omega^2 + (2.7855 \times 10^{-2})\omega + 1.1739 \qquad (2)$$

6.5.2 Peak Flywheel Speed Method

For the peak flywheel speed method of analysis the flywheel drag energy was calculated at each sample interval and then this value was summed over one cycle period. To calculate the efficiency, the flywheel energy at the succeeding peak was added to the lost drag energy and divided by the preceding peak flywheel energy. The equation used for this calculation is given below as equation 3. The constant of 0.25 sec is the time between sample periods which, when multiplied by the angular speed in radians per second, yields the flywheel drag energy

expended between sample periods. The drag torque was calculated using equation 2. This was done for the first four peaks and then these values were averaged to obtain the efficiency listed in Table 6.2.

$$N = \frac{\text{Flywheel Energy}_{(n+1)} + \Sigma \text{ Drag Energy}}{\text{Flywheel Energy}_{n}}$$

$$N_{RT} = \frac{1/2\ J\omega^2{}_{(n+1)} + \Sigma\ 0.25\ T\omega}{1/2\ J\omega^2{}_{n}} \qquad (3)$$

This method assumes that at each peak flywheel speed the energy remaining in the accumulator is constant. When performing this analysis, this energy was noted to vary by 15.7 in-lb (1.8 N-m). This change in accumulator energy was neglected because it was insignificant when compared to the flywheel and drag loss energies. Typical flywheel energies were 550,000 in-lb (62,100 N-m). Typical drag energies were 4,000 in-lb (450 N-m).

6.5.3 Accumulator Energy Transfer Method

For this method of calculating the regenerative cycling efficiencies, the energy transferred into or out of the accumulators during each sample period had to be calculated. This energy was then summed during the acceleration and deceleration periods of the flywheel. Comparing the total energy transferred to the energy

obtained allowed for an efficiency to be determined during acceleration and deceleration of the flywheel. Multiplying the two efficiencies together yielded the round trip efficiency for a cycle.

The transferred accumulator energy was determined by multiplying the accumulator's piston force by the piston displacement. The sampled data for the accumulator gas pressures and piston position was used to calculate the transferred energy. This average gas pressure between succeeding sample periods when multiplied by the piston area is the approximated force during a sample period. This force in reality is not constant since the gas pressure is changing during the sample period. The maximum change in gas pressure between sample periods was noted to be 60 psig (413 kPa). The piston force when multiplied by the change in piston displacement is the energy transferred.

Since only one accumulator was instrumented with an LVDT, the other accumulator's piston was assumed to move the same amount as the instrumented accumulator's piston. This assumption is not entirely valid since stiction or varying coefficients of friction would cause slight differences in each piston's position. The energy transferred during one sample period for the accumulators is given by the following relationship:

$$E_{Acc} = [(\overline{P1})A1 + (\overline{P2})A2]\Delta L1$$

$$E_{Acc} = \left[\left(\frac{P1_n + P1_{(n+1)}}{2}\right) A1 + \left(\frac{P2_n + P2_{(n+1)}}{2}\right) A2\right]\left(L1_{(n+1)} - L1_n\right) \quad (4)$$

Once the accumulator energy is known, the efficiencies can be obtained from the following equations:

$$N_{Accel} = \frac{E_{Flywheel} + E_{Drag}}{E_{Acc}} \quad (5)$$

$$N_{Decel} = \frac{E_{Acc} + E_{Drag}}{E_{Flywheel}} \quad (6)$$

$$N_{RT} = N_{Accel}N_{Decel} \quad (7)$$

6.7 Results

Table 6.2 lists the results of the analysis showing the calculated efficiencies for each method. The calculated round trip efficiencies show a high degree of correlation between the two analysis methods. The data show that larger P/M displacements have a higher regenerative cycling efficiency. This is expected since the P/M is more efficient at larger displacements. Results of the energy transfer method show that the P/M is more efficient as a pump and has higher losses when it functions as a motor to accelerate the flywheel.

TABLE 6.2: REGENERATIVE CYCLING EFFICIENCIES

TEST NUMBER	FILE NAME	ANALYSIS METHOD			
		PEAK FLYWHEEL SPEED	ACCUMULATOR ENERGY TRANSFER		
		N_{RT}	N_{Accel}	N_{Decel}	N_{RT}
9	020H	75.1	82.9	91.0	75.5
1	020C	77.7	83.4	93.6	78.1
8	015H	78.8	82.9	96.1	79.7
7	010H	74.9	82.4	91.3	75.3
2	010C	72.0	80.6	88.7	71.5
6	05H	62.8	74.2	82.0	60.7
4	03H	47.7	64.0	73.3	46.9
3	03C	47.8	65.4	73.2	47.7

The calculated efficiencies seem somewhat low, however, most of the losses are due to the P/M. To verify this point the manufacturer's efficiency data for the P/M were determined for the operating range of the P/M during Tests 1 and 9. Tests 1 and 9 were run using a displacement of 20 degrees. The various efficiencies are listed in Table 6.3. The P/M efficiency was determined by multiplying the pump efficiency by the motor efficiency. This was done since one regenerative cycle transfers the energy once through the P/M as a motor and once through the P/M as a pump. The P/M efficiencies are shown plotted in Figure 6.10. As seen in the diagram, the maximum efficiency for the unit under these conditions is 83 percent. Based on this figure the average P/M efficiency for the cycle was assumed to be 80 percent. If this number is then multiplied by the accumulator efficiency of 96.5 percent for a fast charge, fast discharge cycle (Chapter 5) the estimated round trip efficiency is determined to be 77.2 percent. This result agrees well with the calculated efficiency values.

PRESSURE psig)	735			1470			2205			2940		
SPEED (rpm)	Nm	Np	Np/m	Nm	Np	Np/m	Nm	Np	Np/m	Nm	Np	Np/m
50	.700	.746	.522	.770	.771	.594	.762	.742	.565	.737	.720	.531
100	.757	.789	.597	.816	.817	.667	.812	.800	.650	.797	.770	.614
200	.809	.830	.650	.857	.858	.735	.856	.847	.725	.844	.826	.697
400	.851	.865	.736	.892	,892	.796	.895	.888	.795	.889	.875	.778
800	.866	.877	.759	.909	.908	.825	.912	.908	.828	.915	.903	.826
1500	.836	.855	.715	.896	.897	.804	.911	.906	.825	.918	.908	.834

TABLE 6.3: P/M EFFICIENCIES 20 DEGREES DISPLACEMENT

(Values Obtained from Manufacturer's Data)

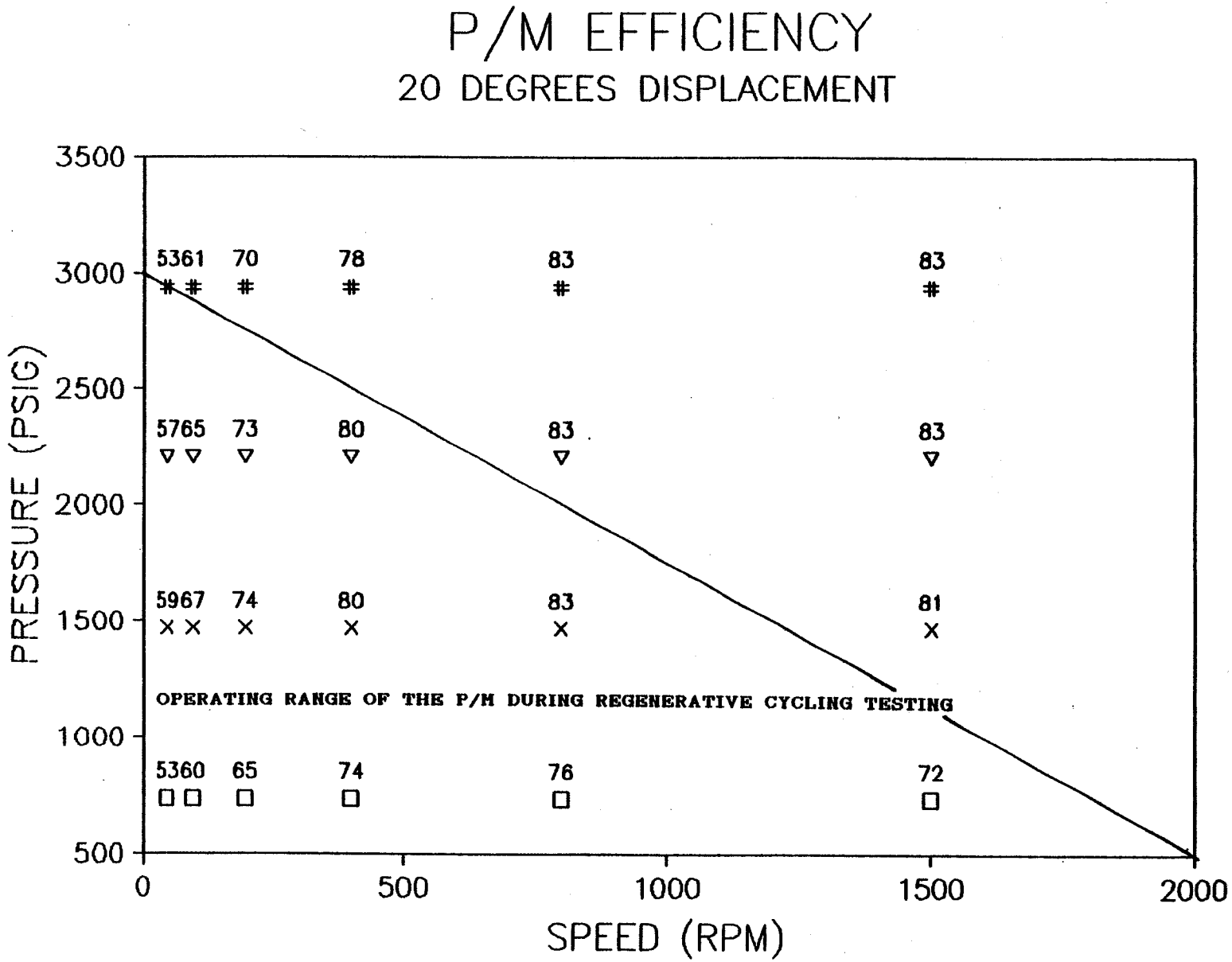


FIGURE 6.10: P/M EFFICIENCY 20 DEGREES DISPLACEMENT

7.0 HYBRID VEHICLE CONTROL TESTING

7.1 Introduction

This section presents the results of hybrid vehicle simulation control tests. The tests were performed to evaluate the controllability of the system, and to record significant system parameters. Tests were run using several different initial conditions and driving cycles. The initial condition variations were the starting accumulator pressure and engine operating state. A typical driving cycle consisted of an acceleration of the flywheel, a period of constant speed, and a deceleration. Several rates of accelerations and decelerations and several constant speed durations were tested. Data were also collected on random driving cycles. During all of the driving cycles, a data acquisition system recorded nine variables: driver's input command voltage, flywheel speed, flywheel torque, pump/motor stroke-control piston position, accumulator pressure, accumulator piston position, the simulated engine speed, the simulated engine torque, and the pump stroke control pressure.

7.2 Control of System

The system was controlled using an IBM personal computer Model PC and a Data Translation DT2801 series analog and digital input/output system. A control flowchart is shown in Figure 7.1 and the control program is included in Appendix A. The overall control strategy is such that control of the pump and of the P/M are separate subsystems with the accumulator pressure being the only connecting link. The control program operates the routines which control the P/M at the start of each control loop. The routines which control the pump are then operated only if the engine is on or being turned on.

The first subsystem consists of the P/M and the flywheel. Depending on its displacement, the P/M either acts as a pump and drives the flywheel, or acts as a motor and is driven by the flywheel (regenerative braking mode). The controller controls the P/M displacement through two high-speed solenoid valves. The solenoid valves control poppet valves, which in turn control a cylinder attached to the P/M. The P/M displacement is a function of the driver's input (a voltage signal), accumulator pressure, and accumulator precharge pressure. An input to the controller is interpreted as a torque command. The P/M displacement function was written such that the P/M torque was proportional to the driver's input for all accumulator

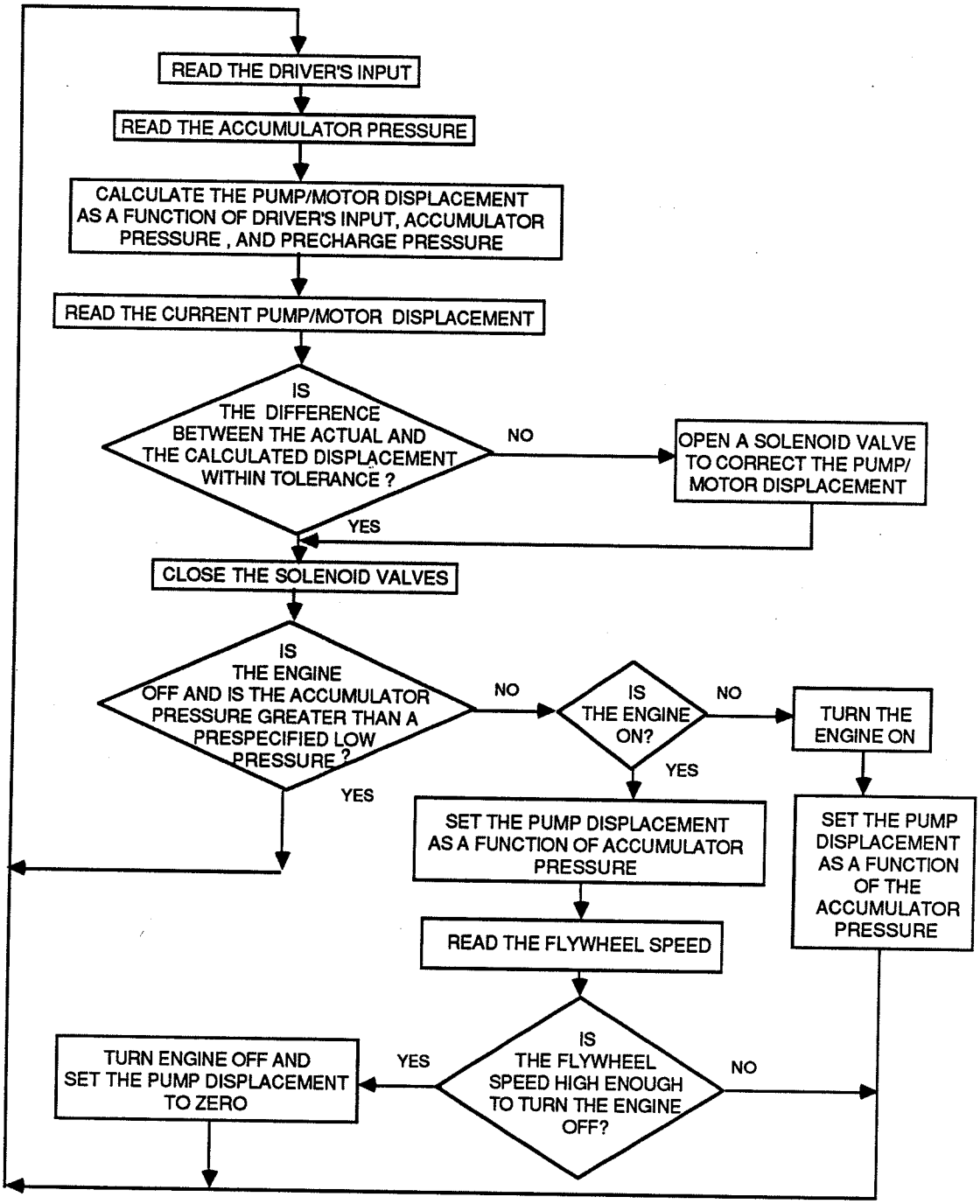


FIGURE 7.1: COMPUTER CONTROL FLOW CHART

pressures. If the driver maintained a constant input, the displacement of the P/M was increased to keep the torque constant as the accumulator pressure decreased. The opposite occurred if the accumulator pressure increased. In this way the subsystem compensated for the variation in accumulator pressure. For the simulation the actual P/M displacement was read from the position LVDT and solenoid valves were opened or closed to bring the displacement to the desired value when the displacement was outside an error band of less than half a degree.

The simulated IC engine was operated using an on/off strategy. When engine power was required, the engine would come on at this power level and the computer algorithm would adjust the pump stroke to maintain this power level until the engine was shut off. The engine was turned on when the accumulator pressure reached a low, prespecified value (1,200 psig). The pump displacement was set as a function of the accumulator pressure so that the simulated IC engine operated near its ideal point, an ideal point being an output torque and speed for which the engine has highest efficiency.

The simulated IC engine remained on until the accumulator charge increased to a calculated shutoff pressure. The shutoff pressure was determined such that the accumulator can absorb all the braking energy. This

engine shutoff strategy allowed for regenerative braking at any time during the system's operation. In the actual automobile this policy would be modified slightly. Since emergency braking infrequently occurs during the typical driving cycle, less capacity would be reserved in the accumulator for regenerative braking. The friction brakes of the car or fluid flow over a relief valve would handle any additional braking requirements.

In addition to the control section of the program, there was also an emergency shutdown procedure could be triggered by the operator. The engine was shut off; P/M and pump displacements were set to zero. A small charged accumulator on the test stand was connected to the flywheel brake which upon opening of a valve provided pressure to the brake cylinder stopping the flywheel.

7.3 Test Configuration

The hydraulic circuit used for studying the dual P/M hybrid vehicle is shown in Figure 2.1. This diagram also shows the location of the various transducers used for data acquisition. The following variables were recorded: command voltage, flywheel speed, flywheel torque, P/M stroke control position, accumulator pressure, accumulator piston position, engine speed, engine torque, and pump control pressure.

Calibration information for the various transducers used for data acquisition can be found in Appendix E. This appendix also contains information on the error bands for each recorded variable.

During the vehicle simulation the simulated IC engine was operated near a single ideal point rather than over an ideal line. The operating point chosen for the simulation was an engine speed of 1100 rpm and torque of 725 in-lb (81.9 N-m) which produced 12.6 hp (9.4 kW). This value was chosen on the basis of hydraulic power supply limitations, simulated engine cycling time, and similarity to actual IC engine data. The entire torque versus speed curve for the simulated IC engine can be seen in Figure 7.2. This figure also shows the hydraulic power supply pressure Ps, represented by the higher line on the graph. It should be noted that our power supply did not have sufficient capacity to maintain adequate pressure for faster simulated engine speeds. This limitation caused the simulated IC engine torque to drop off abruptly above 1,800 rpm as the supply pressure dropped. It did not affect the hybrid vehicle simulation since the engine was never operating in this range during the testing.

Future work will entail having the simulated IC engine operate along the ideal line maintaining a low BSFC while still allowing a wider range of simulated IC engine power

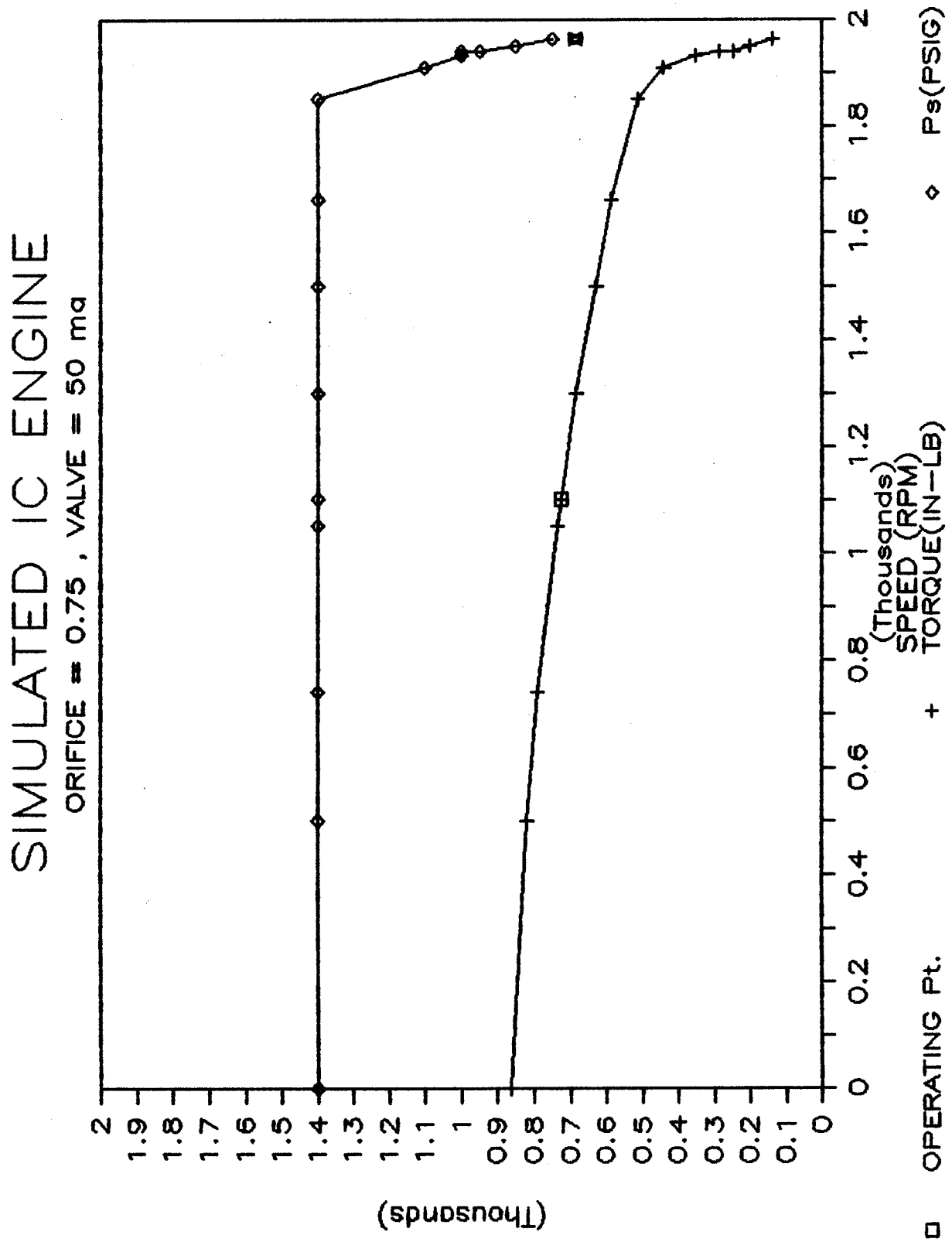


FIGURE 7.2: TORQUE/SPEED CURVE SIMULATED ENGINE

output. This strategy will allow for reduced engine cycling time. The additional control strategy is not expected to have any effect on controllability since the engine and the P/M can be treated as two separate systems due to the isolating effect of the accumulators. Because the simulated IC engine was not being operated over an ideal line, the servovalve shown in Figure 2.1 was not used similar to a "throttle"; instead the valve was operated either in a fully open or closed position.

7.4 Test Procedure

The system was run with periods of constant acceleration, constant speed, and constant deceleration. These tests were conducted utilizing two different methods. The first method involved using "push button driving". In this method the control computer was fed a constant voltage from one of three potentiometers through a panel of pushbuttons used to switch the signal. The first potentiometer was set to give a voltage signal which would produce the desired acceleration, the second was set for the constant speed voltage, and the last for the deceleration voltage. A driving cycle consisted of starting with the flywheel at rest and then switching the control voltage with the push buttons in order to change from acceleration to constant speed to braking. In the second method the

acceleration and braking were run with the constant voltage from the potentiometers; however, the constant speed phase of the cycle was manually controlled by means of a driver monitoring flywheel speed and making small adjustments to maintain a more constant flywheel speed. In each of the methods the acceleration and deceleration rates were changed in order to provide more complete data on system performance.

In addition to the defined driving cycle tests, two random driving cycles were run to provide data on system performance and response to a continuously varying driver signal. These were done using a driver who sent varying voltage signals to the controller, accelerating or decelerating the flywheel.

During each of the test runs a brake load was applied to the flywheel to simulate a road load. An accumulator was in the hydraulic circuit that actuated the brake. The accumulator was charged to the required pressure for the desired load and helped to maintain a constant brake pressure. The brake load however, was not always constant due to heating, cooling, and wear of the brake pads. The drag torque used for the simulation was approximately 200 in-lb (22.6 N-m). That is, the brake was adjusted so that it took approximately 200 in-lb (22.6 N-m) to drive the flywheel at a constant speed. The inertia of the flywheel is 34.783 lb-in/sec^2 (3.93 kg-m^2).

A typical run consisted of driving the "car" to adjust the constant speed voltage to compensate for brake wear and heating. Since it was desired to have the simulated IC engine turn on during different parts of the driving cycle, the accumulator pressure was adjusted so that the simulated IC engine would either turn on immediately, during the acceleration period, during constant speed driving, or during the deceleration period. Once these variables were set, the data acquisition was started and the driving cycle was completed using one of the methods described above.

Seven tests were run with various starting conditions and driving cycles. Table 7.1 lists the various conditions for the tests.

7.5 Results

Typical results can be seen in Figures 7.3 through 7.11. These figures are for the data obtained during test number 5. Figure 7.3 shows the command voltage sent to the controller. Figure 7.4 shows the resulting flywheel (vehicle) speed. As seen in the figure, the flywheel was accelerated to 1,100 rpm then maintained at a constant speed and then was decelerated (braked regeneratively) to a stop. Figure 7.6 shows the P/M position, which as stated earlier is a function of driver command signal and accumulator pressure. As seen in the figure during the

TABLE 7.1: TEST IDENTIFICATION HYBRID VEHICLE CONTROL TESTING

TEST NO.	FILE NAME	STARTING ACCUMULATOR STATE	STARTING ENGINE STATE	TEST PATTERN AND COMMENTS
1	O1B	charged	off	random driving cycle
2	O2B	charged	off	fast acceleration, engine turns on and off during cruise, fast deceleration
3	O3B	discharged	on	start with engine on during fast acceleration; engine did not maintain constant speed
4	O4B	low	off	engine turns on during slow acceleration and off during cruise; fast deceleration
5	O5B	charged	off	medium acceleration, engine turns on and off during cruise, manual correction of input command by driver to maintain more constant speed during cruise, slow deceleration
6	O6B	low	off	engine turns on during slow acceleration, manual correction of input command by driver (as in test #5), medium deceleration
7	O7B	charged	off	random driving cycle; engine did not maintain constant speed
8	O8B	low	off	engine turns on during medium acceleration, manual correction of input command by driver (as in test #5), medium deceleration

first 15 seconds of the cycle the P/M displacement is automatically increased by the control algorithm to maintain the constant torque asked for by the driver since the accumulator pressure is dropping (Figure 7.7). Figure 7.9 shows the simulated engine speed being maintained near the ideal point. This particular driving cycle required the engine to recharge the accumulator twice. Comparing this figure to Figure 7.7 shows that the engine is turned on by the control algorithm, as stated above, when the accumulator pressure drops to 1,200 psig (8.3 MPa). In order to maintain the simulated engine near the ideal point, the pump is destroked by the control algorithm as the pressure increases in the accumulator. This is shown in Figure 7.11. Lastly, flywheel torque and engine torque are shown in Figures 7.5 and 7.10 respectively.

The entire system was found to be very controllable and responded well to the driver's input command. Whether the engine was on or off, there was sufficient power to drive the flywheel. Transitions from engine-driving to accumulator-driving were smooth. This was largely due to the accumulators, which served as the link between the two halves of the system. The accumulators isolated much of each subsystem's dynamics.

Results of the simulation show the engine-pump subsystem's speed occasionally was not constant. This is

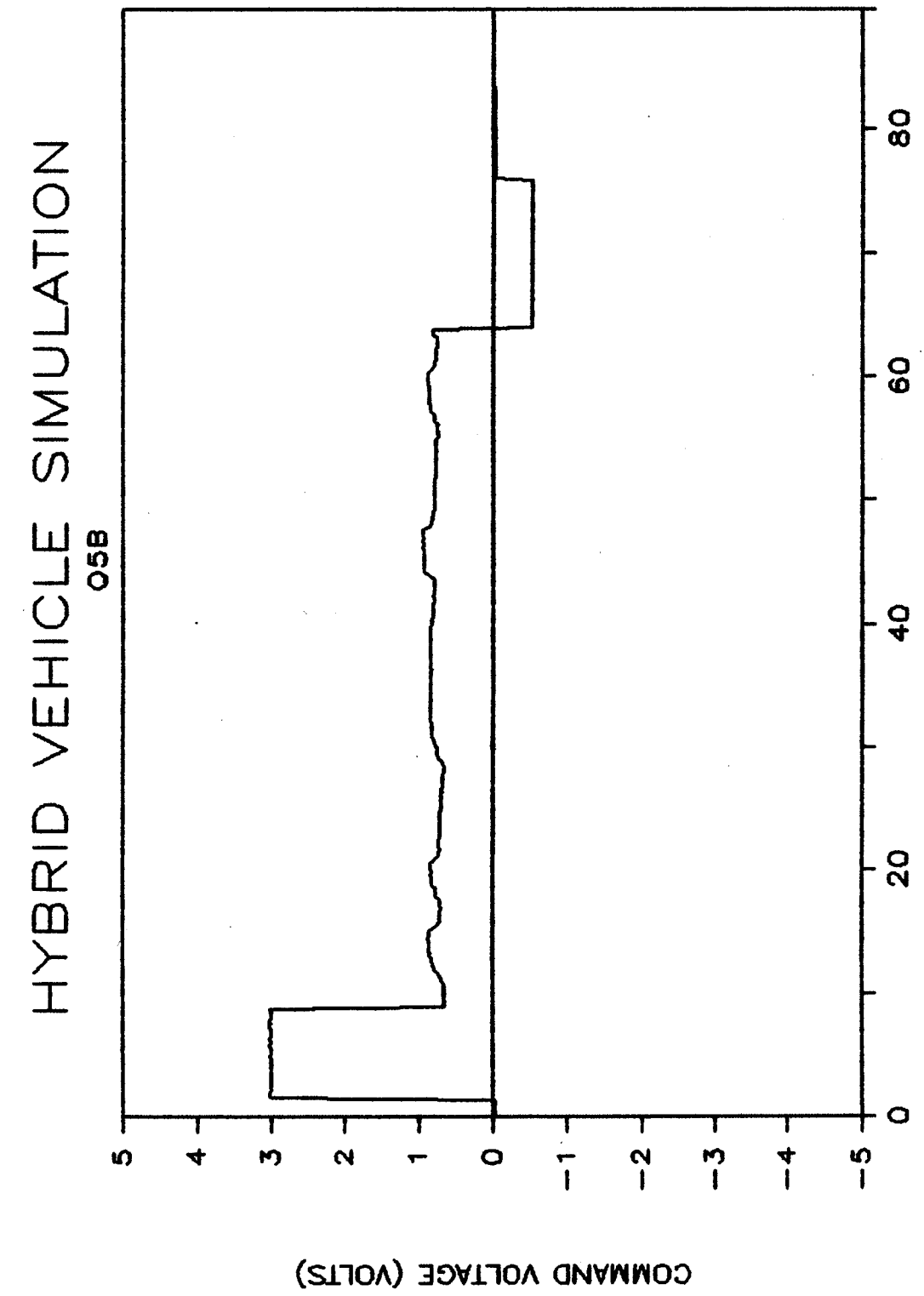


FIGURE 7.3: COMMAND VOLTAGE

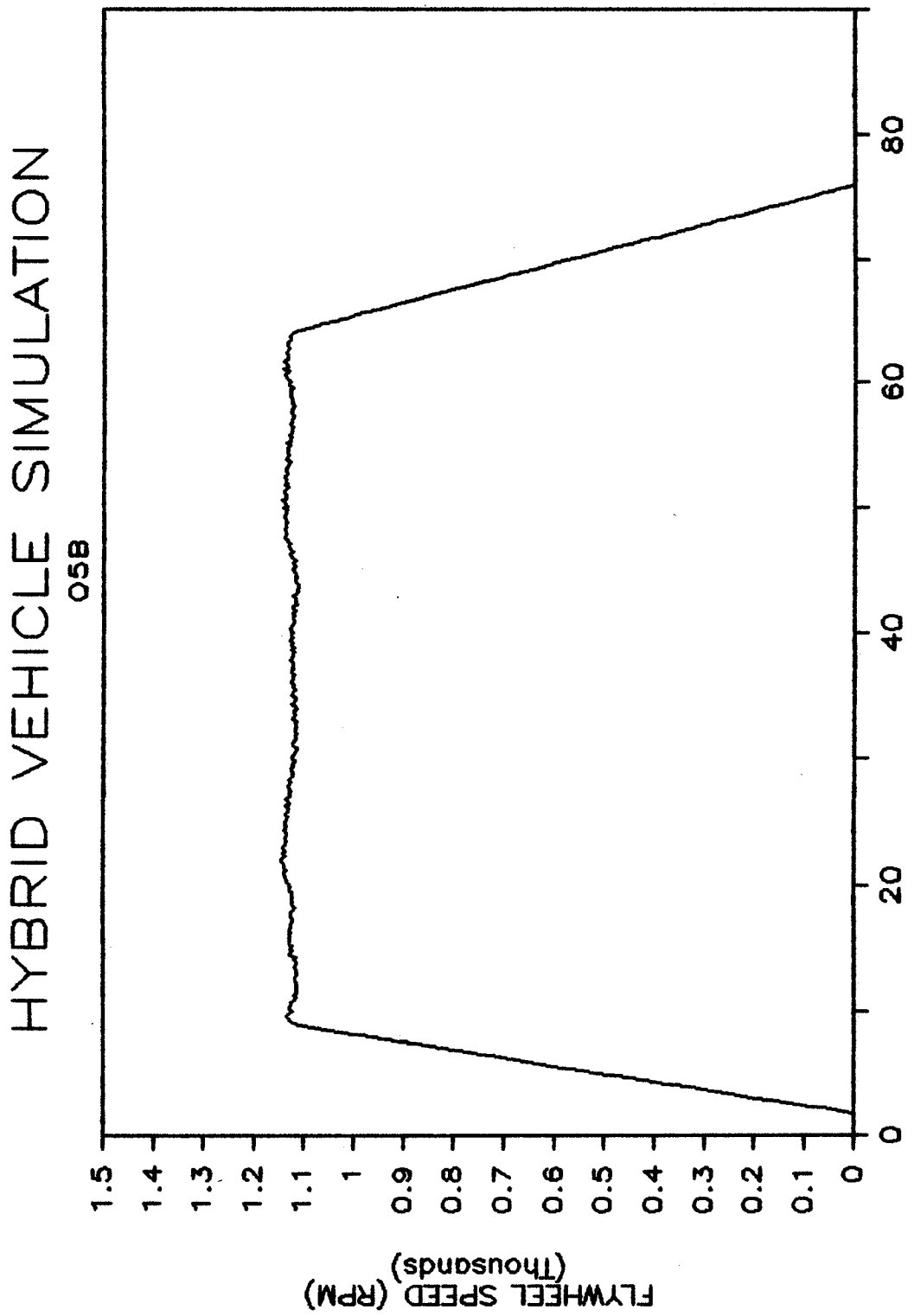


FIGURE 7.4: FLYWHEEL SPEED

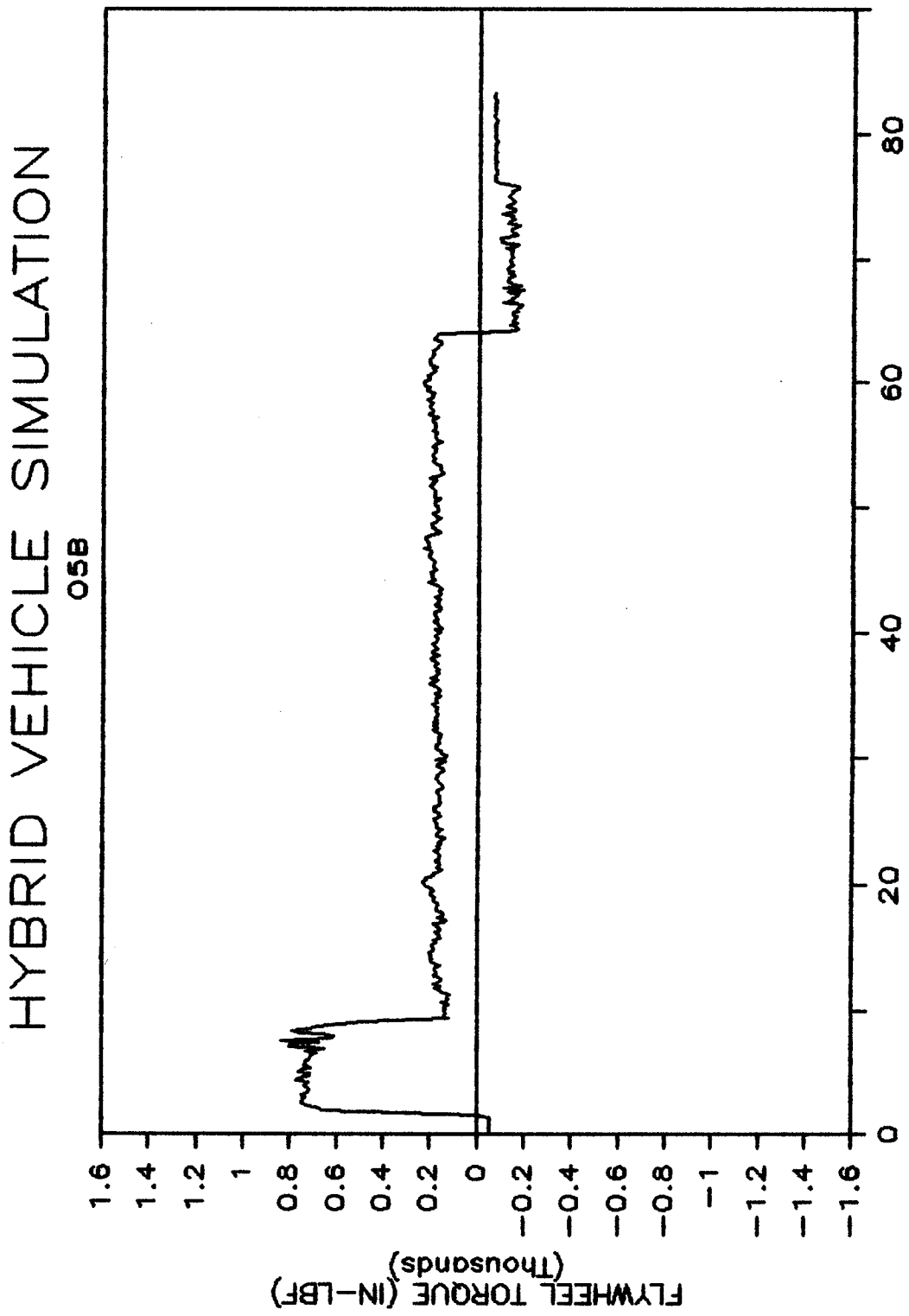


FIGURE 7.5: FLYWHEEL TORQUE

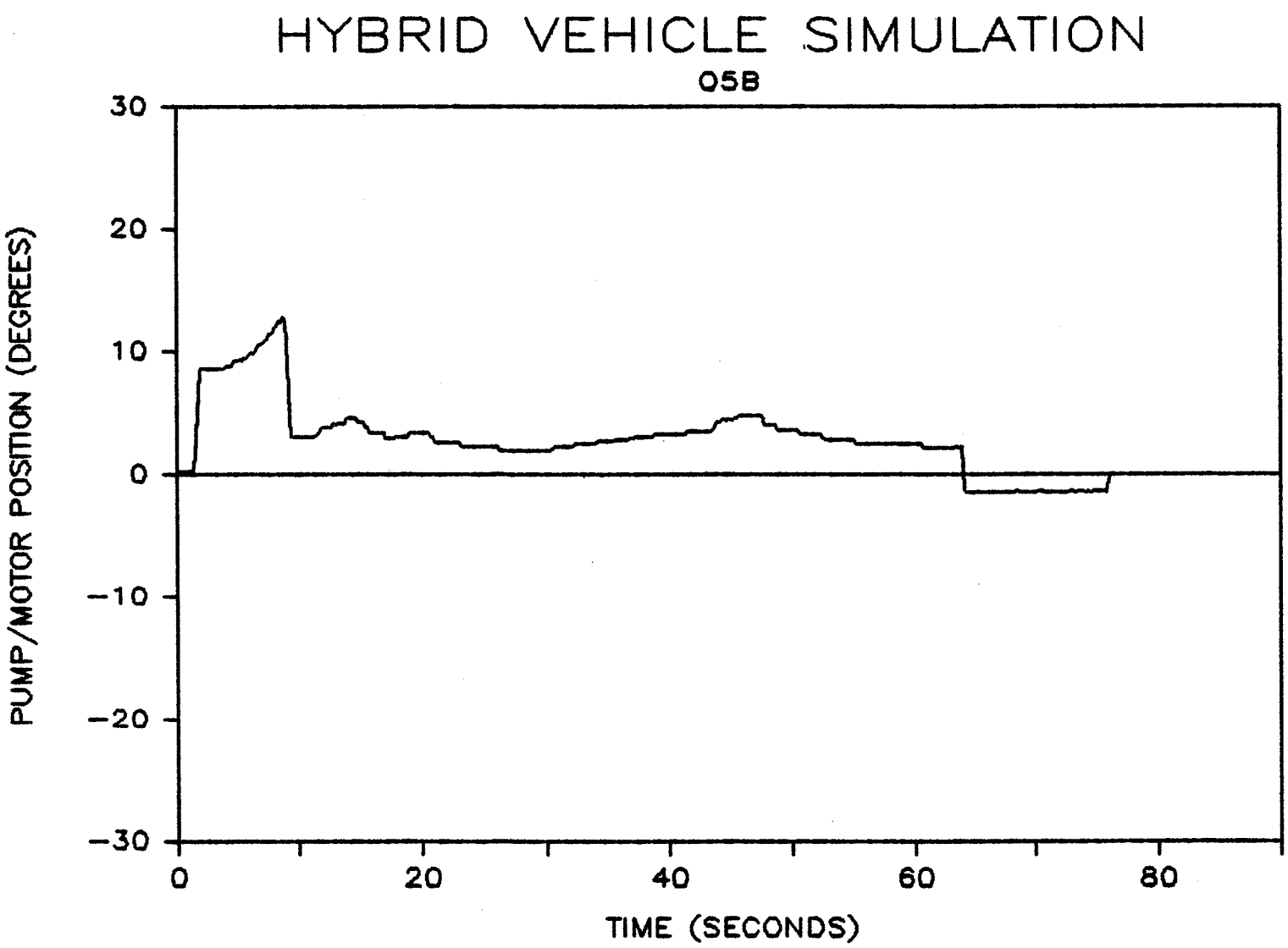


FIGURE 7.6: PUMP/MOTOR POSITION

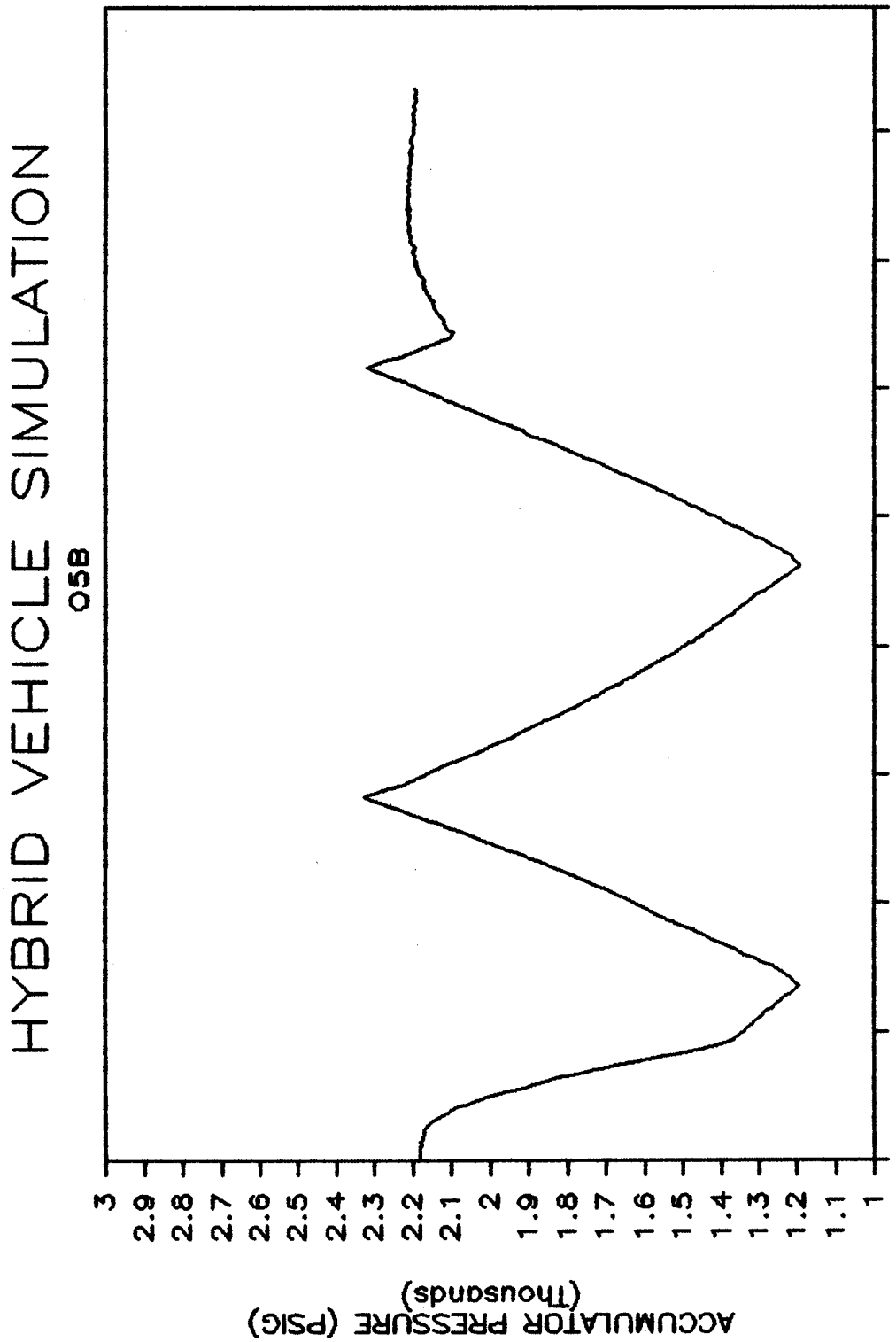


FIGURE 7.7: ACCUMULATOR PRESSURE

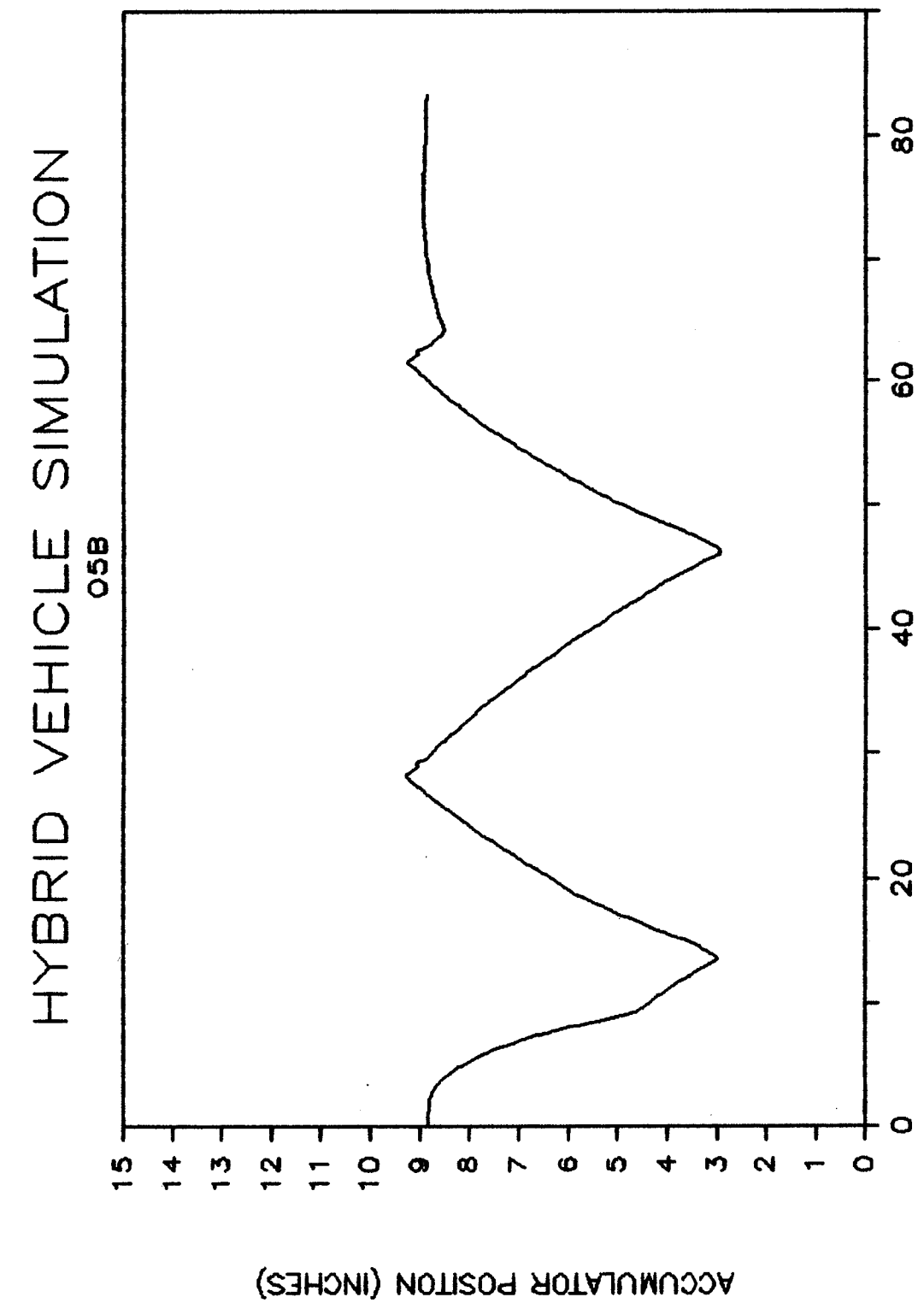


FIGURE 7.8: ACCUMULATOR POSITION

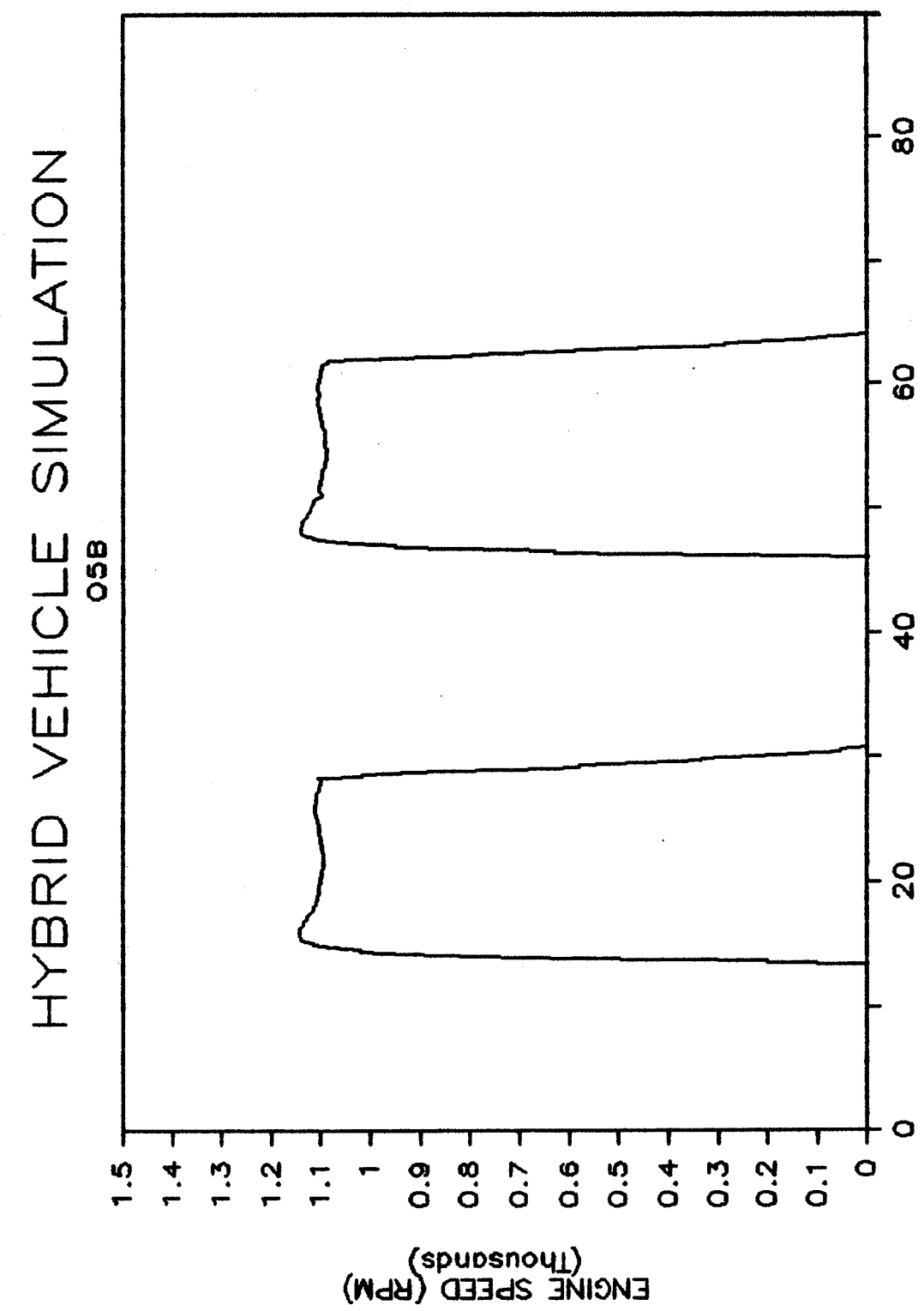


FIGURE 7.9: ENGINE SPEED

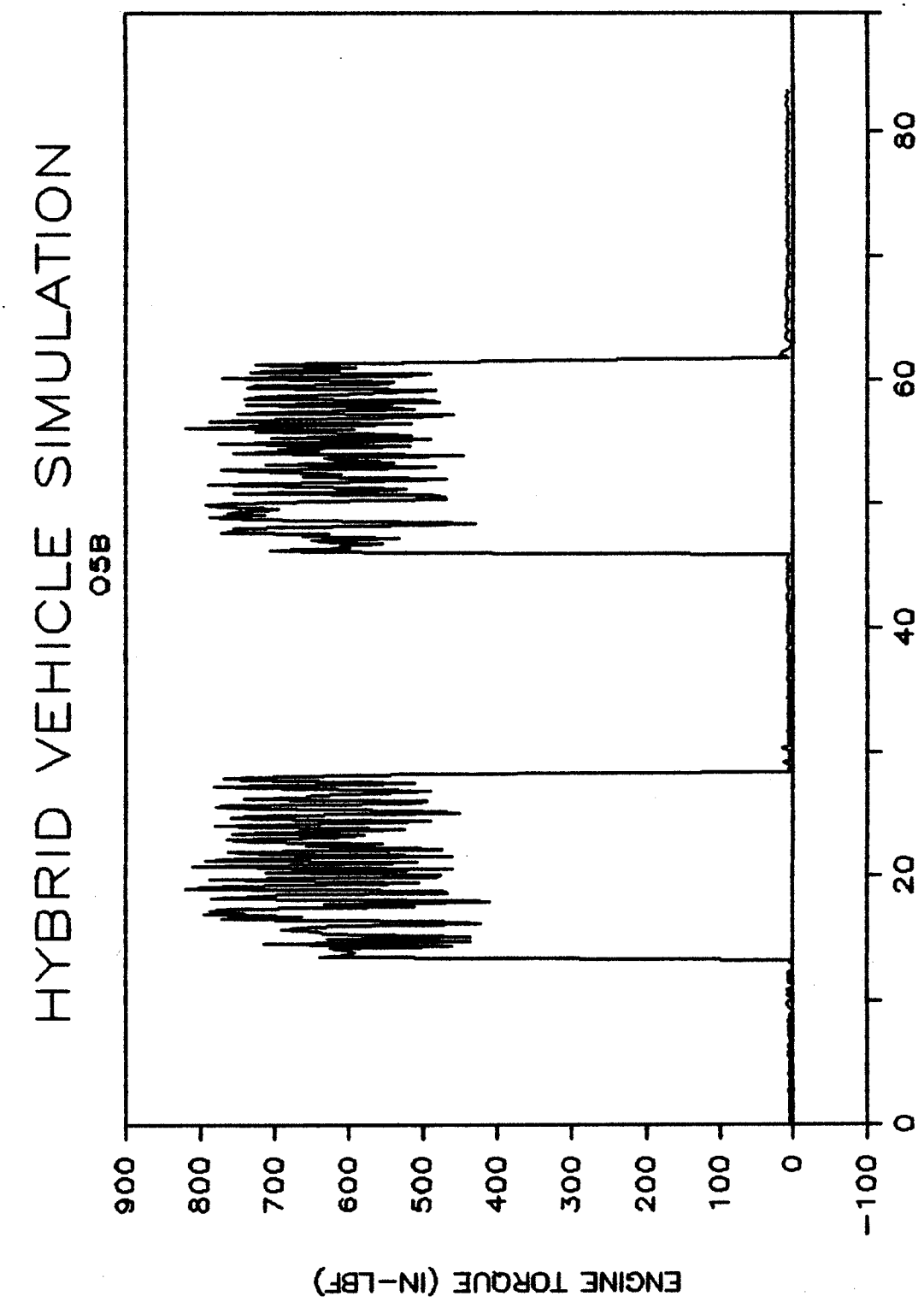


FIGURE 7.10: ENGINE TORQUE

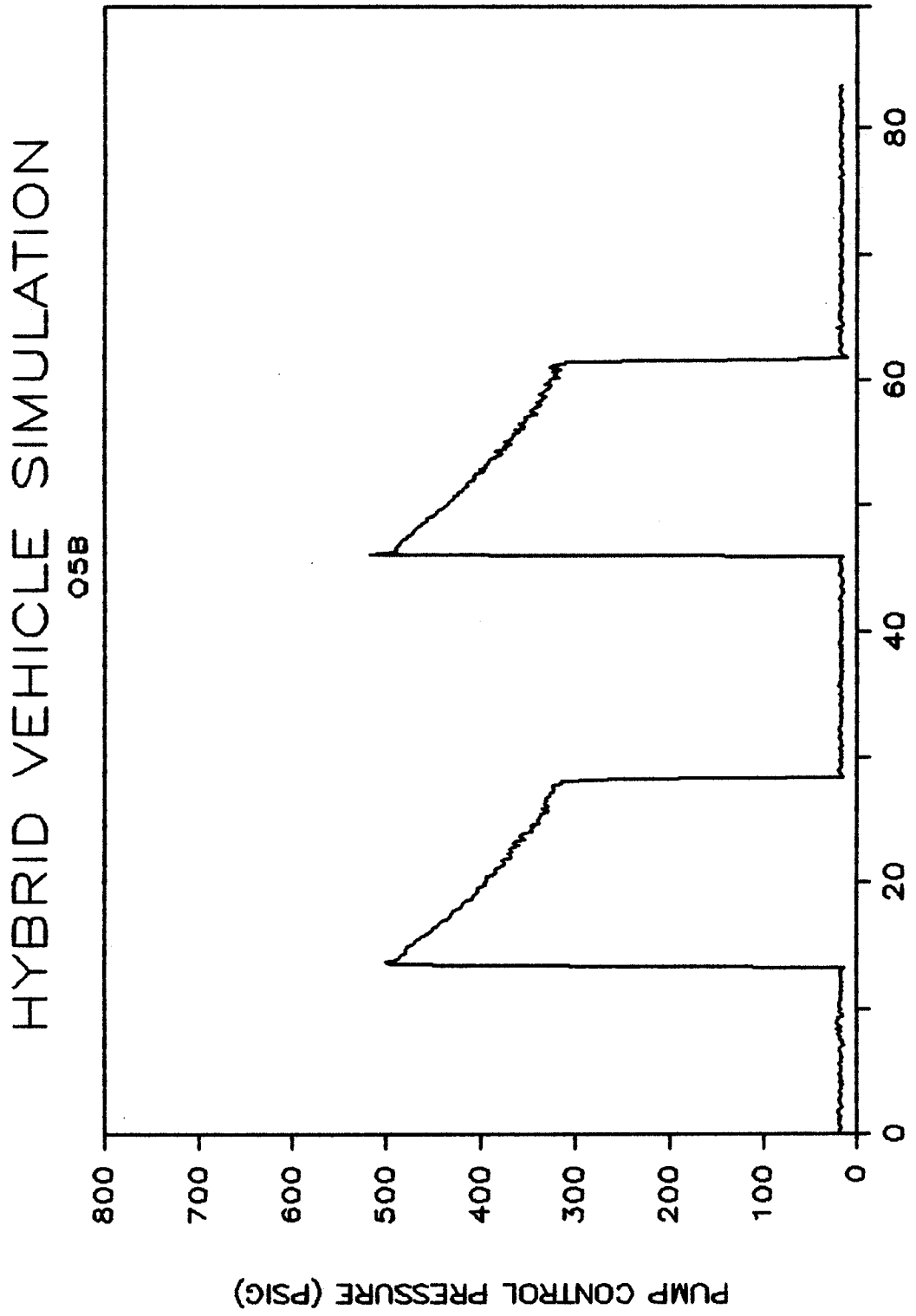


FIGURE 7.11: PUMP CONTROL PRESSURE

especially apparent in tests 3 and 7. In both cases the accumulator pressure was very low. The speed fluctuation of the engine is attributed to two sources. First, the accumulator pressure transducer (channel 5) was measuring the gas pressure inside one accumulator, not the oil pressure. There is a slight difference between these two due to the force needed to move the accumulator piston and to compress the foam. For this reason it is recommended that future implementations of this system monitor the oil pressure, not the gas pressure. Second, the pump displacement for constant torque was probably not properly determined for low pressures. It should have been increased for this range. In all of the tests, the engine tended to overshoot the desired speed. Increasing pump displacement would result in the engine operating at a higher torque, lower speed condition. The speed deviation of the simulated IC engine is only about ± 100 rpm. This problem of a non-constant engine speed is not critical to the whole system. Since an IC engine has a wide area of high efficiency near the ideal point, the overall system efficiency will not be significantly reduced. It is felt if the above two changes were implemented, the speed deviation of the engine would be significantly reduced.

One problem with the P/M subsystem is that it is difficult to maintain an exactly constant flywheel speed as

the accumulator pressure varied without manual driver correction. In general, as the accumulator pressure increased during the "constant speed" parts of the tests, the flywheel speed increased. The reverse occurred when the pressure decreased. The reason for this is due to the control algorithm. In the algorithm no correction in displacement is made unless the error is greater than about one third of a degree. Suppose that the displacement was set exactly right when the accumulator pressure started rising. To maintain constant torque, the P/M must be destroked. But this does not occur until the error is one third of a degree. In the mean time the extra torque accelerates the flywheel. This process repeats itself, and the flywheel continues to speed up. Another problem with the algorithm is that it calculates the proper displacement based on the equation that displacement equals torque divided by pressure. No correction was made for torque efficiency, which varies considerably at low displacements. Decreasing the error band on the P/M controller and modifying the displacement algorithm for the actual efficiency of the P/M used should eliminate most of this problem. However, maintaining an exactly constant speed is not critical to this system. In an automobile the driver provides the final feedback loop. He adjusts his foot to achieve the desired speed.

In both subsystems the torque measurements show large oscillations (Figures 7.5 and 7.10). The engine torque fluctuates perhaps 400 in-lb (45.2 N-m), while the flywheel torque fluctuates about 100 in-lb (11.3 N-m). This fact is attributed to the dynamics of the hydraulic units, the pump pulsations from the pistons. Frequency analysis of the torque signal by fast fourier transform confirmed that the fluctuations were caused by pump pulsations. The frequency of the oscillations was high enough to be damped out effectively by the system inertia. The torque fluctuations did not cause any problems with regard to system stability or controllability.

8.0 CONCLUSIONS

The hybrid vehicle test stand was built to study component efficiencies, determine system efficiencies, and verify control policies. Previous to this testing, the studies of the dual P/M system had been performed by computer analysis. While this is a useful method of analysis, this method does not prove that a system is technically feasible or verify control policies. In addition, the efficiencies calculated by a computer simulation are only as valid as the assumptions on which they were based. The data obtained from this work can now be compared to the results obtained from the computer studies. A comparison of this type would determine if the modeling assumptions were correct and would also allow for improvements in the developed models.

The first three areas of study with the hybrid vehicle test stand focused on obtaining experimental results for determining system efficiencies. Data were collected to determine P/M efficiencies, accumulator efficiencies, and system regenerative cycling efficiencies.

The P/M efficiency testing (Chapter 4) was done at conditions of low displacement. The results of this testing when compared to the manufacturer's data showed that the P/M unit tested obtained efficiencies greater than

the manufacturer's efficiencies. The P/M experimental efficiencies were 20-30 percent greater than the published values. The unit, however, was only tested at displacements up to 5 degrees. It is unlikely that at higher displacements the measured efficiencies would be this much larger than the manufacturer's values. Further testing of the P/M at larger displacements is needed to completely determine its efficiency at all displacements, speeds, and pressures.

The ESU used for the dual P/M system was a hydraulic accumulator. Determination of its efficiency was done through experimental testing (Chapter 5) with and without elastomeric foam in the nitrogen side of the accumulator. When the foam was not present in the accumulator, the cycle efficiency for a charge, hold, discharge cycle ranged from 59.5 to 90 percent. The same accumulator when filled with an elastomeric foam had efficiencies ranging from 95.2 to 95.6 percent under otherwise identical conditions. Based on these results, hybrid vehicles using an accumulator ESU should modify the accumulator with elastomeric foam to take advantage of the increased cycling efficiencies the use of foam offers.

Regenerative cycling efficiencies were determined for the test stand for various P/M displacements (Chapter 6). A regenerative cycle consisted of transferring the energy

from the ESU to the flywheel and back to the ESU. The calculated efficiencies obtained ranged from 47 to 78 percent for displacements varying from 3 to 20 degrees respectively. A more efficient P/M (5) unit would increase these efficiencies since the results of the test for a P/M displacement of 20 degrees showed the P/M was approximately 80 percent efficient while the accumulator was 96 percent efficient. Additional testing with a highly efficient P/M unit should be performed to see how much improvement in cycling efficiencies can be obtained.

The last area of study was hybrid vehicle control testing (Chapter 7). This was conducted to evaluate controllability of the system and to record significant system parameters. Results of these tests confirmed that the system was stable and relatively easy to control. These results also showed small modifications in the control algorithm may be desired to maintain a more constant vehicle speed. The control routine utilized had error band on the P/M displacement of approximately 1/3 degree. This was enough to allow the flywheel speed to vary by as much as 150 rpm depending on accumulator pressure. This would not pose a significant driving problem since the driver of an automobile would provide the final feedback loop adjusting his foot position accordingly.

Based on the above, continued development work should be performed on accumulator hybrid vehicles. In particular the test stand should be utilized to drive the vehicle while operating the engine along the "ideal line" which was not done during this study. Use of a hydraulic pump that does not go "over center" employing valving so it can function as a P/M should be studied to determine its feasibility. This is desirable since a hydraulic pump which does not go "over center" can be made more efficient than one which does. This is possible since less clearance volume is required improving volumetric efficiency. In addition to these studies which can be performed on the designed test stand, development work should begin on designing and constructing a dual P/M system for installation in an automobile. Development of a hybrid automobile would allow for obtaining actual fuel consumption data for comparison to the same vehicle which does not employ this system.

REFERENCES

1. Wu, Peirong, et al., "Fuel Economy and Operating Characteristics of a Hydropneumatic Energy Storage Automobile", SAE paper 851678, 1985

2. Tollefson, S., et al., "Studies of an Accumulator Energy-Storage Automobile Design with a Single Pump/Motor Unit", SAE paper 851677, 1985

3. Beachley, N. H. and Frank, A. A., "Practical Considerations for Energy-Storage Motor Vehicles", Proceedings, 16th Intersociety Energy Conversion Engineering Conference, Atlanta, GA, Aug. 1981

4. Frazer, H. I., "Broader Horizons with High Efficiency Pumps and Motors", Proceedings, 39th National Conference on Fluid Power, 1983

5. Beachley, N. H., "Preliminary Test Results of the Ifield 3.5T Hydrostatic Continuously-Variable Transmission", Internal Report, April 1982

6. Rohde, S. M. and Schilke, N. A., "The Fuel Economy Potential of Heat Engine/Flywheel Hybrid Vehicles", SAE paper 810264, 1981

7. Frank, A. A. and Beachley, N. H., "Evaluation of the Flywheel Drive Concept for Passenger Vehicles", SAE paper 790049, 1979

8. Beachley, N. H. and Otis, D. R., "A Study of Accumulator Passenger Cars Based on the Ifield Hydrostatic Pump/Motor Unit", Lawrence Livermore Laboratory Report No. VCRL-15390, Aug. 1981

9. Beachley, N. H., "Control Strategies for an Internal Combustion Engine/Accumulator Automobile", Proceedings, Symposium on Advanced and Hybrid Vehicles, University of Strathclyde, Glasgow, Scotland, Sept. 1984, pp. 72-82.

10. Lewandowski, E. J., "Design of a Test Facility for Hydropneumatic Accumulator Energy Storage Vehicle Research", M. S. Thesis, University of Wisconsin-Madison, 1987

11. Beachley, N. H., et al., "Minimization of Energy Storage Requirements for Internal Combusion Engine Hybrid Vehicles", ASME Journal of Dynamic Systems, Measurement, and Control, June 1983, Vol. 105, pp. 113-119.

12. Otis, D. R. and Pourmovahed, A., "Improving Performance of Gas-Charged Accumulators Using Elastomeric Foams", Proceedings, International Symposium on Advanced and Hybrid Vehicles, University of Strathclyde, Glasgow, Scotland, Sept. 1984

13. Benson, D. J., "Experimental Evaluation of the Controllability of a Dual Pump/Motor Hydraulic Accumulator Energy Storage Automobile", M.S. Thesis, University of Wisconsin-Madison, 1987

14. Pourmovahed, A., et al., "Experimental Evaluation of Hydraulic Accumulator Efficiency With and Without Elastomeric Foam", Paper to be Presented, IECEC Conference, 1987

APPENDIX A: Computer Control Programs

The following pages contain a listing of the control programs used for Regenerative Cycling Testing (Chapter 6) and Hybrid Vehicle Control Testing (Chapter 7). The programs were written using IBM Personal Computer's BASIC language.

Computer Control Program: Regenerative Cycling Testing

```
10    REM $LIST+
20    ''
30    ''
40    '' define constants
50    ''
60    ''
70    DEFINT A-Z
80    BASE.ADDRESS     = &H2EC
90    COMMAND.REGISTER = BASE.ADDRESS + 1
100   STATUS.REGISTER  = BASE.ADDRESS + 1
110   DATA.REGISTER    = BASE.ADDRESS
120   COMMAND.WAIT     = &H4
130   WRITE.WAIT       = &H2
140   READ.WAIT        = &H5
150   ''
160   CCLEAR  = &H1
170   CADIN   = &HC
180   CSTOP   = &HF
190   CSOUT           =&H5
200   CDIOOUT =&H7
210   ''
220   ADGAIN    = 0
230   BASE.FACTOR#=4096
231   BEG = 1
240   ''
250   '' stop and clear DT2801 board
260   ''
261   STP = 0
270   OUT COMMAND.REGISTER, CSTOP
280   TEMP = INP(DATA.REGISTER)
290   WAIT STATUS.REGISTER, COMMAND.WAIT
300   OUT  COMMAND.REGISTER, CCLEAR
310   ''
320   '' get a/d and d/a channels
321   INPUT "IS THE TRIGGER ON (Y/N/) ";TAN$
322   TFLAG = 0
323   IF TAN$ = "Y" OR TAN$ = "y" THEN TFLAG = 1
330    ''
335   INPUT "IS THE PUMP/MOTOR ON THE POSITIVE SIDE (Y/N) ",ANS$
336   COUNT = 0
337   IF ANS$ = "Y" OR ANS$ = "y" THEN COUNT = 1
340   INPUT "ENTER THE TRIGGER CHANNEL (0-7) ",TRCHANNEL
350   INPUT "ENTER THE A/D CONTROLLED CHANNEL (0-7) ",ADCHANNEL
360   INPUT"DIGITAL PORT 0,1";DIOPORT
370   INPUT "POSITION ACCURACY (DEAD BAND/2), VOLTS";ACC#
385   INPUT "ENTER THE LOW SWITCHING VOLTAGE ",LSV#
390   INPUT "ENTER THE SWITCHING DEADBAND VOLTAGE ",DSV#
391   INPUT "ENTER THE HIGH CONTROLLED VOLTAGE ",HCV#
392   INPUT "ENTER THE LOW CONTROLLED VOLTAGE ",LCV#
400   A$ = ""
```

```
410   '' wait until DT2801 ready
420   WAIT  STATUS.REGISTER, COMMAND.WAIT
430   OUT  COMMAND.REGISTER, CSOUT
440   WAIT  STATUS.REGISTER, WRITE.WAIT, WRITE.WAIT
450   OUT DATA.REGISTER, DIOPORT
460   WHILE A$=""
470    ''
480    WAIT STATUS.REGISTER, COMMAND.WAIT
490    OUT  COMMAND.REGISTER, CADIN
500    ''
510    '' wait until the DT2801 DATA IN FULL flag is clear
520    '' ,then write a/d gain to the data in register
530    ''
540    WAIT STATUS.REGISTER, WRITE.WAIT, WRITE.WAIT
550    OUT  DATA.REGISTER, ADGAIN
560    '' wait until the DT2801 board DATA IN FULL flag is clear,
570    '' then write the a/d channel to data in register
580    ''
590    WAIT STATUS.REGISTER, WRITE.WAIT, WRITE.WAIT
600    OUT  DATA.REGISTER, TRCHANNEL
610    ''
620    '' read two bytes from data out register after DATA OUT ready
630    ''
640    WAIT  STATUS.REGISTER, READ.WAIT
650    LOW = INP(DATA.REGISTER)
660    WAIT  STATUS.REGISTER, READ.WAIT
670    HIGH = INP(DATA.REGISTER)
680    RAWVALUE#=HIGH*256+LOW
682    VOLTS#=RAWVALUE#*(20/BASE.FACTOR#)-10
685    IF VOLTS# > (LSV# + DSV#) AND TFLAG = 1 THEN TFLAG = 0
691    IF VOLTS# < LSV# AND TFLAG = 0 THEN 695 ELSE 692
692    IF ANS$ = "N" AND BEG = 1 THEN REF# = LCV#
693    IF ANS$ = "Y" AND BEG = 1 THEN REF# = HCV#
694    GOTO 700
695    IF COUNT = 1 THEN 698 ELSE 696
696    COUNT = 1 : REF# = HCV# :TFLAG = 1
697    GOTO 700
698    COUNT = 0 : REF# = LCV# :TFLAG = 1
700    OUT  COMMAND.REGISTER, CADIN
701    BEG = 0
710    ''
720    '' wait until the DT2801 DATA IN FULL flag is clear
730    '' ,then write a/d gain to the data in register
740    ''
750    WAIT STATUS.REGISTER, WRITE.WAIT, WRITE.WAIT
760    OUT  DATA.REGISTER, ADGAIN
770    '' wait until the DT2801 board DATA IN FULL flag is clear,
780    '' then write the a/d channel to data in register
790    ''
800    WAIT STATUS.REGISTER, WRITE.WAIT, WRITE.WAIT
810    OUT  DATA.REGISTER, ADCHANNEL
820    ''
830    '' read two bytes from data out register after DATA OUT ready
```

```
840     ''
850     WAIT  STATUS.REGISTER, READ.WAIT
860     LOW = INP(DATA.REGISTER)
870     WAIT  STATUS.REGISTER, READ.WAIT
880     HIGH = INP(DATA.REGISTER)
890     RAWVALUE#=HIGH*256+LOW
900     VOLTS#=RAWVALUE#*(20/BASE.FACTOR#)-10
910     E#=REF#-VOLTS#
920     IF ABS(E#)>ACC#  THEN GOTO 940
930     DATA.VALUE=0 :GOTO 950
940     IF E#<0 THEN DATA.VALUE=1  ELSE DATA.VALUE=2
950     ''
960     '' Binary output
970     '' wait until DT2801  ready, then write the WRITE DAC IMMEDIATE
980     '' command to command register
990     WAIT  STATUS.REGISTER, COMMAND.WAIT
1000    OUT  COMMAND.REGISTER, CDIOOUT
1010    ''
1020    '' wait until DATA IN FULL flag is clear, then write dachannel
1030    '' to DATA IN REGISTER
1040    WAIT  STATUS.REGISTER, WRITE.WAIT, WRITE.WAIT
1050    OUT DATA.REGISTER, DIOPORT
1060    '' write low and high to DATA IN REGISTER after a clear of
1070    '' DATA IN FULL flag
1080    ''
1090    WAIT STATUS.REGISTER, WRITE.WAIT, WRITE.WAIT
1100    OUT DATA.REGISTER, DATA.VALUE
1110    ''
1120    '' wait until DT2801 board ready, then go back to execute
1130    '' again
1140    ''
1141    IF STP =1 THEN 1170
1150    A$=INKEY$
1160    IF A$="" THEN GOTO 1171 ELSE GOTO 1161
1161    STP = 1
1162    LCV# = 0# : HCV# = 0# : REF# = 0
1163    PRINT "KEYBOARD SET DISPLACEMENT TO 0 "
1170    A$ = ""
1171  WEND
1180  PRINT"ERROR"
1190  ''
1200  END
```

Computer Control Program: Hybrid Vehicle Control Testing

```
10    REM $LIST+
20    ''
30    ''
40    '' define constants
50    ''
60    ''
70    DEFINT A-Z
80    BASE.ADDRESS     = &H2EC
90    COMMAND.REGISTER = BASE.ADDRESS + 1
100   STATUS.REGISTER  = BASE.ADDRESS + 1
110   DATA.REGISTER    = BASE.ADDRESS
120   COMMAND.WAIT     = &H4
130   WRITE.WAIT       = &H2
140   READ.WAIT        = &H5
150   ''
160   CCLEAR  = &H1
170   CADIN   = &HC
180   CSTOP   = &HF
190   CSOUT          =&H5
200   CDIOOUT =&H7
210   ''
220   ADGAIN    = 0
230   BASE.FACTOR#=4096
240   ''
250   '' stop and clear DT2801 board
260   ''
270   OUT COMMAND.REGISTER, CSTOP
280   TEMP = INP(DATA.REGISTER)
290   WAIT STATUS.REGISTER, COMMAND.WAIT
300   OUT  COMMAND.REGISTER, CCLEAR
310   ''
320   '' get a/d and d/a channels
330   ''
340   INPUT "ENTER THE TRIGGER CHANNEL (0-7) ",TRCHANNEL
350   INPUT "ENTER THE A/D CONTROLLED CHANNEL (0-7) ",ADCHANNEL
360   INPUT"DIGITAL PORT 0,1";DIOPORT
370   INPUT "POSITION ACCURACY (DEAD BAND/2), VOLTS";ACC#
380   INPUT "ENTER THE HIGH SWITCHING VOLTAGE ",HSV
390   INPUT "ENTER THE LOW SWITCHING VOLTAGE ",LSV
391   INPUT "ENTER THE HIGH CONTROLLED VOLTAGE ",HCV
392   INPUT "ENTER THE LOW CONTROLLED VOLTAGE ",LCV
400   A$ = ""
410   '' wait until DT2801 ready
420   WAIT  STATUS.REGISTER, COMMAND.WAIT
430   OUT  COMMAND.REGISTER, CSOUT
440   WAIT  STATUS.REGISTER, WRITE.WAIT, WRITE.WAIT
450   OUT DATA.REGISTER, DIOPORT
460   WHILE A$=""
470     ''
480     WAIT STATUS.REGISTER, COMMAND.WAIT
```

```
490     OUT  COMMAND.REGISTER, CADIN
500     ''
510     '' wait until the DT2801 DATA IN FULL flag is clear
520     '' ,then write a/d gain to the data in register
530     ''
540     WAIT STATUS.REGISTER, WRITE.WAIT, WRITE.WAIT
550     OUT  DATA.REGISTER, ADGAIN
560     '' wait until the DT2801 board DATA IN FULL flag is clear,
570     '' then write the a/d channel to data in register
580     ''
590     WAIT STATUS.REGISTER, WRITE.WAIT, WRITE.WAIT
600     OUT  DATA.REGISTER, TRCHANNEL
610     ''
620     '' read two bytes from data out register after DATA OUT ready
630     ''
640     WAIT  STATUS.REGISTER, READ.WAIT
650     LOW = INP(DATA.REGISTER)
660     WAIT  STATUS.REGISTER, READ.WAIT
670     HIGH = INP(DATA.REGISTER)
680     RAWVALUE#=HIGH*256+LOW
690     VOLTS#=RAWVALUE#*(20/BASE.FACTOR#)-10
691     IF VOLTS# > HSV THEN REF# = HCV
692     IF VOLTS# < LSV THEN REF# = LCV
700     OUT  COMMAND.REGISTER, CADIN
710     ''
720     '' wait until the DT2801 DATA IN FULL flag is clear
730     '' ,then write a/d gain to the data in register
740     ''
750     WAIT STATUS.REGISTER, WRITE.WAIT, WRITE.WAIT
760     OUT  DATA.REGISTER, ADGAIN
770     '' wait until the DT2801 board DATA IN FULL flag is clear,
780     '' then write the a/d channel to data in register
790     ''
800     WAIT STATUS.REGISTER, WRITE.WAIT, WRITE.WAIT
810     OUT  DATA.REGISTER, ADCHANNEL
820     ''
830     '' read two bytes from data out register after DATA OUT ready
840     ''
850     WAIT  STATUS.REGISTER, READ.WAIT
860     LOW = INP(DATA.REGISTER)
870     WAIT  STATUS.REGISTER, READ.WAIT
880     HIGH = INP(DATA.REGISTER)
890     RAWVALUE#=HIGH*256+LOW
900     VOLTS#=RAWVALUE#*(20/BASE.FACTOR#)-10
910     E#=REF#-VOLTS#
920     IF ABS(E#)>ACC#  THEN GOTO 940
930     DATA.VALUE=0 :GOTO 950
940     IF E#<0 THEN DATA.VALUE=1  ELSE DATA.VALUE=2
950     ''
960     '' Binary output
970     '' wait until DT2801  ready, then write the WRITE DAC IMMEDIATE
980     '' command to command register
990    WAIT  STATUS.REGISTER, COMMAND.WAIT
```

```
1000    OUT  COMMAND.REGISTER, CDIOOUT
1010    ''
1020    '' wait until DATA IN FULL flag is clear, then write dachannel
1030    '' to DATA IN REGISTER
1040    WAIT  STATUS.REGISTER, WRITE.WAIT, WRITE.WAIT
1050    OUT DATA.REGISTER, DIOPORT
1060    '' write low and high to DATA IN REGISTER after a clear of
1070    '' DATA IN FULL flag
1080    ''
1090    WAIT STATUS.REGISTER, WRITE.WAIT, WRITE.WAIT
1100    OUT DATA.REGISTER, DATA.VALUE
1110    ''
1120    '' wait until DT2801 board ready, then go back to execute
1130    '' again
1140    ''
1150    A$=INKEY$
1160    IF A$="" THEN GOTO 1170 ELSE GOTO 370
1170  WEND
1180  PRINT"ERROR"
1190  ''
1200  END
```

APPENDIX B: Rexroth Test Data

The following pages contain the experimental results of the Rexroth P/M Efficiency Testing (Chapter 4).

TABLE 4.1: TORQUE REQUIRED TO SPIN PUMP

ANGLE (DEGREES)	SPEED (RPM)	INLET TORQUE (IN-LB)
0	0	59.2
0	100	10.5
0	200	14.3
0	400	17.0
0	800	25.8
0	1100	29.5
1	0	59.3
1	100	11.5
1	200	15.8
1	400	21.6
1	800	30.6
1	1100	36.6
3	0	63.8
3	100	13.4
3	200	17.4
3	400	24.0
3	800	33.4
3	1100	38.5
5	0	64.5
5	100	14.1
5	200	19.3
5	400	23.5
5	800	32.3
5	1100	38.4
10	0	64.7
10	100	15.6
10	200	20.5
10	400	27.4
10	800	45.9
10	1100	48.0
15	0	71.3
15	100	18.1
15	200	24.0
15	400	34.6
15	800	46.9
15	1100	54.7
20	0	77.8
20	100	21.8
20	200	28.6
20	400	42.8
20	800	52.8
20	1100	64.2
25	0	82.6
25	100	20.8
25	200	32.9
25	400	51.0
25	800	62.7
25	1100	71.2

TABLE 4.2: SPIN LOSSES FOR MOTOR

ANGLE (DEGREES)	SPEED (RPM)	INLET PRESSURE (PSI)	OUTLET PRESSURE (PSI)	DIFFERENTIAL PRESSURE (PSI)	TEMPERATURE (FAHRENHEIT
1	3200	1354.0	3.0	1351.0	127.0
1	1500	732.5	0.1	732.4	126.8
1	800	507.7	0.0	507.7	126.6
1	400	400.1	0.0	400.1	124.6
1	200	413.4	0.0	413.4	121.8
1	0	3250.0	0.0	3250.0	----
1	0	3280.0	0.0	3280.0	----
1	0	3410.0	0.0	3410.0	----
-1	3200	1450.0	5.4	1444.6	127.6
-1	1500	752.0	2.4	749.6	126.5
-1	800	510.0	1.8	508.2	125.3
-1	400	377.0	1.4	375.6	124.9
-1	204	301.0	1.3	299.7	124.0
-1	182	292.0	1.3	290.7	128.0
-1	188	298.0	1.3	296.7	----
-1	0	3000.0	0.0	3000.0	----
-1	0	2900.0	0.0	2900.0	----
-1	0	3350.0	0.0	3350.0	----
-1	0	2650.0	0.0	2650.0	----
-2	3200	716.2	6.8	709.4	134.2
-2	1500	398.6	3.0	395.6	133.2
-2	800	274.2	1.9	272.3	131.7
-2	400	188.0	1.4	186.6	131.0
-2	200	147.5	1.0	146.5	130.7
-2	200	148.7	1.0	147.7	128.0
-2	155	152.0	0.9	151.1	128.5
-2	155	146.0	0.8	145.2	128.0
-2	0	940.0	0.0	940.0	----
-2	0	1150.0	0.0	1150.0	----
-2	0	1050.0	0.0	1050.0	----
-2	0	1050.0	0.0	1050.0	----
-2	0	1120.0	0.0	1120.0	----
3	3200	581.0	10.9	570.1	120.0
3	1500	325.3	3.6	321.7	120.2
3	800	229.5	1.3	228.2	120.2
3	400	164.9	0.4	164.5	121.1
3	200	139.2	0.1	139.1	120.0
3	100	183.3	0.0	183.3	118.1
3	0	627.0	0.0	627.0	----
3	0	615.0	0.0	615.0	----
3	0	690.0	0.0	690.0	----
3	0	710.0	0.0	710.0	----
-3	3200	500.0	13.0	487.0	126.9
-3	1500	300.0	6.2	293.8	125.4

TABLE 4.2: Continued

-3	800	192.5	3.7	188.8	125.2
-3	400	138.2	2.9	135.3	122.2
-3	200	105.2	2.7	102.5	120.2
-3	156	106.0	2.6	103.4	116.5
-3	0	670.0	0.0	670.0	----
-3	0	670.0	0.0	670.0	----
-3	0	650.0	0.0	650.0	----
-3	0	640.0	0.0	640.0	----
-3	0	680.0	0.0	680.0	----
-3	0	520.0	0.0	520.0	----
-3	0	700.0	0.0	700.0	----
-3	0	600.0	0.0	600.0	----
5	3200	394.8	26.7	368.1	107.1
5	1500	227.7	9.3	218.4	108.4
5	800	166.2	3.9	162.3	109.4
5	400	119.8	1.7	118.1	110.3
5	200	107.6	0.8	106.8	110.4
5	100	117.7	0.1	117.6	113.7
5	0	346.0	0.0	346.0	----
5	0	338.0	0.0	338.0	----
-5	1500	234.5	12.7	221.8	110.0
-5	800	180.0	7.0	173.0	108.6
-5	400	144.0	4.7	139.3	107.7
-5	200	114.5	3.9	110.6	106.2
-5	100	82.0	3.6	78.4	98.7
-5	50	74.3	3.2	71.1	98.1
10	2620	221.9	50.5	171.4	121.5
10	1500	128.1	18.7	109.4	120.9
10	800	85.4	6.6	78.8	121.0
10	400	61.2	1.7	59.5	121.0
10	200	57.4	0.0	57.4	120.7
10	100	82.6	0.0	82.6	119.7
10	0	177.0	0.0	177.0	----
10	0	161.0	0.0	161.0	----
10	0	177.0	0.0	177.0	----
10	0	180.0	0.0	180.0	----
-10	2593	228.0	54.4	173.6	119.3
-10	1500	130.0	22.3	107.7	118.1
-10	800	82.4	12.0	70.4	116.1
-10	400	54.1	6.4	47.7	115.3
-10	200	40.7	4.2	36.5	114.2
-10	100	42.6	3.4	39.2	112.3
15	1750	151.9	50.2	101.7	121.7
15	1500	125.7	37.4	88.3	123.1
15	800	69.6	13.1	56.5	122.4
15	400	46.8	3.9	42.9	122.3
15	200	40.3	0.7	39.6	122.1
15	100	50	0.0	50.0	121.9
15	50	73.2	0.0	73.2	----
15	0	112	0.0	112.0	----
15	0	94	0.0	94.0	----

TABLE 4.2: Continued

20	1340	127.0	50.8	76.2	122.5
20	800	71.5	21.5	50.0	122.0
20	400	42.1	7.5	34.6	121.8
20	200	32.8	2.5	30.3	121.5
20	100	38.8	0.6	38.2	121.3
20	50	53.7	0.0	53.7	120.9
20	59	51.0	0.0	51.0	----
20	0	55.0	0.0	55.0	----
20	0	52.0	0.0	52.0	----
25	1080	113.1	52.0	61.1	122.5
25	800	79.1	30.2	48.9	122.9
25	400	40.9	9.9	31.0	123.1
25	200	31.6	3.6	28.0	122.3
25	100	35.5	1.0	34.5	121.0
25	50	45.1	0.4	44.7	120.5
25	17	57.9	0.6	57.3	----
25	0	70.0	0.0	70.0	----

TABLE 4.3: START-UP AND STALL ANGLES FOR MOTOR

INLET PRESSURE (PSI)	ANGLE AT WHICH MOTOR STARTS TURNING (DEGREES)	ANGLE AT WHICH MOTOR STOPS TURNING (DEGREES)
3000	-0.89	-0.18
3000	-0.72	-0.18
3000	1.52	0.20
2000	-1.55	-0.2
2000	-1.50	0.26
2000	0.92	0.26
2000	1.33	
1000	-2.04	-0.74
1000	-1.78	-0.34
1000	-1.78	0.40
1000	2.13	
750	-2.48	-0.87
750	-2.25	-0.87
500	-3.65	-1.35
500	-3.57	-0.60
500	3.45	0.67
500	3.23	
250	-6.99	-2.27
250	-5.83	-1.09
100	-17.19	-2.88
100	-18.13	-2.93

TABLE 4.4: REXROTH PUMP DATA

ANGLE = 1 DEGREE

PUMP SPEED (RPM)	DIFFERENTIAL PRESSURE (BAR)	VOLUMETRIC EFFICIENCY	MECHANICAL EFFICIENCY	TOTAL EFFICIENCY	CHAIN EFFICIENCY
201.3	5.98	0.781	0.214	0.167	0.621
201.0	48.02	0.531	0.647	0.344	0.852
201.7	121.50	0.264	0.737	0.195	0.941
403.7	4.40	0.904	0.130	0.118	0.645
420.8	51.17	0.721	0.609	0.439	0.853
402.8	98.83	0.524	0.731	0.384	0.908
805.5	3.88	0.944	0.009	0.008	0.664
812.4	48.43	0.768	0.511	0.393	0.920
807.6	99.49	0.591	0.687	0.405	0.930
809.8	148.58	0.438	0.768	0.337	0.928
807.4	204.96	0.208	0.819	0.171	0.916
1089.3	2.86	1.145	0.005	0.005	0.736
1089.6	49.32	0.824	0.475	0.392	0.840
1087.1	99.20	0.660	0.648	0.356	0.885
1088.9	150.40	0.485	0.735	0.356	0.937
1086.3	196.60	0.314	0.805	0.253	0.900
1083.1	246.30	0.009	0.819	0.007	0.940

TABLE 4.5: REXROTH PUMP DATA

ANGLE = 3 DEGREES

PUMP SPEED (RPM)	DIFFERENTIAL PRESSURE (BAR)	VOLUMETRIC EFFICIENCY	MECHANICAL EFFICIENCY	TOTAL EFFICIENCY	CHAIN EFFICIENCY
99.2	3.84	0.959	0.364	0.349	0.686
100.4	49.98	0.714	0.829	0.592	0.895
95.6	102.65	0.589	0.869	0.512	0.969
101.2	162.78	0.378	0.891	0.337	0.970
105.2	235.80	0.151	0.896	0.135	0.978
198.4	2.88	0.972	0.239	0.232	0.720
199.5	49.57	0.884	0.812	0.717	0.912
198.1	97.16	0.816	0.868	0.708	0.952
199.0	151.59	0.751	0.885	0.665	0.967
203.3	203.78	0.553	0.866	0.479	0.998
197.7	244.01	0.476	0.875	0.416	0.974
399.8	2.59	1.052	0.168	0.176	0.739
402.7	50.29	0.942	0.777	0.732	0.897
399.6	100.59	0.866	0.869	0.753	0.938
401.5	150.34	0.802	0.905	0.725	0.951
395.8	200.73	0.737	0.920	0.678	0.964
404.4	252.77	0.647	0.934	0.604	0.975
396.8	319.08	0.550	0.938	0.515	0.983
812.3	2.89	1.012	0.150	0.151	0.740
792.4	49.93	0.956	0.746	0.714	0.884
791.0	101.48	0.896	0.851	0.763	0.943
806.4	148.82	0.828	0.888	0.735	0.968
799.2	199.86	0.782	0.928	0.726	0.952
811.3	251.33	0.690	0.924	0.638	0.967
800.7	317.10	0.618	0.942	0.582	0.978
1094.5	3.36	1.003	0.158	0.158	0.744
1096.8	48.38	0.952	0.706	0.672	0.903
1093.4	98.90	0.894	0.846	0.756	0.925
1093.0	147.56	0.833	0.892	0.743	0.947
1094.0	197.32	0.773	0.915	0.707	0.981
1086.7	252.40	0.702	0.942	0.661	0.956
1084.0	321.52	0.607	0.943	0.573	0.984

TABLE 4.6: REXROTH PUMP DATA

ANGLE = 5 DEGREES

PUMP SPEED (RPM)	DIFFERENTIAL PRESSURE (BAR)	VOLUMETRIC EFFICIENCY	MECHANICAL EFFICIENCY	TOTAL EFFICIENCY	CHAIN EFFICIENCY
100.0	5.09	0.944	0.525	0.496	0.783
97.9	50.24	0.840	0.867	0.728	0.956
97.5	100.92	0.747	0.898	0.671	0.978
100.7	147.00	0.625	0.911	0.569	0.983
92.8	199.50	0.500	0.914	0.457	0.985
199.7	4.62	0.976	0.371	0.363	0.813
199.9	49.50	0.919	0.858	0.789	0.938
198.0	99.30	0.849	0.872	0.741	0.983
201.2	159.30	0.803	0.884	0.710	0.974
196.9	247.20	0.618	0.892	0.551	0.984
197.7	328.00	0.433	0.887	0.384	0.991
404.4	4.47	1.000	0.434	0.434	0.770
401.2	51.20	0.956	0.868	0.829	0.941
398.3	101.80	0.903	0.908	0.820	0.969
388.2	150.70	0.870	0.923	0.803	0.978
401.2	212.60	0.787	0.934	0.735	0.982
397.8	254.10	0.737	0.941	0.693	0.980
403.4	320.30	0.627	0.938	0.588	0.984
812.7	4.25	1.010	0.361	0.365	0.704
804.5	51.59	0.968	0.854	0.826	0.936
806.1	100.11	0.923	0.905	0.835	0.960
800.5	151.03	0.881	0.932	0.822	0.963
810.8	201.63	0.842	0.948	0.798	0.978
829.0	247.47	0.785	0.956	0.751	0.979
805.0	319.85	0.727	0.942	0.687	0.992
1087.8	5.08	1.037	0.327	0.339	0.776
1082.1	50.31	0.990	0.818	0.810	0.941
1077.2	94.55	0.969	0.899	0.871	0.952
1117.4	149.35	0.877	0.922	0.809	0.978
1110.2	210.84	0.832	0.944	0.786	0.980
1101.7	250.19	0.805	0.955	0.769	0.982
1091.7	315.37	0.734	0.949	0.696	0.987

TABLE 4.7: CHAIN BOX DATA

INPUT SPEED (RPM)	INPUT TORQUE (IN-LB)	CHAIN EFFICIENCY
364.3	15.5	0.621
179.5	15.9	0.686
359.0	17.3	0.720
730.5	18.0	0.645
181.0	21.2	0.783
723.4	21.5	0.739
1457.6	22.4	0.664
731.8	23.0	0.770
361.4	26.2	0.813
1971.1	26.9	0.736
1469.9	26.9	0.740
1470.6	28.8	0.704
1980.5	29.5	0.744
363.7	30.0	0.852
728.9	33.9	0.853
1968.4	34.4	0.776
1470.1	35.4	0.920
1971.7	42.5	0.840
728.9	51.2	0.908
1461.4	53.6	0.930
1967.1	59.5	0.885
365.0	60.3	0.941
361.0	69.0	0.912
181.7	69.5	0.895
1465.4	71.7	0.928
728.7	74.4	0.897
1970.4	75.2	0.937
1433.9	78.1	0.884
1984.7	78.2	0.903
1965.7	93.4	0.900
1461.0	93.9	0.916
177.2	104.1	0.956
361.7	105.8	0.938
726.0	107.9	0.941
1959.9	110.0	0.940
1455.8	110.9	0.936
1958.1	112.3	0.941
358.5	121.3	0.952
173.0	125.7	0.969
723.1	127.3	0.938
1978.5	130.4	0.925
1431.3	130.5	0.943
1459.2	178.7	0.968
726.5	180.1	0.951
1977.8	180.2	0.947
360.1	182.7	0.967
1949.2	189.9	0.952
183.1	194.2	0.970
176.4	197.3	0.978
1458.7	197.8	0.960

TABLE 4.7: Continued

720.7	198.8	0.969
358.3	198.9	0.983
1979.6	226.9	0.981
1446.2	233.2	0.952
716.2	233.5	0.964
367.9	243.1	0.998
190.4	277.7	0.978
182.2	282.0	0.983
2022.0	284.4	0.978
731.8	286.5	0.975
702.5	286.6	0.978
1448.5	289.0	0.963
1966.4	289.0	0.956
1468.1	290.0	0.967
357.7	295.4	0.974
364.1	317.8	0.974
1448.9	355.0	0.978
1961.5	357.0	0.984
718.0	357.0	0.983
1467.2	373.4	0.978
167.9	380.5	0.985
2008.9	391.4	0.980
726.0	398.2	0.982
1500.1	454.6	0.979
1993.6	458.4	0.982
719.8	472.9	0.980
356.3	483.6	0.984
1975.5	578.1	0.987
1456.7	585.5	0.992
730.0	595.9	0.984
357.7	640.9	0.991

APPENDIX C: Rexroth Pump/Motor Data

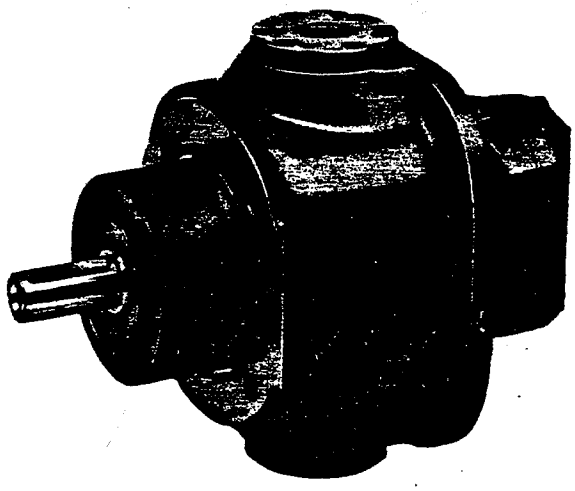
The following pages contain the manufacturer's data for the Rexroth A2V107HD. General information about the unit has been included with the rated efficiency characteristics.

Variable Displacement Pumps

Product Group AA2 · Basic units without Controls

AA2V

Sheet No. 2
Issue A 2/74



Contents	Page
Ordering Code	2
Description	3
Programme Structure	3
Design Features	3
Sizes according	4
Hydraulic Data	4
Calculating Sizes and Technical Data	5
Unit Dimensions for Sizes 12–225	6/7
Boost Pump	7
Unit Dimensions for Sizes 468–1830	8/9
Unit Dimensions for Valve Assembly for Sizes 12–225	10/11
Symbols	12
Performance Curve of Variable Displacement Pump	13
Q-n/P-n Characteristics	14
Adjustment	15
Input/Output Drive	16/17
Summary of Control Devices	18/19

HYDROMATIK
A MEMBER OF THE REXROTH-GROUP

Ordering Code

Item	Short code 1	2	3	4	5	6	7	8	9	10
	AA2V	107	AHd	g	r	1	G	2	1	P

1 Pump Type

Product group	AA2
Variable	V

2 Size

(displ. 0.708 in³/rev.)	12
(displ. 1.714 in³/rev.)	28
(displ. 3.364 in³/rev.)	55
(displ. 6.528 in³/rev.)	107
(displ. 13.729 in³/rev.)	225
(displ. 28.567 in³/rev.)	468
(displ. 55.867 in³/rev.)	915
(displ. 111.847 in³/rev.)	1830

3 Control Devices [1])

without controls	OV
const. HP contr., direct op.	Ld
const. HP contr., pilot op.	Lv
constant pressure control	ADr
handwheel control	AMa
mechanical rod control	Ge
electrical control	AEl
hydr. contr., flow related	AHm
hydr. contr., pressure related	AHd
hydr. manual servo control	AHw

4 Type of Circuit

open circuit	O
closed circuit	C
half-closed circuit [2])	H

5 Direction of Rotation

clockwise	R
counter-clockwise	L
both directions	W

6 Series

series no.	1

7 Design

submersible pump [3])	S
housed pump	G

8 Valve Assembly (up to Size 225)

without valve assembly	0
with pressure relief valve	1
with valve block	2

9 Boost Pump (Size 28—225)

without boost pump	0
with boost pump	1

10 Shaft End

keyed	P

Add code details for control device.

Ld	Constant HP control, direct operated	**2-1**
Lv	Constant HP control, pilot operated	**2-2**
ADr	Constant pressure control	**2-3**
AMa	Handwheel control	**2-4**
Ge	Mechanical rod control	**2-5**
AEl	Electrical control	**2-6**
AHm	Hydraulic control, flow related	**2-7**
AHd	Hydraulic control, pressure related	**2-8**
AHw	Hydraulic manual servo control	**2-9**

[1]) Suitability of controls and designs for the various pump sizes.

Sizes

Control devices	12	28	55	107	225	468	915	1830
OV	E/G	E/G	E/G	E/G	E/G	E/G	E/G	G
Ld	E/G	E/G	E/G	E/G	E/G			
Lv				E	E	E/G	E/G	
ADr	E/G	E/G	E/G	E/G	E/G			
AMa	G	G	G	G	G			
Ge	G	G	G	G				
AEl	G	G	G	G	G	G	G	
AHm			E/G	E/G	E G	E/G	E G	
AHd			E/G	E/G	E G	E/G	E/G	G
AHw		G	E/G	E/G	E/G			

E = only as submersible pump
G = only as housed pump
E/G = both designs possible

[2]) Size 28 not normally available with control devices Ld, ADr, AMa, Ge, AEl or AHw

[3]) not for size 1830

Description

The variable displacement axial piston pump can operate either as a pump or as a motor. The flow is proportional to the drive speed and the displacement and is infinitely variable by changing the swivel angle at constant speed. Flow increases as the pump is swivelled from '0' to its maximum angle (25). Swivelling the pump over centre or changing the direction of rotation changes the direction of flow.

Programme Structure

The AA2 programme up to size 225 is designed as unit construction system. The basic unit comprises the variable displacement pump without controls. The variable displacement pump is available in design E or G. The Various control devices such as horsepower control, pressure control, etc. are mounted directly on the pump. Design E is for mounting inside the oil tank and design G for mounting outside the tank.

The various control devices for the sizes 468 to 1830 are incorporated in the pump housing.

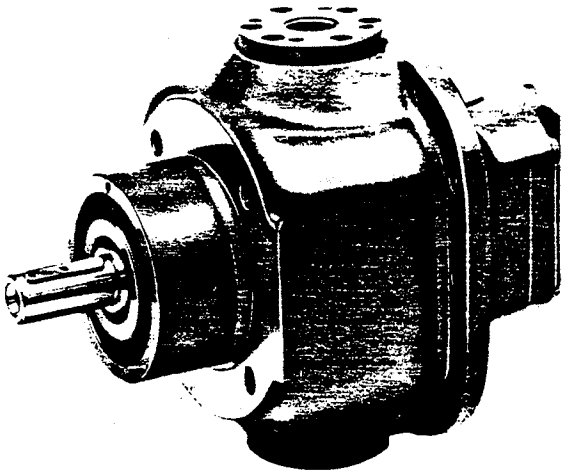
The ordering code is made up of the model code for the basic variable displacement pump (sheet no. 2) and that of the appropriate control device.

Design Features

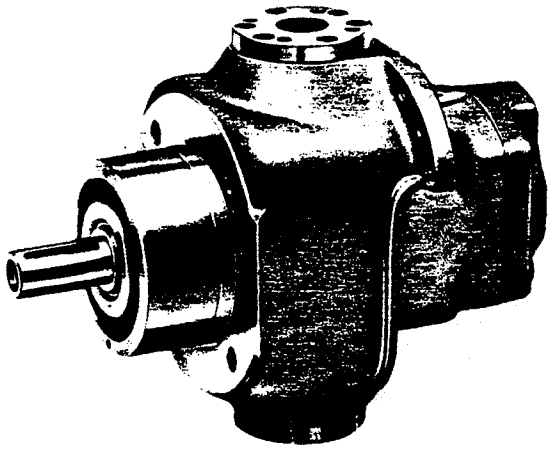
7 Pistons/Piston Rods
Spherical control surface cylinder positioning
Rigid shaft support
Swivel range from 0 to ± 25°
Oil channeling via a turning connection
The units are force controlled and can work as a pump or motor. In pump operation, the rate of flow is proportional to the turning speed and the stroke volume and can be infinitely adjusted without throttling by changing the swivel angle. By swivelling the pump through the zero position ($\alpha = 0$) or reversing the direction of rotation, the direction of flow smoothly changes its direction. In motor operation, the output speed is proportional to the rate of consumption and vice versa proportional with the stroke volume. The output torque increases with the pressure drop between the high and low pressure sides.

Special Characteristics

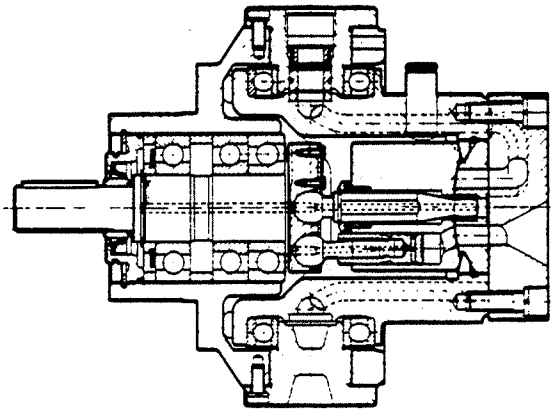
High efficiencies
Low positioning forces
Insensibility to contamination
Favourable starting characteristics
Open constructional design possible
Good suction characteristics even at higher speeds
Good supplementary suction capabilities



Design G (housed pump)



Design E (submersible pump)



Sectional drawing of the variable displacement pump

Sizes according

Design: Variable displacement axial piston pump in bent axis design.

Mounting Method: Flange or foot
Weight [lb] (see unit dimensions)

Mounting Position: optional

Direction of Flow

Position Indicator		CW-Rotation open circuit	CW-Rotation closed and half-closed circuit	CCW-Rotation open circuit	CCW-Rotation closed and half-closed circuit
Swivel direction	Right	S to B A plugged	A to B	S to A B plugged	B to A
	Left	S to A B plugged	B to A	S to B A plugged	A to B

Direction of Rotation: With variable displacement pumps, direction of rotation is normally clockwise viewed on the shaft end. If direction of rotation is counter-clockwise the direction of flow is reversed.
With boost pump direction of rotation normally clockwise viewed on the shaft end. With counter-clockwise rotation the direction of flow is unchanged, but the gerotor insert is turned through 180°.

Drive Speed Range
Minimum speed n_{min} no limitations.
Maximum speed n_{max} [Rpm] (see table, page 5)

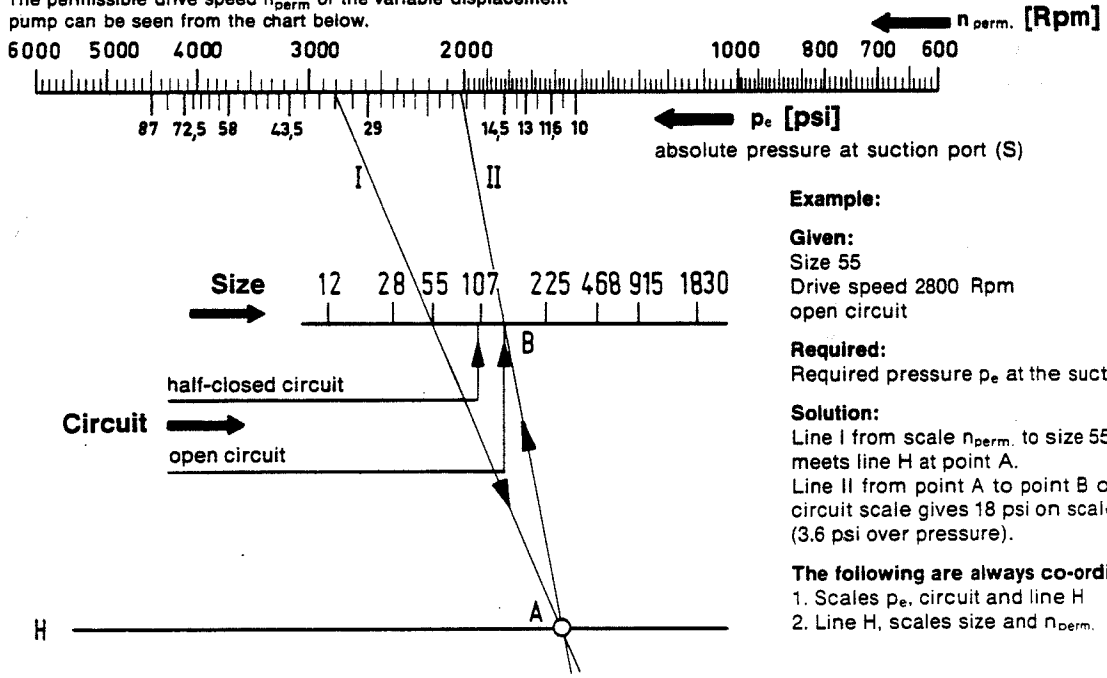
In half-closed circuit the full flow is drawn off.

The maximum drive speed can be increased at swivel angle $15° < \alpha < 25°$ so that the flow remains constant. However, the speeds shown for boosted operation may not be exceeded.

Should it be necessary to exceed the values indicated, please obtain prior approval from us.

The maximum drive speed for self-priming operation ($\alpha = 25°$) can be increased when inlet pressure $p_e > 14.5$ psi, but must be reduced when $p_e < 14.5$ psi.

The permissible drive speed n_{perm} of the variable displacement pump can be seen from the chart below.



Example:

Given:
Size 55
Drive speed 2800 Rpm
open circuit

Required:
Required pressure p_e at the suction port

Solution:
Line I from scale $n_{perm.}$ to size 55 meets line H at point A.
Line II from point A to point B on the circuit scale gives 18 psi on scale p_e (3.6 psi over pressure).

The following are always co-ordinated:
1. Scales p_e, circuit and line H
2. Line H, scales size and $n_{perm.}$

Hydraulic Data

Operating pressure range, inlet side
Variable displacement pump and boost pump:
(absolute pressure at suction inlet S)
$p_{e\,min}$ 11.6 psi, $p_{e\,max}$ 29 psi (14.5 psi over pressure)

Operating pressure range, outlet side

Variable displacement pump:

Ports A, B
Max. continuous operating pressure ____ p_D 4640 psi
Peak pressure ____ p_{max} 5800 psi

Boost pump:
Operating pressure range, outlet side

Pressure at port G
Max. operating pressure ____ p_D 435 psi

Variable Displacement Pump and Boost Pump:

Fluid temperature range
ϑ_{min} ____ − 13° F ϑ_{max} ____ + 176° F

Viscosity range
ν_{min} ____ 60 SUS ν_{max} ____ 4635 SUS

Optimum operating viscosity
ν_{opt} ____ 80 . . . 120 SUS

Hydraulic Medium
Mineral oils. Detailed information on mineral oils, fire-resistant fluids, etc. is contained in our oil recommendation sheet no. 0-1

Filtration of Hydraulic Medium
recommended filtration ____ 25—40 µm

It should be noted that the finer the filtration, the greater the working life of the oil.

Calculation of Sizes and Technical Data

Flow	$Q = \frac{Vg \cdot n \cdot \sin\alpha \cdot \eta_v}{231 \cdot \sin 25°}$	[gpm]
Torque	$M = \frac{Vg \cdot \Delta p \cdot \sin\alpha}{24 \cdot \pi \cdot \sin 25° \cdot \eta_{mh}}$	[lb ft]
Power	$P = \frac{M \cdot n}{5252} = \frac{Q \cdot \Delta p}{1715 \cdot \eta_{mh}}$	[HP]

Vg = Max. geometric displacement [in³/rev.]
M = Torque [lb ft]
Δp = Differential pressure [psi]
n = Speed [Rpm]
η_v = volumetric efficiency
η_t = overall efficiency
η_{mh} = mechanical-hydraulic efficiency
α = swivel angle [°]

Technical Data

Size	Dim.	12	28	55	107	225	468	915	1830
Displacement Vg^3 of the Variable Pump ($\alpha = 25°$)	in³/rev.	0.708	1.714	3.344	6.529	13.729	28.557	55.837	111.67
Displacement of the Boost Pump	in³/rev.	–	0.226	0.824	1.428	2.325	–	–	–
Torque Constants[4] ($\alpha = 25°$)	$\frac{lb \cdot ft}{100\ psi}$	0.938	2.270	4.424	8.630	18.158	37.812	73.827	148.152
Maximum Speed Boosted n_{max}	rpm	6000	4750	3750	3000	2360	1900	1500	1200
Maximum Speed in Open Circuit n_{oc}[1])	rpm	4000	3000	2500	2000	1500	1200	1000	–
Maximum Speed in Half-Closed Circuit n_{hc}[1])	rpm	3650	2750	2200	1750	1350	1100	875	690
Maximum Speed with mounted Boost Pump p_{max} = 435 psi	rpm	–	3150	2500	2000	1600	–	–	–
Moment of Inertia GD^2	lb · ft²	0.0408	0.1614	0.4983	1.5899	5.0545	21.357	66.682	237.30

Performance (theoretical values, not taking into accout η_{mh} and η_v)

Size		Dim.	12	28	55	107	225	468	915	1830
Electric Motor Speed		rpm	1800	1800	1800	1800	1200	1200	900	900
Flow at Electric Motor Speed		gpm	5.52	13.36	26.06	50.87	71.32	148.4	217.5	435.1
Power at Electric Motor Speed	Δp = 3000 psi	HP	9.7	23.4	45.6	89	125	259	380	761
	Δp = 4500 psi	HP	14.5	35.1	68.4	134	187	389	571	1142
	Δp = 5800 psi	HP	18.7	45.2	88.1	172	241	502	736	1471
Flow at Speed n_{max}		gpm	18.39	35.24	54.29	84.79	140.3	234.9	362.5	580.1
Power at Speed n_{max}	Δp = 3000 psi	HP	32.2	61.6	95.0	148	245	411	634	1015
	Δp = 4500 psi	HP	48.3	92.4	143	222	368	616	951	1522
	Δp = 5800 psi	HP	62.2	119.0	184	287	475	794	1226	1962
Flow at Speed n_{oc}[2])		gpm	11.89	21.59	35.10	54.83	86.47	143.9	234.5	–
Power at Speed n_{oc}	Δp = 3000 psi	HP	20.8	37.8	61.4	95.9	151	252	410	–
	Δp = 4500 psi	HP	31.2	56.6	92.1	144	227	378	615	–
	Δp = 5800 psi	HP	40.2	73.0	119	185	292	487	793	–
Torque at	Δp = 3000 psi	lb · ft	28.1	68.10	133	259	545	1134	2215	4445
	Δp = 4500 psi	lb · ft	42.2	102	199	388	817	1701	3322	6667
	Δp = 5800 psi	lb · ft	54.4	132	257	500	1053	2193	4282	8593

1) Values apply when absolute pressure at suction inlet S = 14.5 psi and when operated on mineral oil as well as an oil viscosity ν = 60 . . . 4635 SUS.

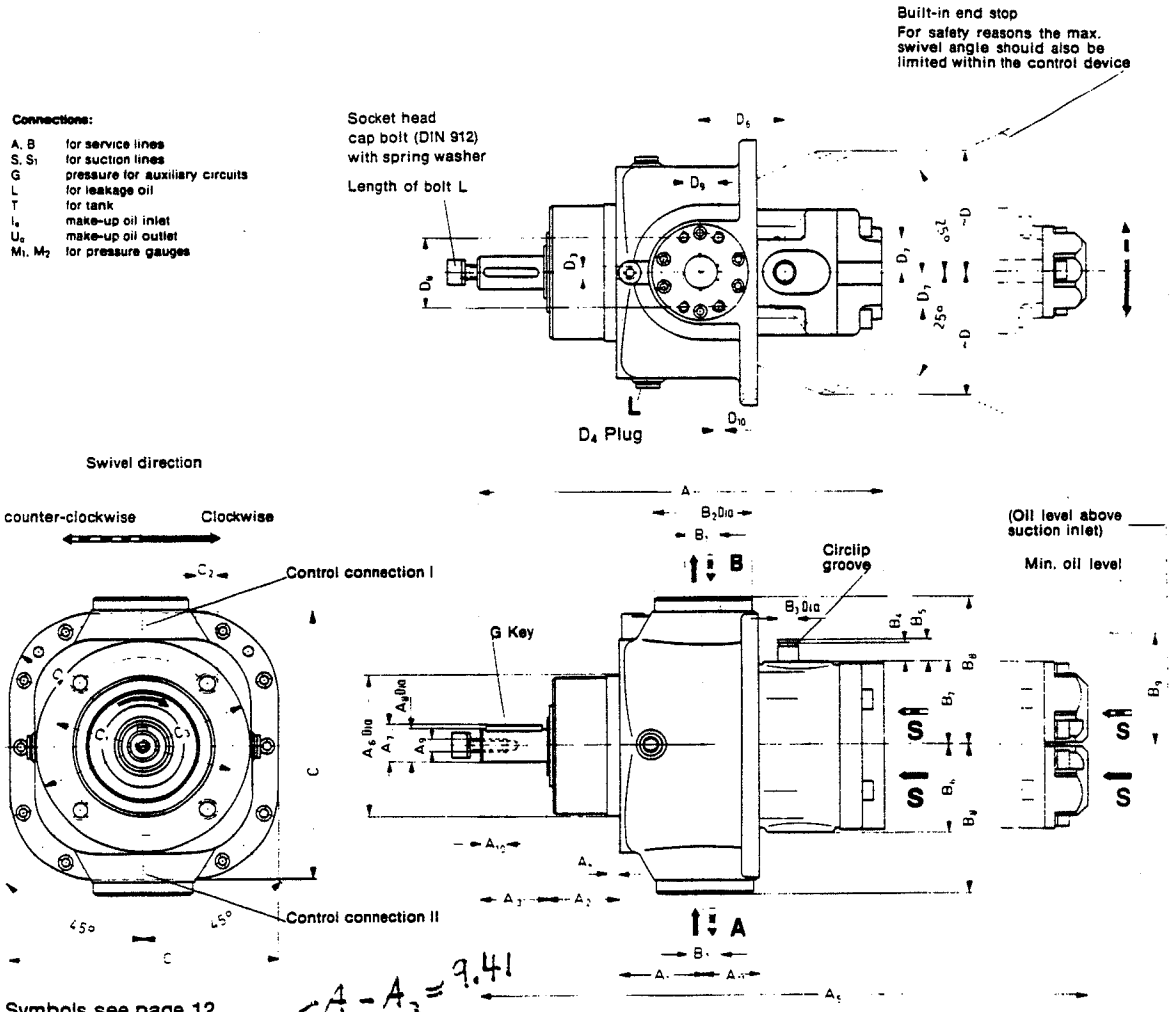
2) 3 % displacement losses included.

3) In open and half-closed circuits, Vg is 3 % less.

4) Without considering η_{mh}.

Unit Dimensions, Sizes 12–225

Design G



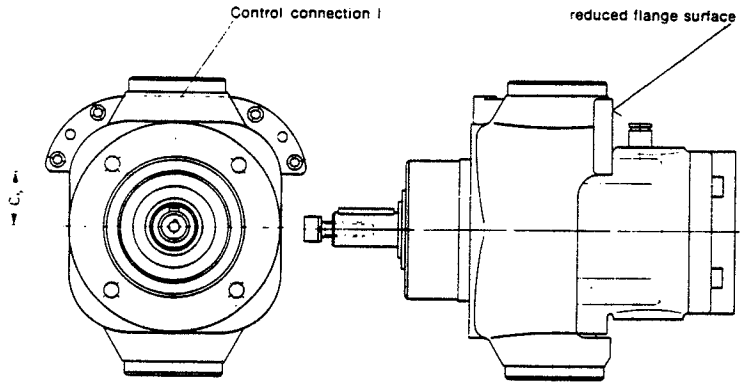
Symbols see page 12

$A - A_3 = 9.41$

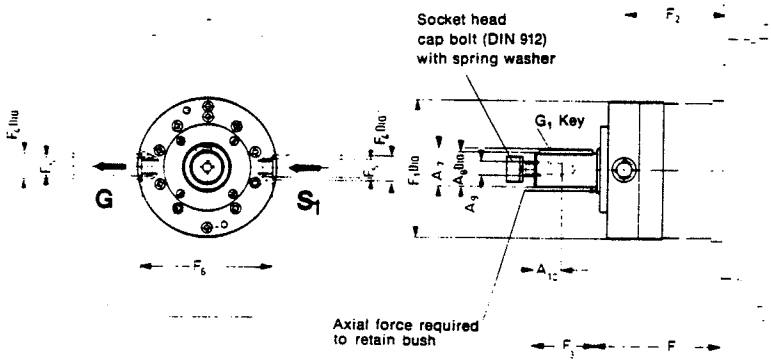
Size	A	A_1	A_2	A_3	A_4	A_5	A_6 max.	A_6 min.	A_7	A_8 max.	A_8 min.	A_9 thread	A_{10}	A_{11}	B_1 DIA	B_2 DIA	B_3 max.	B_3 min.
12	8.93	1.96	1.57	1.57	0.23	9.84	3.1496	3.1461	0.885	0.7879	0.7874	M 6	0.47	1.26	0.50	2.36	0.4718	0.4711
28	11.37	2.44	1.96	1.96	0.31	12.60	3.9370	3.9335	1.098	0.9848	0.9843	M 8	0.63	1.57	0.75	2.87	0.6299	0.6285
55	14.17	3.03	2.48	2.36	0.39	15.74	4.9212	4.9173	1.295	1.1818	1.1811	M 12	1.00	1.96	0.75	3.46	0.7866	0.7857
107	17.71	3.54	3.15	3.15	0.47	19.68	6.2992	6.2952	1.696	1.5755	1.5748	M 12	1.00	2.48	1.00	4.33	0.9834	0.9826
225	22.24	4.41	3.93	3.93	0.63	24.68	7.8740	7.8694	2.106	1.9693	1.9685	M 16	1.25	2.95	1.25	5.11	1.2588	1.2578

Size	D_6	D_7	SAE – 6000 PSI D_8 ± 0.01	D_9 ± 0.01	D_{10} UNC - 2 B	depth	F	F_1	F_2	F_3	F_4	F_5 thread	depth	with Adapter thread*	part-no	F_6
12	1.96	0.84	1.594	0.718	5/16 - 18	0.81	–	–	–	–	–	–	–	–	–	–
28	2.36	0.99	2.000	0.937	3/8 - 16	0.94	3.54	3.89	2.69	1.96	–	M 16×1.5	0.47	3/4 - 16	70222	3.78
55	2.95	1.24	2.000	0.937	3/8 - 16	0.94	4.37	4.90	3.66	2.12	1.10	M 22×1.5	0.55	7/8 - 14	70223	4.74
107	3.74	1.57	2.250	1.093	7/16 - 14	1.06	5.51	6.26	4.62	2.83	1.10	M 22×1.5	0.55	1 1/16 - 12	70224	6.06
225	4.64	1.96	2.625	1.250	1/2 - 13	1.00	6.53	7.83	5.51	3.93	1.26	M 26×1.5	0.63	1 3/16 - 12	70225	7.63

Design E

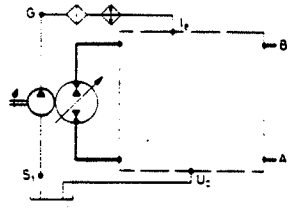


Mounting of boost pump, from size 28, designs G and E

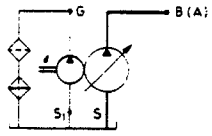


Boost Pump

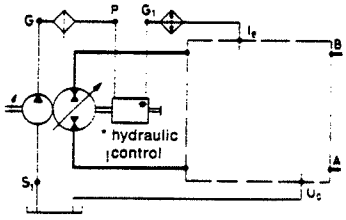
It is possible to fit an auxiliary pump on the sizes 28, 55, 107 and 225. This is used mainly as a boost pump, but can also be used as a pilot pressure pump or for cooling and filtering circuits.



Auxiliary pump as boost pump



Auxiliary pump for cooling and filtering circuit



Auxiliary pump as control and boost pump

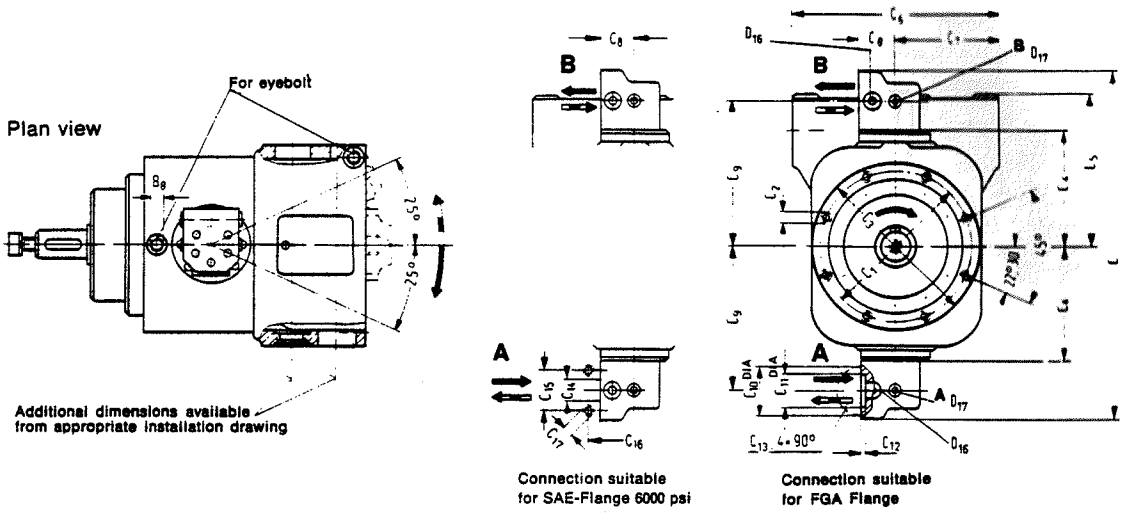
Size	B_4	B_5	B_6	B_7	B_8	B_9	C	C_1 ± 0.008	C_2 UNC - 2 B depth	C_3	C_4	C_5	D	D_3 UNC - 2 B depth		D_4 UNF - 2 B
12	0.433	0.47	1.93	1.87	4.13	3.93	5.28	3.93	5/16 - 18	0.47	4.64	1.92	0.98	2.67	–	–	1/2 - 20
28	0.511	0.59	2.42	2.36	5.08	4.33	7.28	4.92	3/8 - 16	0.59	5.90	2.38	1.26	3.42	–	–	9/16 - 18
55	0.677	0.78	3.05	2.95	6.10	4.72	9.29	6.30	5/8 - 11	0.94	7.48	3.07	1.65	4.33	–	–	3/4 - 16
107	0.834	0.94	3.83	3.74	7.20	5.11	11.26	7.87	5/8 - 11	0.94	9.29	3.34	2.26	5.37	5/16 - 18	0.94	3/4 - 16
225	1.043	1.18	4.80	4.64	8.46	5.51	14.01	9.84	3/4 - 10	1.18	11.81	4.25	2.75	6.83	1/2 - 13	1.00	7/8 - 14

* Straigth Thread 0-Ring Boss UNF - 2 B

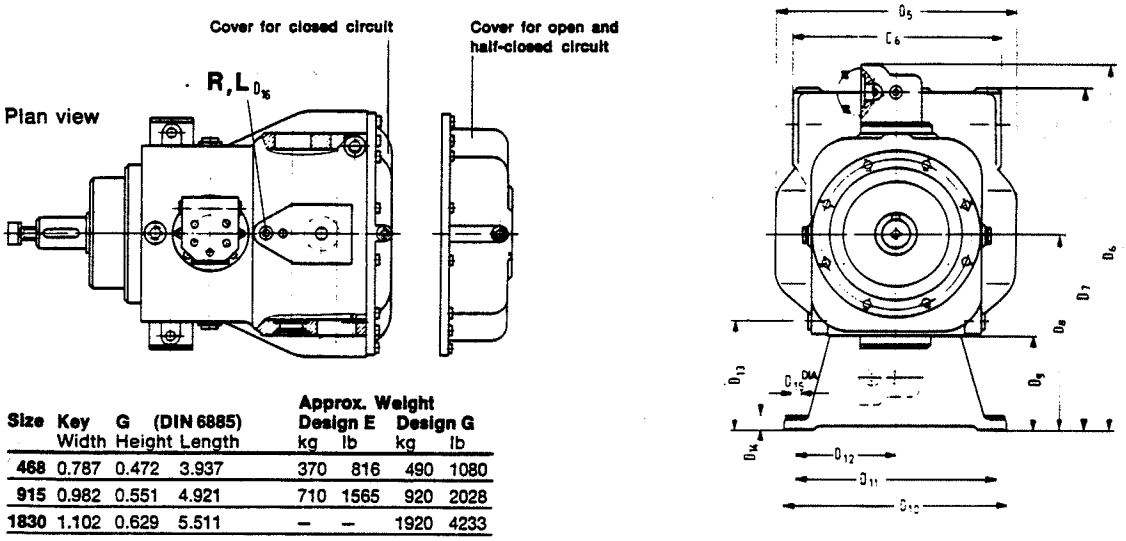
Size	Key Width	G (DIN 6885) Height	Length	Key Width	G_1 (DIN 6885) Height	Length	L	Approx. Weight Var. displ. pump E kg	Design lb	G kg	lb	Boost pump kg	lb	Relief valve kg	lb	Valve block kg	lb
12	0.236	0.236	1.26	–	–	–	0.98	9	19.8	10	22.0	–	–	1.0	2.2	9	19.8
28	0.315	0.275	1.57	0.315	0.275	1.57	1.18	17	37.5	18	39.7	0.5	1.1	1.4	3.1	10	22.0
55	0.315	0.275	1.96	0.315	0.275	1.77	1.57	35	77.2	37	81.6	1.0	2.2	2.2	4.9	12	26.5
107	0.472	0.315	2.48	0.427	0.315	2.48	1.57	63	139.0	67	148.0	3.0	6.6	3.9	8.6	20	44.1
225	0.511	0.354	3.14	0.551	0.354	3.14	1.96	120	265.0	130	287.0	6.0	13.2	6.9	15.2	36	79.4

Unit Dimensions, Sizes 468, 915 and 1830

Design E



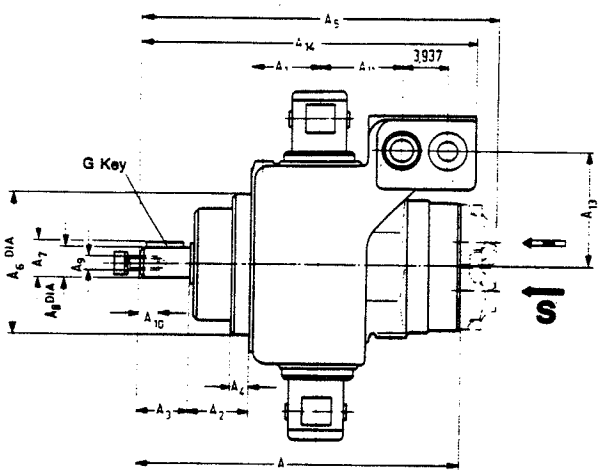
Design G

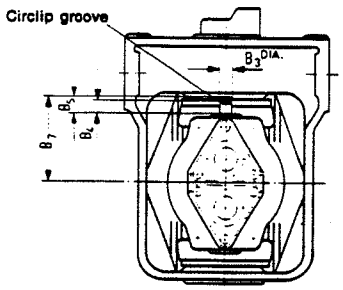


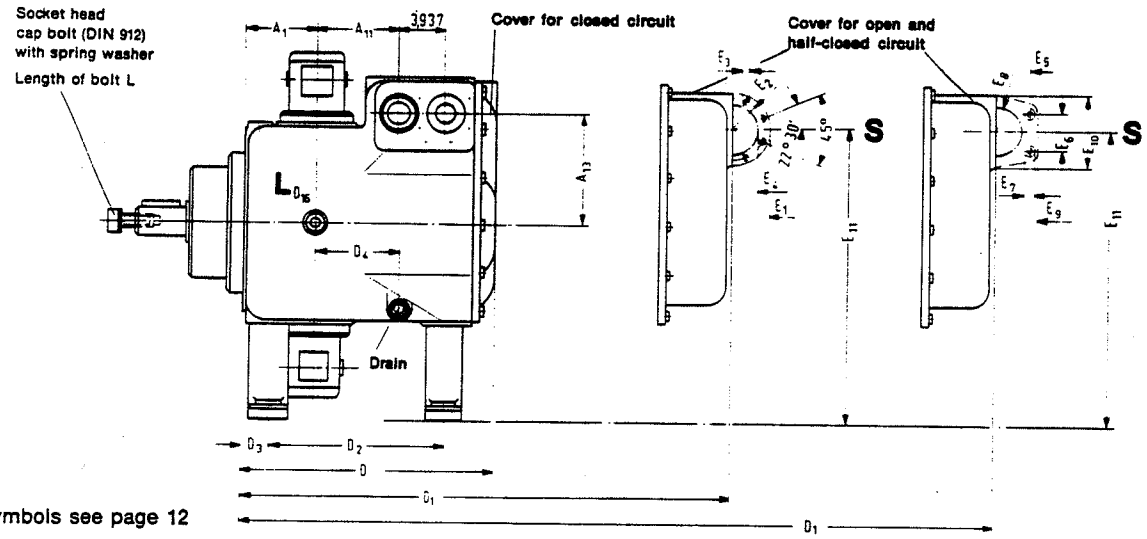
Size	Key Width	G Height	(DIN 6885) Length	Approx. Weight Design E kg	Design E lb	Design G kg	Design G lb
468	0.787	0.472	3.937	370	816	490	1080
915	0.982	0.551	4.921	710	1565	920	2028
1830	1.102	0.629	5.511	–	–	1920	4233

Size	A	A_1	A_2	A_3	A_4	A_5	A_6 max.	A_6 min.	A_7	A_8 max.	A_8 min.	A_9 thread	A_{10}	A_{11}	A_{12}	A_{13}	B_3 max.	B_3 min.	B_4	B_5
468	27.67	6.29	4.40	4.33	1.26	31.02	12.5984	12.5949	2.937	2.7567	2.7559	M 20	1.53	7.28	29.01	9.84	1.3769	1.3759	1.24	1.33
915	34.64	7.87	5.31	5.51	1.57	38.77	15.7480	15.7442	3.752	3.5442	3.5434	M 24	1.96	8.89	34.29	12.59	1.7706	1.7696	1.85	1.96
1830	–	9.84	6.88	6.69	1.96	–	19.6850	19.6812	4.566	4.3316	4.3308	M 24	1.96	11.41	–	15.35	2.2035	2.2023	2.04	2.16

Size	SAE 6000 psi C_{14}	C_{15} ± 0.01	C_{16} ± 0.01	C_{17} UNC - 2 B depth	D	D_1	D_2	D_3	D_4	D_5	D_6	D_7	D_8	D_9	D_{10}	D_{11}	D_{12}	D_{13}	D_{14}	D_{15}
468	1.50	3.125	1.437	5/8 - 11	1.38	21.65	26.58	15.74	1.96	4.72	22.04	30.90	29.13	15.75	6.69	20.07	17.71	8.85	8.07	1.26	1.02
915	2.0	3.815	1.750	3/4 - 10	1.50	25.98	32.09	17.71	2.75	5.90	27.36	36.81	35.63	18.70	7.28	23.62	20.86	10.43	8.85	1.57	1.30
1830	–	–	–	–	–	47.04	54.13	21.26	3.34	7.87	34.64	43.70	42.51	22.04	7.67	29.52	26.37	13.18	9.25	1.96	1.53







Symbols see page 12

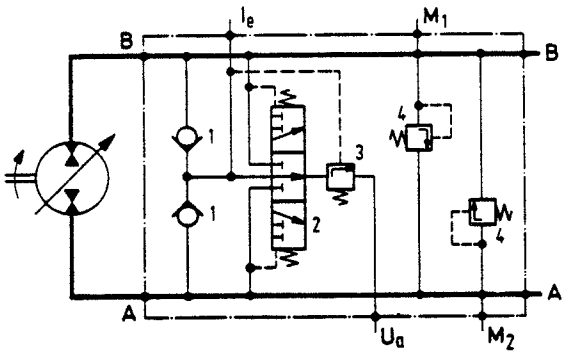
B_7	B_8 UNC - 2 B	depth	C	C_1 ± 0.008	C_2 UNC - 2 B	depth	C_3	C_4	C_5	C_6	C_7	C_8	C_9	FGA-Flange C_{10}	C_{11}	C_{12}	C_{13} UNC - 2 B	depth
7.63	1 - 8	1.49	30.31	14.17	5/8 - 11	0.94	15.74	9.84	13.38	18.66	9.33	3.34	12.59	–	–	–	–	–
9.84	1 1/8 - 7	1.77	36.22	17.71	3/4 - 10	1.18	19.68	12.40	16.93	22.24	11.12	3.93	15.35	–	–	–	–	–
12.00	1 1/2 - 6	2.12	43.30	22.04	1 - 8	1.41	24.80	15.35	20.47	26.85	13.42	4.72	18.50	5.70	3.58	0.23	1 - 8	1.49

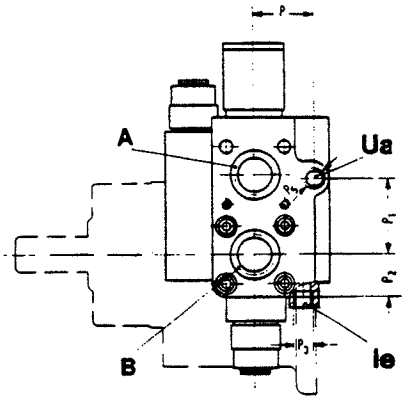
Straight thread D_{16} UNF - 2 B	depth	0-Ring Boss D_{17} UNF - 2 B	depth	E_1	E_2	E_3 thread	depth	E_4	E_5 ± 0.01	E_6 ± 0.01	E_7 UNC - 2 B	depth	E_8	E_9	E_{10}	E_{11}	L
1 5/16 - 12	0.91	3/4 - 16	0.67	–	–	–	–	–	6.000	3.625	5/8 - 11	1.31	5.00	7.40	7.28	24.57	2.36
1 5/8 - 12	0.91	3/4 - 16	0.67	10.71	8.86	5/8 - 11	1.1	5.90	–	–	–	–	–	–	–	29.72	2.75
1 7/8 - 12	0.91	3/4 - 16	0.67	12.99	11.02	5/8 - 11	0.94	7.87	–	–	–	–	–	–	–	34.65	2.75

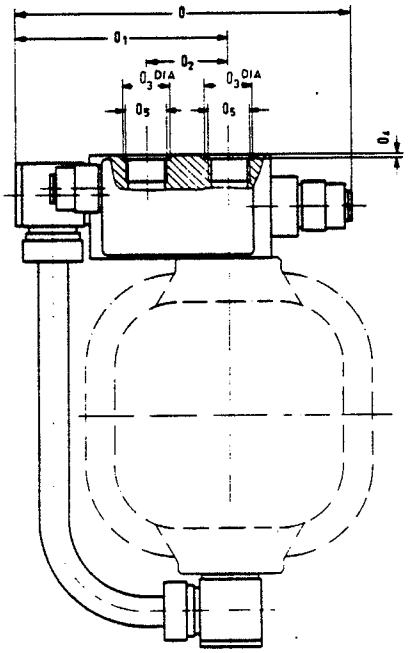
Dimensions for Valve Assembly, Sizes 12–225

Built-on valve block (pressure side A, B varying) for closed circuits.

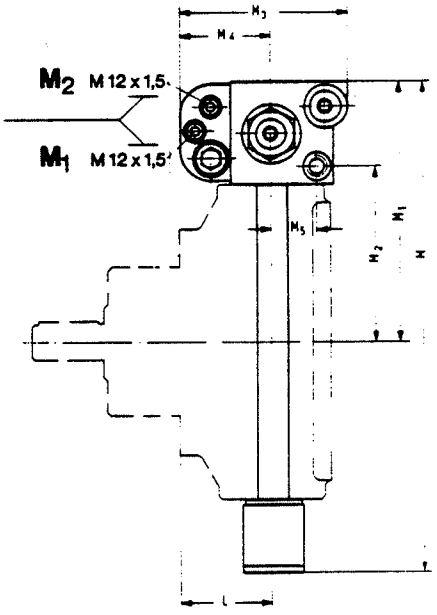
2 pressure sides permit 2 moment directions at the power take-off with a hydraulic motor as consumer.





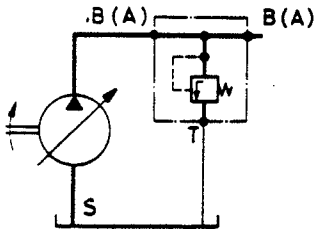


with adapter thread * 7/16 - 20 part-no. 70569

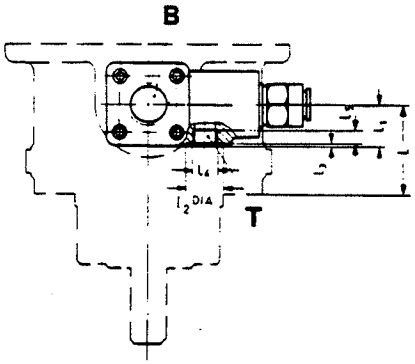


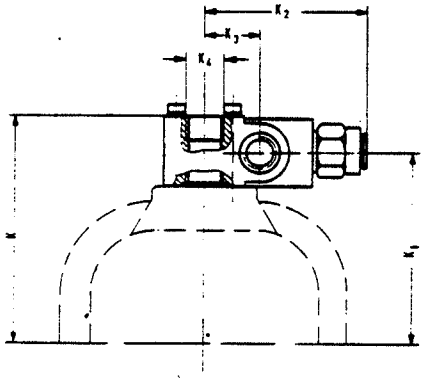
Size	K	K1	K2	K3	K4 thread	depth	with adapter thread *	part-no.	L	L1	L2	L3	L4 thread	L5	with adapter thread *	part-no.	M	M1	M2	M3	M4
12	5.15	4.25	4.31	1.26	M 22 x 1.5	0.55	7/8 - 14	70223	1.96	0.88	–	–	M 18 x 1.5	0.47	3/4 - 16	70230	15.51	8.97	6.33	4.40	2.40
28	6.14	5.15	4.54	1.57	M 27 x 2	0.63	1 1/16 - 12	70226	2.44	1.08	1.10	0.04	M 22 x 1.5	0.55	7/8 - 14	70223	13.93	7.40	4.76	4.40	2.40
55	7.42	6.31	5.25	1.81	M 33 x 2	0.71	1 5/16 - 12	70227	3.03	1.30	1.30	0.06	M 27 x 2	0.63	1 1/16 - 12	70226	16.28	8.60	5.80	5.43	2.95
107	8.85	7.57	6.53	2.28	M 42 x 2	0.79	1 5/8 - 12	70228	3.54	1.57	1.57	0.06	M 33 x 2	0.71	1 5/16 - 12	70227	19.60	10.39	7.00	6.37	3.46
225	10.94	9.40	8.07	2.83	M 48 x 2	0.87	1 7/8 - 12	70229	4.40	1.96	1.96	0.06	M 42 x 2	0.79	1 5/8 - 12	70228	24.68	12.79	8.85	7.91	4.25

Built-on pressure relief valve
for open circuits



Built-on pressure relief valve





Connections:

A, B	for working lines
Ie	Boost fluid inlet
Ua	Make-up fluid outlet
M_1, M_2	Gauge connections
T	Tank

Weights [lb] (see unit dimensions Page 7)

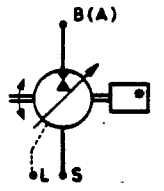
* Straight Thread 0-Ring Boss UNF - 2 B

M_5	O	O_1	O_2	O_3	O_4	O_5 thread	depth	with adapter thread *	part-no.	P	P_1	P_2	P_3 thread	depth	with adapter thread *	part-no.	P_5 thread	depth	with adapter thread *	part-no.
1.33	9.74	6.61	2.20	1.37	0.11	M 27 x 2	0.63	1 1/16 - 12	70226	1.53	2.52	1.33	M 16 x 1.5	0.47	3/4 - 16	70222	M 16 x 1.5	0.47	3/4 - 16	70222
1.33	9.74	6.61	2.20	1.37	0.11	M 27 x 2	0.63	1 1/16 - 12	70226	1.53	2.52	1.33	M 16 x 1.5	0.47	3/4 - 16	70222	M 16 x 1.5	0.47	3/4 - 16	70222
1.49	10.94	6.98	2.63	1.61	0.11	M 33 x 2	0.71	1 5/16 - 12	70227	1.96	2.48	1.37	M 16 x 1.5	0.47	3/4 - 16	70222	M 18 x 1.5	0.47	3/4 - 16	70230
1.89	13.22	8.50	3.22	2.12	0.17	M 42 x 2	0.79	1 5/8 - 12	70228	2.36	3.07	1.65	M 18 x 1.5	0.47	3/4 - 16	70230	M 18 x 1.5	0.47	3/4 - 16	70230
2.44	15.31	9.92	4.01	2.36	0.17	M 48 x 2	0.87	1 7/8 - 12	70229	2.67	4.01	2.10	M 22 x 1.5	0.55	7/8 - 14	70223	M 22 x 1.5	0.55	7/8 - 14	70223

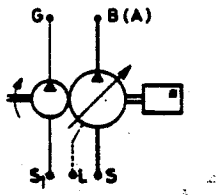
Symbols

Open circuit

without valve assembly

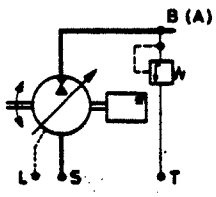


without boost pump

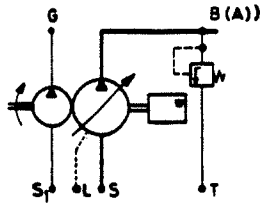


with boost pump
Sizes 28–225

with valve assembly
(up to size 225)



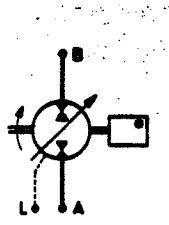
without boost pump



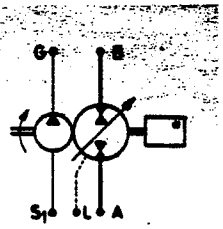
with boost pump
which can be used
as make-up pump

Closed Circuit

without valve assembly

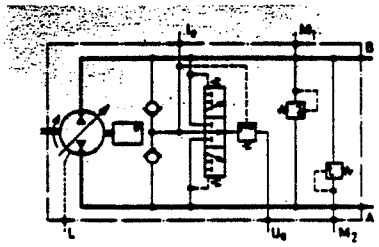


without boost pump

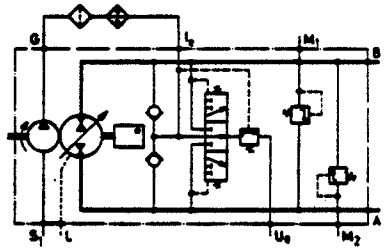


with boost pump
Sizes 28–225

with valve assembly
(up to size 225)



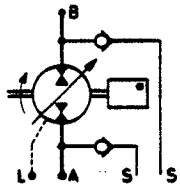
without
boost pump



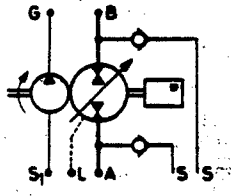
with
boost pump

Half-closed Circuit

without valve assembly



without boost pump



with boost pump
Sizes 28–225

Connections:

A, B	for service lines
S, S_1	for suction lines
G	pressure for auxiliary circuits
L	for leakage oil
T	for tank
I_e	boost oil inlet
U_a	make-up oil outlet
M_1, M_2	for pressure gauges

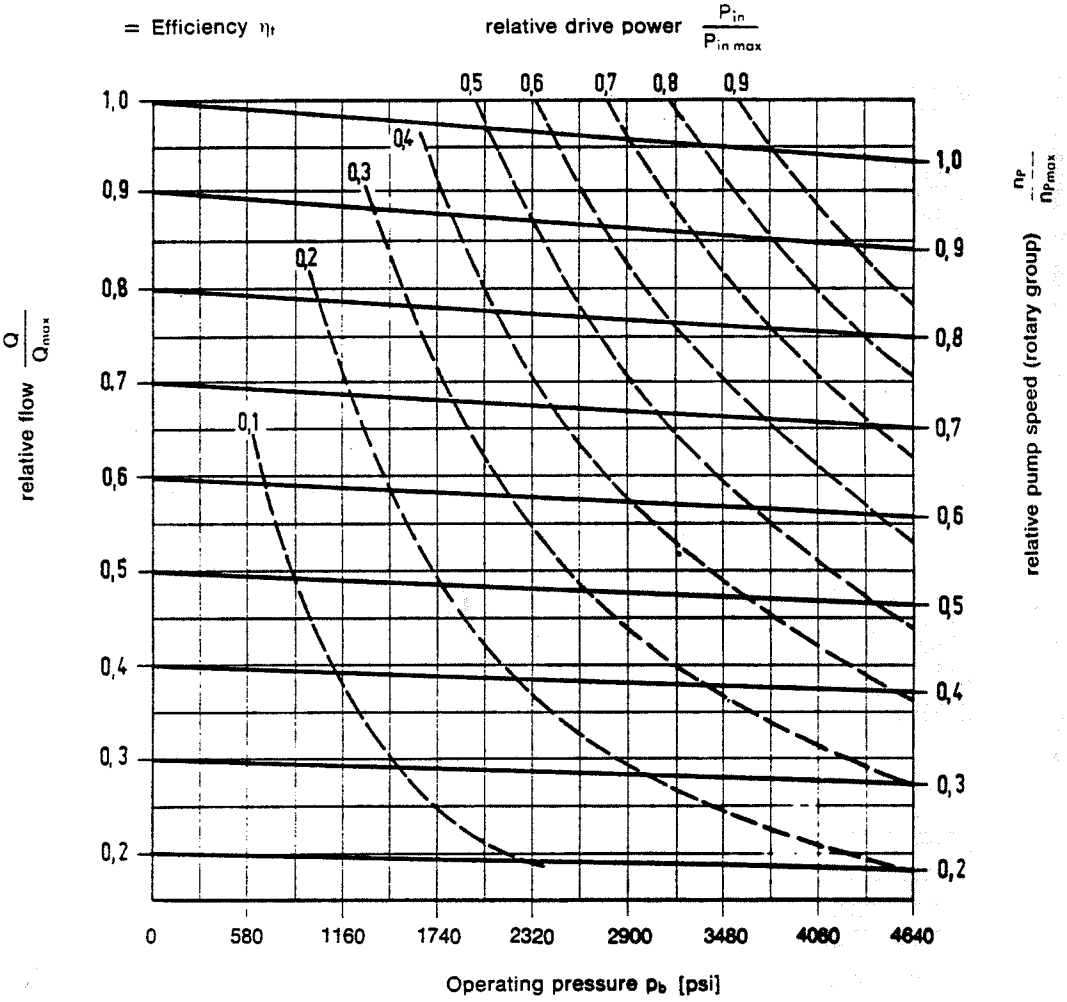
* Swivel trunnion

Variable Displacement Pump — Performance Curve ($\alpha = 25^\circ$)

The values shown are averages for the various sizes, at 122° F and 164 SUS
For further details of the mechanical and hydraulic efficiency, please contact us.

Size	12	28	55	107	225	468	915	1830
n_{max} [rpm]	6000	4750	3750	3000	2360	1900	1500	1200
Q_{max} [gpm]	18.39	35.24	54.29	84.79	140.3	234.9	362.5	580.1
P_{max} [HP]	48.3	92.4	143	222	368	616	951	1522

(These values are only computational and refer to this performance curve)

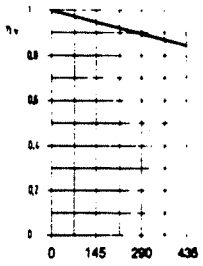


Boost Pump (for size 28–225)

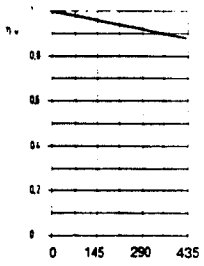
Volumetric efficiency at 122° F and 164 SUS

Mechanical/hydraulic efficiency
η_{mh} = 0.7 (average value)

Speed n = 1000 Rpm

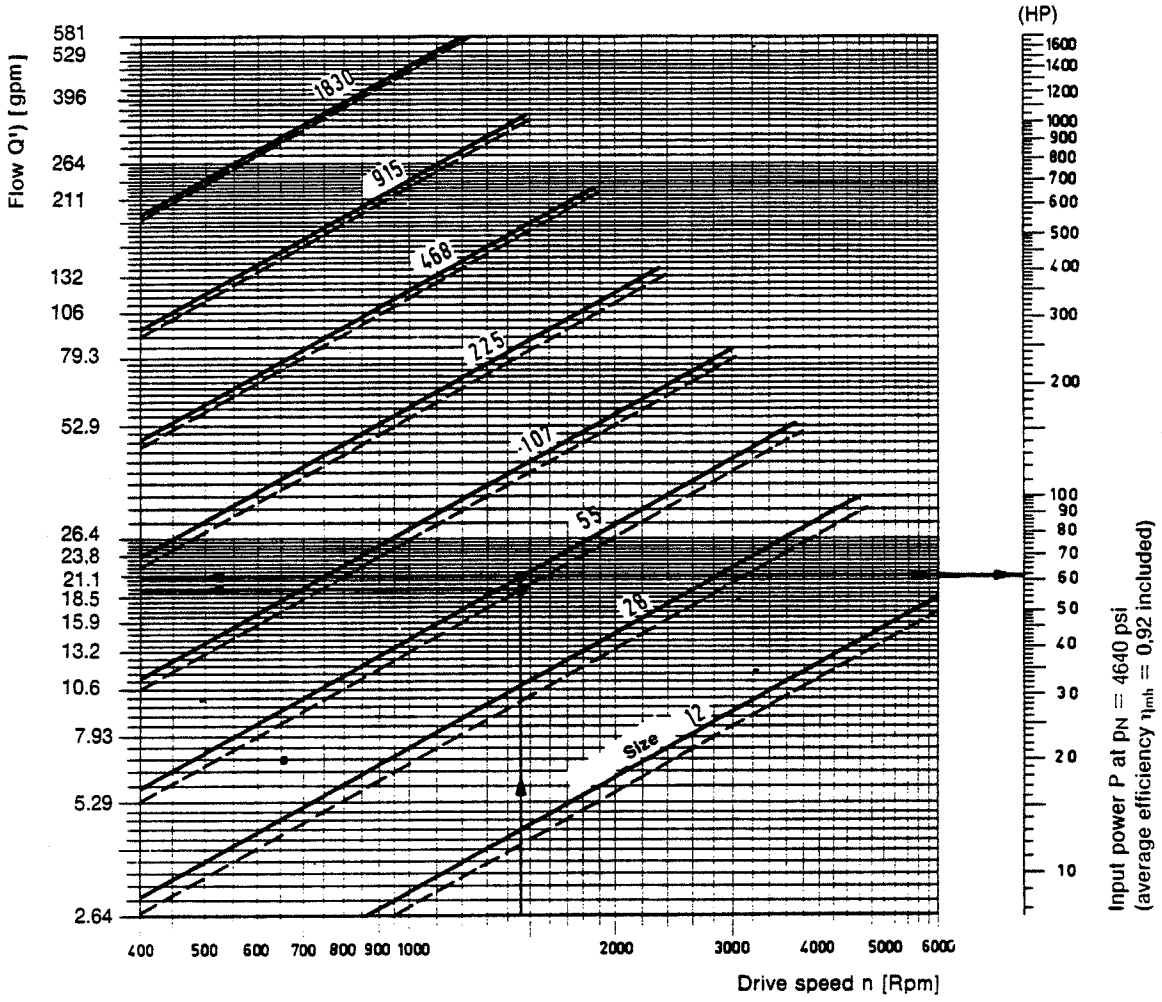


Speed n = 1500 Rpm



Q-n/P-n Characteristics

Variable Displacement Pump



Characteristics at $p_b = 0$

Characteristics at p_N = 4640 psi

¹) Q to be reduced by 3 % for open and half-closed circuits.

Example: **Given:**

n = 1450 Rpm
Size = 55

From the Diagram it follows:

Q = 21 gpm at $p_b = 0$
Q = 19.5 gpm at p_N = 4640 psi
P = 62 HP at p_N = 4640 psi

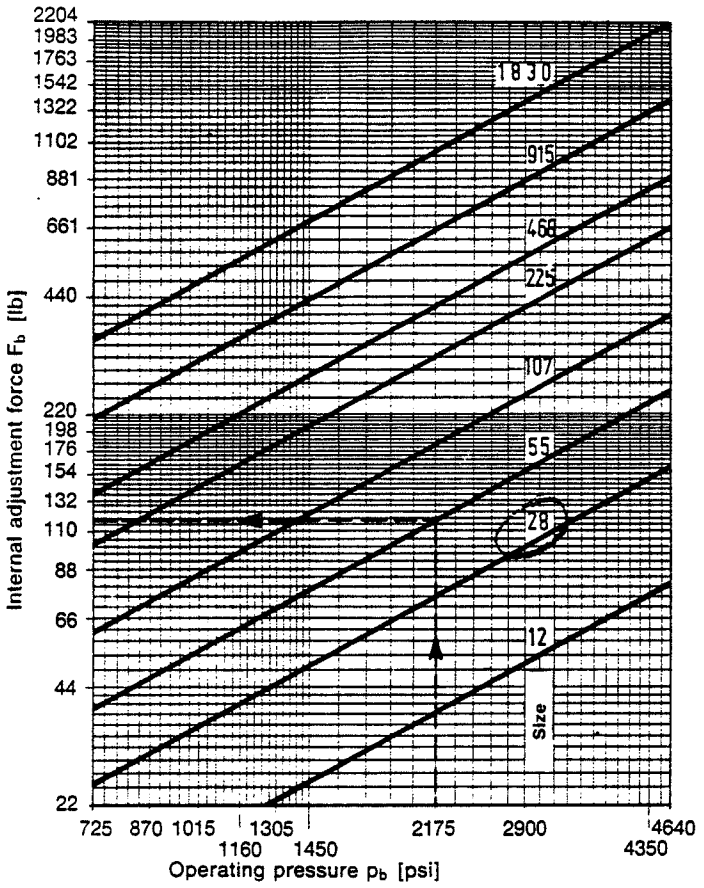
Adjustment (via trunnion or control device)

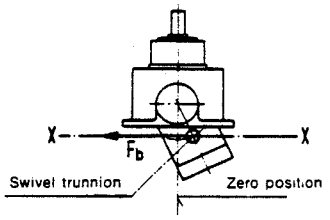
Adjustment stroke s [in]

Size	12	28	55	107	225	468	915	1830
Adjustment stroke s	0.84	0.99	1.24	1.57	1.96	2.82	3.48	4.40

Adjustment Angle α [°] ± 25°

Adjustment Force F_b [lb]
(Internal adjustment force. without acceleration force)





Example:
p_b = 2175 psi
Size 55
from the diagram, F_b = 119 lb

Adjustment force F_b* [lb] taking into consideration the acceleration force.

$$F_b^* = F_b - \frac{m_r \cdot b}{32.174}$$

m_r [lb mass] = equivalent inertia of the swivel body at the swivel trunnion

b [ft/s²] = acceleration in direction x–x

Values for m_r [lb mass]

Size	12	28	55	107	225	468	915	1830
open and closed circu	3.8	22	44	88	189	280	588	1135
half-closed circuit	3.9	35	68	123	242	440	904	1852

Adjustment force F_b [lb] with n_{max} with pump drive, the adjustment force F_b is directed to the zero position.

Input and Output Power

Motor-driven via coupling, gears or V-belts.
When using boost pump, drive via coupling only.

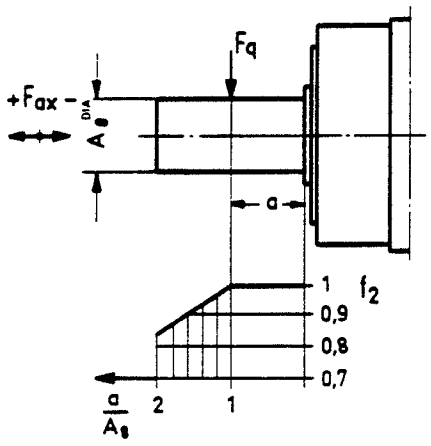
Gear Drive: The maximum permissible radial force $F_{q\,perm.}$ is based on a minimum pinion diameter of $2 \cdot A_8$ at 20° involute gearing. For the maximum permissible axial force $F_{ax\,perm.}$ the effective force direction must be taken into consideration (+, −). Forces penetrating into the unit (−) increase the bearing life, while forces from the opposite direction (+) decrease it. At operating pressure p_b = 0, the force $F_{ax\,perm.}$ (−) must not exceed the bearing tension F_V.

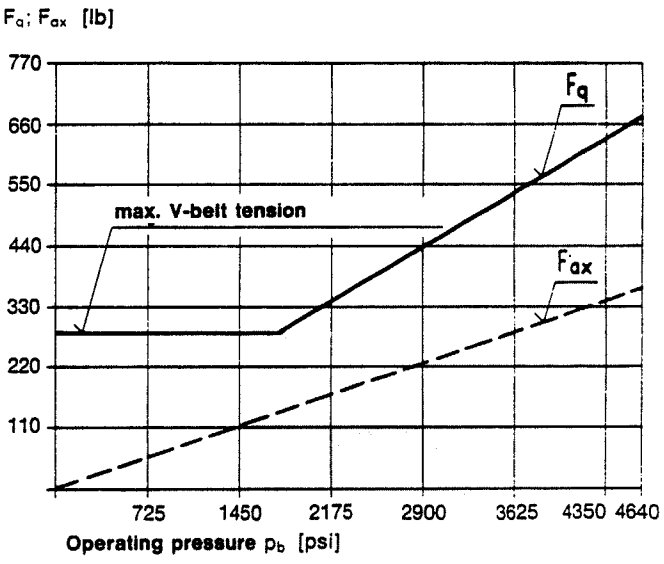
V-Belt Drive: When using Continental Ultraflex V-belts, the smallest diameter of the disc is $5 \cdot A_8$.

Special Conditions: If the force effectiveness line F_{ax} (−) is identical to the centre of the shaft end, then $F_{ax\,perm.}$ (−) can be determined by the formula $F_{ax\,perm.} \leq f_3 \cdot p_b + F_V$.
p_b [psi] = operating pressure.

$F_{q\,perm.}$ and $F_{ax\,perm.}$ can be determined as follows:
$F_{q\,perm.} \leq f_1 \cdot f_2 \cdot F_q$
$F_{ax\,perm.} \leq f_1 \cdot F_{ax} + F_V$

Size	A_8 dia	F_V [lb]	f_1 [−]	f_3 [in²]
12	0.7879	70.5	1	0.217
28	0.9848	110.2	2	0.387
55	1.1818	176.4	3.2	0.620
107	1.5755	275.6	4.6	0.945
225	1.9693	440.9	7.8	1.565
468	2.7567	551.1	11.5	2.480
915	3.5442	705.5	17.6	3.875
1830	4.3316	881.8	28.2	6.200



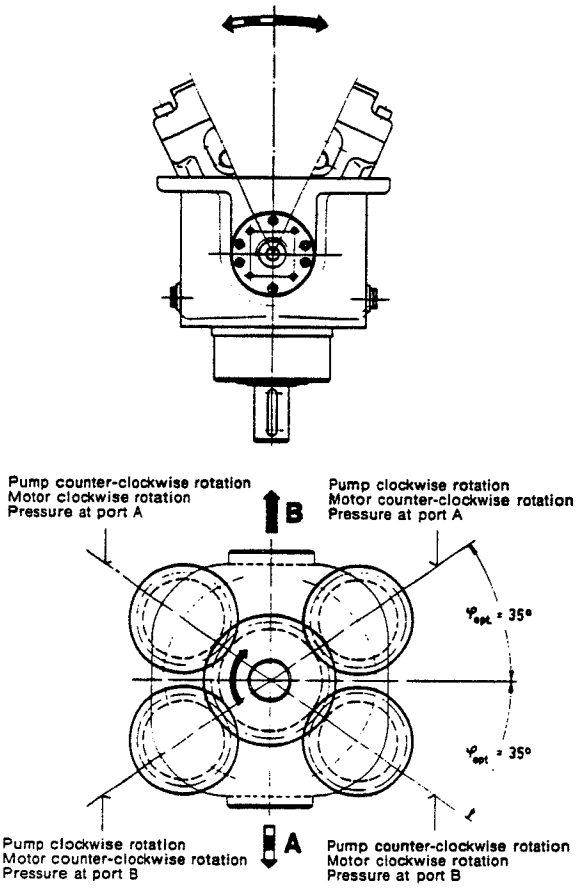


All rights reserved – subject to revision.

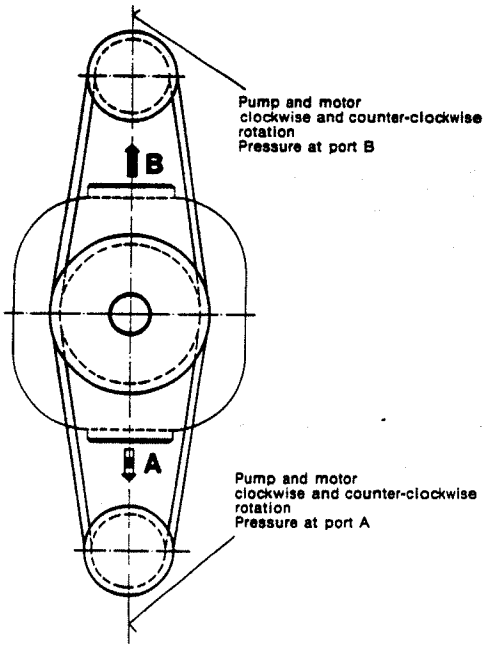
Optimum direction φ_{opt} of input or output drive with gears or V-belt.

Given then suitable effective force direction of F_q the bearing load can be reduced by means of the internal rotary group forces. The following input and output directions are recommended when using gear or V-belt drives.

Gear Drive, Input or Output



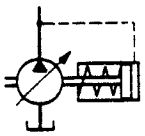
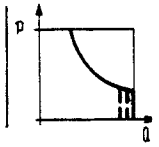
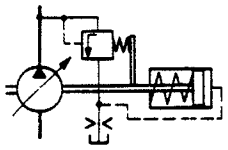
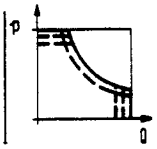
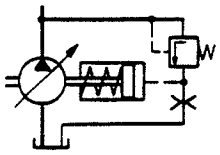
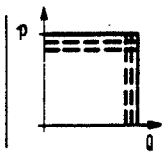
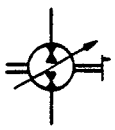
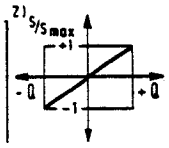
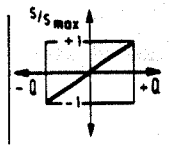
V-Belt Drive, Input or Output

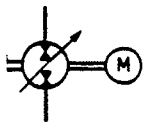
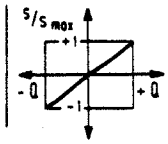
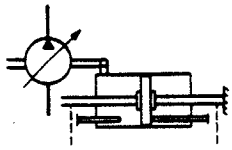
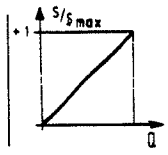
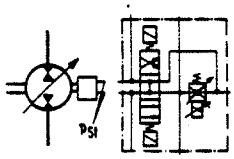
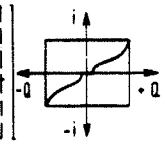
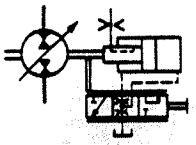
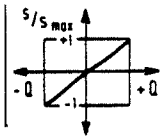


For gear input or output drive, deviation of ± 35° from the optimum angle is permissible.

If greater deviation is necessary, please consult us.

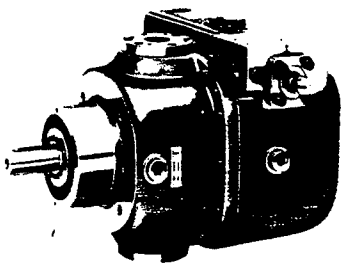
Summary of Controls

Description	Symbol	Performance Curve
Ld Constant HP Control Direct Operated Sheet 2-1		
Lv Constant HP Control Pilot Operated Sheet 2-2		
ADr Pressure Control Sheet 2-3		
AMa Handwheel Control Sheet 2-4		
Ge Mechanical Rod Control Sheet 2-5		

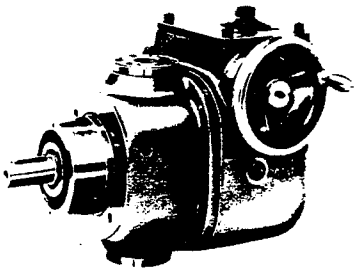
Description	Symbol	Performance Curve
AEl Electrical Control Sheet 2-6		
AHm Hydraulic Control Flow Related Sheet 2-7		
AHd Hydraulic [1] Control Pressure Related Sheet 2-8		
AHw Hydraulic Manual Servo Control Sheet 2-9		

1) With additional devices for regulating drive, pneumatic and electrical remote flow control and mooring control

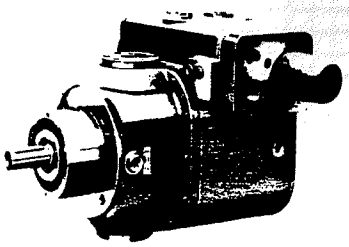
Variable Displacement Pumps with Control Devices



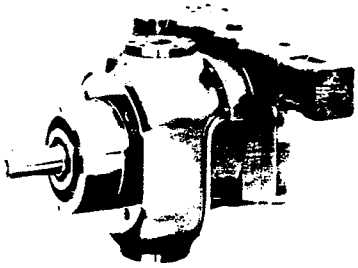
Constant HP Control **Ld**



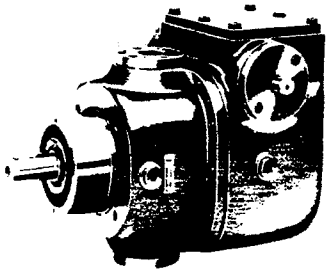
Handwheel Control **AMa**



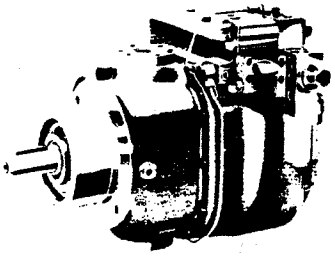
Hydraulic Control,
Flow Related **AHm**



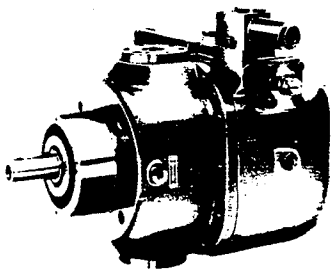
HP Control, Pilot Operated **Lv**



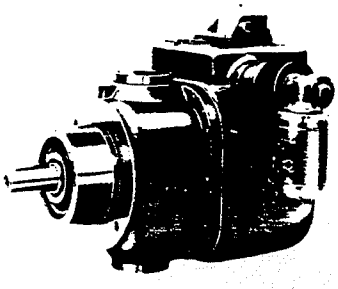
Mechanical Rod Control **Ge**



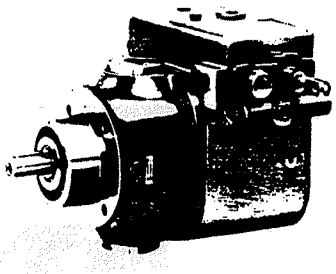
Hydraulic Control,
Pressure Related **AHd**



Constant Pressure Control **ADr**



Electrical Control **AEl**



Hydraulic Manual
Servo Control **AHw**

Issue 9/78

Ordering codes for

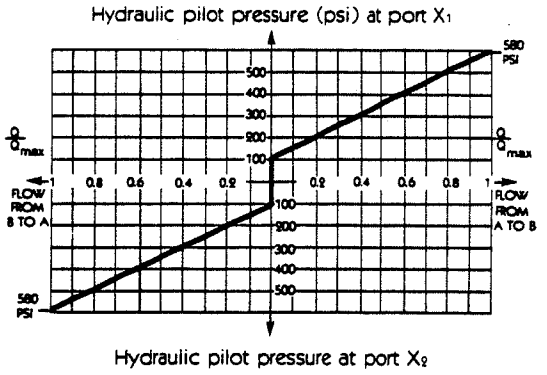
HYDRAULIC CONTROL

PILOT PRESSURE RELATED

TYPE Hd

As fitted to pump types

A2V & F1V



Description

The pilot pressure related hydraulic control converts control signals quickly and accurately into a related swivel position of the pump. It consists of adjusting cylinder, amplifier stage and input valve.

The control signals can be either hydraulic, pneumatic or electrical. An input valve is required only for pneumatic or electrical remote control. Pilot connections X_1 and X_2 can be used directly for hydraulic remote control.

Hydraulic Remote Control with Adjusting Cylinder and Amplifier Stage

The swivel angle (displacement) of the pump is set to suit the pilot pressure at two independent pilot ports, with one pilot line being allocated to each swivel direction. In one swivel direction, with a pilot pressure of between 116 and 580 psi, the pump displacement increases linearly.

Pneumatic and Electrical Remote Control

Fitting of the pneumatic or electrical input valve converts the hydraulic remote control into a pneumatic or electrical remote control.

Horsepower Limiter

By fitting a horsepower limiter the swivel angle (flow) as a function of the high pressure is limited so that a preselected drive power cannot be exceeded.

Principle of Operation

The operating principle of the pilot pressure related control is very simple. The above chart shows the relationship of pump output volume, (Q) as decimal factor of maximum volume (Q_{max}) related to pilot pressure applied to port X_1 or X_2 of the pump control. Referring to the diagram in column 11 on page 2, this pilot pressure, say applied to port X_1, is seen as a force at one end of control spool (3) (Pilot pressure times area of spool end), moving spool to the right, allowing control pressure oil from port P to be fed into left hand side of adjusting cylinder (2), via the biased control spool.

The adjusting cylinder (2) moves to the left (piston and rods are fixed to pump case).

Movement of the adjusting cylinder (2) strokes the pump to one side of center, compressing the spring at the right end of the control spool (3). The cylinder continues to move until the spring force equals the opposing hydraulic force on the control spool (3). When an equilibrium is reached the control spool is returned to its neutral position, blocking control oil to the adjusting cylinder. The pump is maintained in this position until the pilot pressure at X_1 is changed or removed.

REXROTH
HYDROMATIK

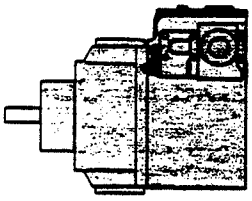
Hydraulic Control, Pressure Related

1 2 3 4 5 6 7 8 9 10
Model code details of basic pump from catalog A2V variable pump or F1V air-cooled power pack.

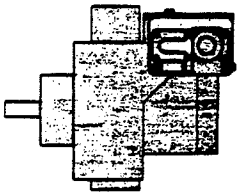
Pump types available with Hd pressure related control.

o - open circuit
g - closed circuit
h - half closed circuit

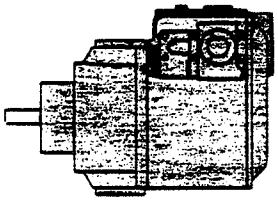
SIZE	Design E (Submersible)	Design G (housed)
55	3oh	6ogh
107	3oh	6ogh
225	3oh	6ogh
468	4oh	7 gh
500	4oh	7 gh



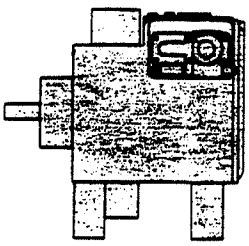
Style E[3]
Sizes 55-225



Style E[4]
Sizes 468-915



Style G[6]
Sizes 55-225



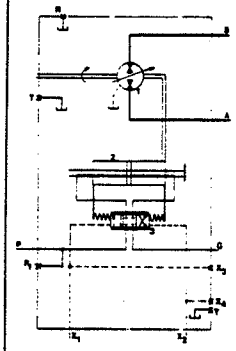
Style G[7]
Sizes 468-915

11 Amplifier stage

K

Adjusting cylinder **k**

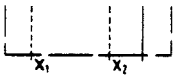
(for external adjustment of swivel time)



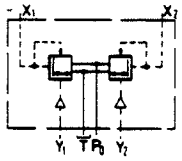
12 Remote Control

h

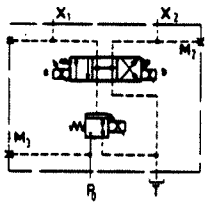
hydraulic **h**
pneumatic **P**
electric **e**



hydraulic h
direct application of pilot pressure to port X_1 or X_2



pneumatic P
with pneumatic amplifier manifold.



electric e
with electric proportional control.

For joystick control to work directly with option h refer to Rexroth data sheet RA 64110

13 Horse-power limiting

1

without horsepower limiting **0**

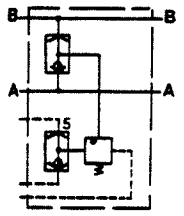
both sides limited via shuttle valve **1**

side A and B independently limited (2 Limiting Valves) **2**

one side only limited. **3**



without horsepower 0 limiting valve



horsepower limiting 1 on both pressure ports with use of shuttle valve

14 Q-P Curve selection (for horsepower limiting)

3

Without horsepower limiting **0**

With horsepower limiting

Size 55	107	225	468	915	Curve No.
11.9	23.6	49.7	71.0	136	1
15.4	29.6	62.2	87.6	170	2
17.7	35.3	74.7	105	204	3
21.2	41.4	88.7	123	239	4
23.6	47.2	99.3	138	270	5
27.1	53.0	113	157	307	6
30.1	59.1	126	175	341	7
33.1	65.1	139	191	376	8
36.6	71.0	151	212	411	9
39.0	77.2	161	226	437	10

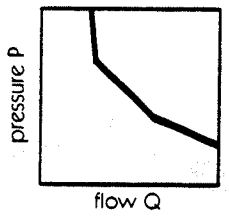
Note Base speeds for the above power curve settings:
Size 55, 107, 225 1750 rpm
Size 468, 915 1160 rpm

To select curve for other speeds

Size 55, 107, 225 $P = \frac{P\ drive \times N\ drive}{1750}$

Size 468, 915 $P = \frac{P\ drive \times N\ drive}{1160}$

Note The above settings are obtained by changing the springs of the limiting valve. Some adjustment is available within the range of the next highest and next lowest curve. Efficiency levels of the pump are included in the above values.



Refer to page 4 for a detailed description of the operating principles.

15 Limit Switch

O

none **0**

1 limit switch **1**

2 limit switches **2**

3 limit switches **3**

4 limit switches **4**

5 limit switches **5**

6 limit switches **6**

Note - limit switch housing comes with visual position indicator

16 Potentiometer

P

without **O**

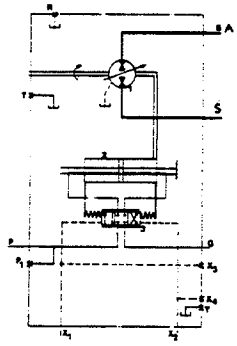
with **P**

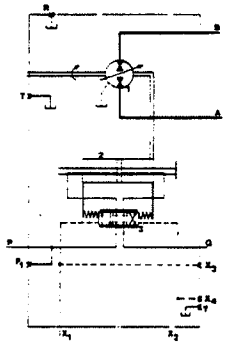
desired resistance ohms [Ω]
feed back potentiometer for use with servo valve.
1000 Ω
2000 Ω
5000 Ω
10000 Ω

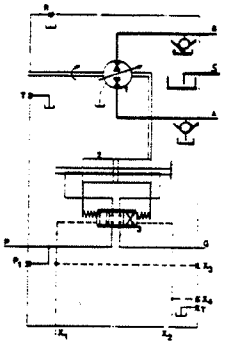
the given resistance values are for the full swivel range of the pump $+Q_{max}$ through $-Q_{max}$

IN CLEAR TEXT

1 drive type
ie. electric motor
gasoline engine
diesel engine.
2 drive speed (N drive)
3 drive power (P drive)


open circuit-o


closed circuit-g


half closed circuit-h

Ordering Example:

A2V.55.Hd.g.r.1.G.0.0.P.-Kh120P-1000/El. mtr. 15 HP @ 1750 rpm.
Variable displacement pump with pilot pressure related control size 55 (3.34 in³/rev), closed circuit, clockwise rotation, housed pump, without valve assembly and without boost pump, keyed shaft, with return line connection for swivel time adjustment, hydraulic remote control, both pressure lines limited by shuttle valve, horsepower curve #2, without limit switches, with 1000Ω potentiometer. The pump is being driven by a 15 HP electric motor at 1750 rpm.

Horsepower Limiting

The pressure related control is available with a horsepower limiting valve to prevent prime mover overloading because of hydraulic load fluctuations or due to an over-zealous operator. The horsepower override works on principle of modifying the input pilot pressure at ports X_1 or X_2. Remembering that the pilot pressure is proportional to the pump displacement and therefore output volume, modifying the input pilot pressure in an inverse relationship to the system operating pressure, enables us to control the hydraulic horsepower output of the pump. This, in turn (allowing for pump efficiencies) ensures that the input horsepower available is never exceeded. In other words, the relationship of input power to hydraulic flow and pressure is always true to the equation.

$$\text{INPUT HORSEPOWER} = \frac{Q \times P}{1714 \times \mu}$$

When - Q = oil flow from port A or B in gallons per minute

P = system pressure in psi

μ = overall efficiency of the pump at given pressure and speed

The override of the pilot pressure is accomplished by a variable pressure, direct-operated relief valve working in principle, as shown in figure 1. The horsepower override valve may be bolted directly to pump control or piped remotely.

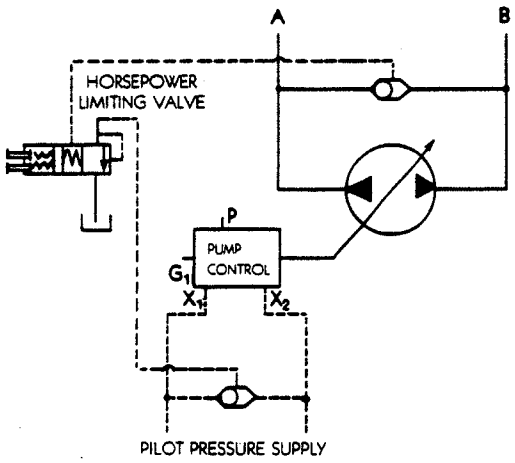


FIGURE 1 OPERATING PRINCIPLE OF HORSEPOWER LIMITING VALVE FOR PILOT PRESSURE RELATED PUMP CONTROL.

This valve is completely hydraulic, and therefore, requires no external signal from electric motor power-sensing device, or governor (for gas or diesel engine prime movers). The horsepower setting is governed by pre-designated spring rates, however, adjustment about the nominal setting may be performed on a hydraulic test bench by regulating the allowable pilot pressure for any given system pressure. If necessary, it can be set in the field by adjusting the valve in relation to the electric motor amperage.

To demonstrate the effect on pilot pressure by the horsepower limiting valve, figure 2 shows a 75 horsepower curve obtained from the valve's horsepower control springs.

The example is for a 13.73 in^3/revolution industrial pump operating at 1750 rpm with 75 input horsepower.

With a pilot pressure of 580 psi applied to the X_1 or X_2 port, the pump will remain on 100% stroke as long as the system pressure remains less than 1200 psi.

As system pressure rises above 1200 psi, due to load resistance, the pump destrokes in accordance with the spring rates of the limiting valve. Again referring to figure 6-2, a system pressure of 2600 psi corresponds to a pump displacement of 0.4 x maximum. This is caused by the direct acting relief section of the limiting valve (figure 6-1) overriding the 580 psi pilot pressure to allow a maximum pilot pressure of only 302 psi and hence causing the pump to destroke at 40% of maximum displacement.

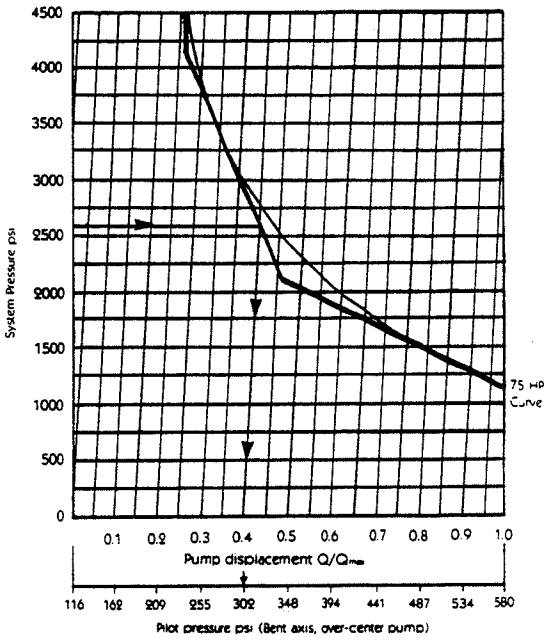


FIGURE 2 HORSEPOWER OVERRIDE CURVE.

It must be remembered that the foregoing acts as an override of the primary control, i.e. pilot pressure related displacement, and should not be compared or confused with true constant horsepower regulators (types Ld & Lv) used as the primary control on open loop pumps.

REXROTH WORLDWIDE HYDRAULICS
The Rexroth Group has design, sales, and service facilities in 31 countries throughout the world.
THE REXROTH CORPORATION
BETHLEHEM, PENNSYLVANIA 18018 • 215-694-8300
REXROTH
HYDROMATIK
BRUENINGHAUS
LOHMANN AND
STOLTERFOHT
INDRAMAT
EXCENTRA
SIGMA
CARRON

EFFICIENCY CHARACTERISTICS

Efficiency is determined by measuring leakage. We differentiate between two types of leakage: mechanical-hydraulic leakage and volumetric leakage.

VOLUMETRIC LEAKAGE

is made up from internal leakage loss between high pressure and low pressure side and the external leakage amount, which occur at a ratio of 2:1.
Volumetric leakage depends upon operational pressure resp. pressure differential between high and low pressure sides, the pump size resp. size of motor and oil viscosity. The influence of drive speed (rpm) can be omitted.

MECHANICAL-HYDRAULIC LEAKAGE

is made up of frictional loss on bearings, pistons, control surfaces, as well as flow leakage caused by fluid friction and shock loss by flow rerouting.
Mechanical-hydraulic leakage depends on operational pressure, drive speed, pump swivel angle (motor swivel angle) and oil viscosity.

OVERALL EFFICIENCY

is made up of efficiency per unit.

$$\eta_t = \eta_v \cdot \eta_{mh}$$

overall efficiency = volumetric efficiency
x mechanical-hydraulic efficiency

Volumetric and mechanical-hydraulic efficiency in the table applies strictly speaking only in case that operational pressure equals pressure differential. (low pressure = 0 bar)
The inaccuracy up to a boost pressure of approx. 15 - 20 bar is relatively small and can be omitted.

Volumetric efficiency refers to a pump in closed circuit. When operating in open circuit a suction loss of max. 3 % must be included in the calculation (tolerance in rotary group, suction loss in open circuit).

The data listed in the table refer to oil viscosity of 36 cSt. They are suitable for the calculation of horse power requirements.

CALCULATION OF SIZE

PUMP:

Flow $$Q = \frac{Vg \cdot n \cdot \sin\alpha \cdot \eta_v}{231 \cdot \sin 25^\circ} \quad [\text{gpm}]$$

Torque $$M = \frac{Vg \cdot \Delta p \cdot \sin\alpha}{24 \cdot \pi \cdot \sin 25^\circ \cdot \eta_{mh}} \quad [\text{lb ft}]$$

Power $$P = \frac{M \cdot n}{5252} = \frac{Q \cdot \Delta p}{1715 \cdot \eta_t} \quad [\text{HP}]$$

MOTOR:

Supply Volume $$Q = \frac{Vg \cdot n \cdot \sin\alpha}{231 \cdot \sin 25^\circ \cdot \eta_v} \quad [\text{gpm}]$$

Torque $$M = \frac{Vg \cdot \Delta p \cdot \sin\alpha \cdot \eta_{mh}}{24 \cdot \pi \cdot \sin 25^\circ} \quad [\text{lb ft}]$$

Power $$P = \frac{M \cdot n}{5252} = \frac{Q \cdot \Delta p \cdot \eta_t}{1715} \quad [\text{HP}]$$

Vg = Max. geometric displacement $[in^3/rev.]$
M = Torque [lb ft]
Δp = Differential pressure [psi]
n = Speed [rpm]
η_v = volumetric efficiency
η_{mh} = mechanical-hydraulic efficiency
η_t = overall efficiency $[\eta_t = \eta_v \cdot \eta_{mh}]$
α = swivel angle [°]
K_M = torque constant $\left[\frac{\text{lb ft}}{\text{psi}}\right]$
P = power [kw] or [HP]
Q = displacement [gpm]

Calculation of size $\frac{\sin\alpha}{\sin 25^\circ}$ is not necessary with fixed displacement pumps and motors, since the geometric displacement and the torque constant cannot be changed. The correct size can be learned from our bulletins.

Efficiency Tables - MOTOR size 107 (6.53 in^3/rev.)

Fixed displacement motor type A2F
Variable displacement motor type A6V

η_v = volumetric efficiency
η_{mh} = mechanical-hydraulic efficiency)
η_t = overall efficiency = (η_v x η_{mh})

All efficiencies x 10^{-3}

swash angle ∢		1°			5°			10°			15°			20°			25°		
efficiencies		η_v	η_{mh}	η_t	η_v	η_{mh}	η_t	η_v	η_{mh}	η_t	η_v	η_{mh}	η_t	η_v	η_{mh}	η_t	η_v	η_{mh}	η_t
speed (min-1)	system pressure (bar)																		
50 U/min	50	-	-	-	790	225	177	875	550	482	920	684	629	946	740	700	957	773	740
	100	-	-	-	685	450	308	796	726	578	865	812	702	902	853	770	925	858	794
	150	-	-	-	593	565	335	730	783	572	812	853	692	860	886	762	890	896	797
	200	-	-	-	480	637	306	655	811	531	756	875	661	814	906	737	853	912	778
	250	-	-	-	345	680	234	528	826	436	662	886	587	745	916	682	795	922	733
	320	52	80	4	205	715	146	377	844	318	522	895	467	636	919	584	705	927	653
100 U/min	50	-	-	-	848	400	339	921	639	589	947	739	699	961	787	757	972	823	801
	100	-	-	-	748	542	405	845	776	656	892	846	755	928	879	816	951	884	840
	150	-	-	-	659	628	414	789	823	650	855	877	750	899	903	812	930	910	846
	200	-	-	-	614	698	428	746	850	634	820	895	734	867	919	797	896	922	827
	250	150	90	13	500	727	363	699	865	604	781	908	709	831	930	774	862	932	804
	320	90	195	17	405	751	304	599	877	525	697	918	640	756	937	708	800	940	752
200 U/min	50	-	-	-	902	490	442	950	701	666	966	784	758	976	828	809	984	850	837
	100	-	-	-	807	632	510	896	813	729	932	872	812	953	899	857	967	905	875
	150	-	-	-	723	705	509	852	856	730	906	899	815	931	919	856	952	925	881
	200	-	-	-	671	751	504	812	877	713	874	915	801	906	932	844	929	936	870
	250	217	228	49	599	774	463	766	890	682	843	927	781	880	942	830	910	946	861
	320	150	304	45	517	800	414	698	902	630	804	936	753	850	949	807	877	951	835
400 U/min	50	-	-	-	936	531	497	968	753	729	980	824	808	986	863	851	990	875	867
	100	-	-	-	871	700	610	934	850	795	959	896	860	972	917	892	979	923	904
	150	-	-	-	802	764	612	900	885	797	940	920	865	957	935	895	968	940	911
	200	370	275	101	753	802	604	866	903	783	916	934	856	940	945	889	954	950	907
	250	280	340	95	703	820	576	836	914	764	893	944	843	920	954	878	942	956	901
	320	216	408	88	628	835	524	797	921	734	863	950	820	897	959	861	927	962	892
800 U/min	50	-	-	-	949	551	523	976	783	764	984	845	832	991	874	866	993	879	873
	100	-	-	-	903	732	661	952	873	832	972	909	884	980	927	909	986	931	918
	150	-	-	-	853	803	685	930	905	841	958	930	892	971	942	912	979	948	928
	200	421	344	144	809	836	676	904	921	833	944	946	894	960	952	915	970	958	830
	250	335	409	137	758	849	644	880	930	819	929	954	886	948	961	911	963	963	928
	320	270	475	128	707	858	607	852	935	797	908	958	870	933	965	900	951	968	921
1500 U/min	50	-	-	-	956	502	480	978	752	736	988	822	812	992	843	836	994	846	842
	100	-	-	-	917	710	651	958	862	826	976	901	879	984	91o	896	989	913	903
	150	-	-	-	870	797	694	940	900	846	966	926	895	977	932	911	983	938	923
	200	456	312	142	838	832	697	921	918	845	954	942	899	969	947	918	978	951	930
	250	376	393	147	790	845	668	903	926	837	843	950	897	961	956	919	972	958	932
	320	309	464	143	741	859	637	877	934	819	926	956	885	949	962	913	963	965	929
3200 U/min	50	-	-	-	963	91	83	892	484	476	991	583	578	993	603	599	995	606	605
	100	-	-	-	926	496	459	966	739	714	980	801	785	987	809	799	990	813	805
	150	-	-	-	890	694	618	949	833	791	971	866	842	980	875	857	986	876	864
	200	490	92	45	856	742	635	933	862	804	963	893	861	975	902	880	981	903	886
	250	415	156	64	823	765	630	922	880	812	954	911	869	967	916	886	976	917	896
	320	345	240	82	769	796	612	896	896	803	940	921	866	959	930	891	969	932	983

Efficiency Tables - PUMP size 107 (6.53 in³/rev.)

Fixed displacement pump type A2F
Variable displacement pump type A2V and A7V

η_v = volumetric efficiency
η_{mh} = mechanical-hydraulic efficiency
η_t = overall efficiency = (η_v x η_{mh})
All efficiencies x 10^{-3}

swash angle a		1°			5°			10°			15°			20°			25°		
efficiencies		η_v	η_{mh}	η_t	η_v	η_{mh}	η_t	η_v	η_{mh}	η_t	η_v	η_{mh}	η_t	η_v	η_{mh}	η_t	η_v	η_{mh}	η_t
speed (min⁻¹)	system pressure (bar)																		
50 U/min	50	240	235	56	738	563	415	855	690	590	910	760	691	940	794	746	952	815	776
	100	-	-	-	349	645	225	738	785	580	837	842	704	885	872	771	912	876	799
	150	-	-	-	329	696	229	622	822	511	757	872	660	826	898	742	866	906	784
	200	-	-	-	-	-	-	-	-	-	-	-	-	-	-	-	-	-	-
	250	-	-	-	-	-	-	-	-	-	-	-	-	-	-	-	-	-	-
	320	-	-	-	-	-	-	-	-	-	-	-	-	-	-	-	-	-	-
100 U/min	50	465	280	129	825	625	515	912	735	670	941	793	746	957	825	789	969	850	823
	100	-	-	-	648	686	444	812	817	664	873	866	756	916	892	817	942	896	844
	150	-	-	-	473	729	344	726	850	617	820	891	730	878	911	800	915	917	839
	200	-	-	-	340	768	261	650	869	565	766	905	693	833	925	770	871	928	808
	250	-	-	-	-	-	-	-	-	-	700	916	641	774	935	723	823	937	771
	320	-	-	-	-	-	-	-	-	-	-	-	-	-	-	-	-	-	-
200 U/min	50	675	342	230	885	662	586	945	770	728	962	822	791	973	853	830	981	870	853
	100	340	462	157	770	731	563	880	843	741	921	886	816	945	908	858	959	913	876
	150	-	-	-	630	772	486	820	874	717	886	909	805	916	925	847	940	930	874
	200	-	-	-	535	800	428	760	891	677	843	922	777	883	936	826	911	940	856
	250	-	-	-	357	815	291	682	901	614	796	932	742	847	945	800	885	949	839
	320	-	-	-	-	-	-	550	911	501	734	940	690	801	952	762	838	954	799
400 U/min	50	788	382	301	935	680	636	965	802	774	977	850	830	983	879	865	987	889	877
	100	530	495	262	860	769	661	926	870	805	951	906	862	965	924	892	972	929	903
	150	-	-	-	765	809	618	883	897	792	927	926	858	946	939	888	958	944	904
	200	-	-	-	665	835	572	837	911	763	896	938	840	923	948	875	939	952	894
	250	-	-	-	600	847	508	793	921	730	864	947	818	897	956	858	922	958	883
	320	-	-	-	440	858	377	730	927	677	820	952	781	864	961	830	900	963	867
800 U/min	50	850	395	335	950	690	655	973	822	800	981	866	850	988	888	877	990	892	883
	100	670	507	340	900	788	710	946	888	840	966	917	885	974	932	908	980	935	916
	150	460	570	262	840	835	701	918	913	838	947	935	886	960	945	908	969	950	921
	200	300	644	193	780	859	670	886	927	821	929	949	881	946	955	903	957	960	918
	250	-	-	-	703	868	610	853	935	797	908	956	868	929	963	894	945	965	912
	320	-	-	-	615	875	538	812	939	763	878	960	842	907	966	876	928	969	899
1500 U/min	50	879	370	325	957	667	639	976	801	782	985	849	836	989	864	855	991	867	859
	100	748	485	362	917	775	710	953	878	837	969	910	882	978	918	897	983	920	904
	150	560	560	313	862	831	717	930	909	846	956	931	890	967	937	906	974	942	917
	200	425	593	250	822	858	706	906	924	837	940	945	888	956	950	908	965	953	920
	250	-	-	-	755	865	653	882	931	821	924	953	881	943	958	903	955	960	917
	320	-	-	-	679	876	595	846	938	793	900	958	862	926	963	892	941	966	909
3200 U/min	50	891	224	199	965	524	505	980	660	646	988	706	697	990	716	708	992	717	711
	100	765	360	275	927	665	616	961	793	762	974	834	812	981	840	824	984	842	829
	150	626	428	267	887	766	679	941	857	806	962	882	848	970	889	858	976	890	869
	200	500	480	240	847	795	673	920	879	808	950	904	858	962	911	876	968	912	882
	250	-	-	-	805	810	652	905	893	808	937	918	860	950	923	876	960	924	887
	320	-	-	-	726	831	603	870	906	788	916	927	849	936	934	875	947	936	886

APPENDIX D: Parker Accumulator Data

The following pages contain the manufacturer's data for the Parker piston accumulators used in the test stand. Since the actual models used were prototypes for a possible new series, some of the data was incomplete and had to be added.